AD-787 472

AN ANALYSIS OF GRAVITY PREDICTION
METHODS FOR CONTINENTAL AREAS

Luman E. Wilcox

Defense Mapping Agency Aerospace Center
St. Louis, Air Force Station, Missouri

August 1974

DMAAC Reference Publication No. 74-001

AN ANALYSIS
OF GRAVITY PREDICTION METHODS
FOR CONTINENTAL AREAS

Luman E. Wilcox

AUGUST 1974

D D C

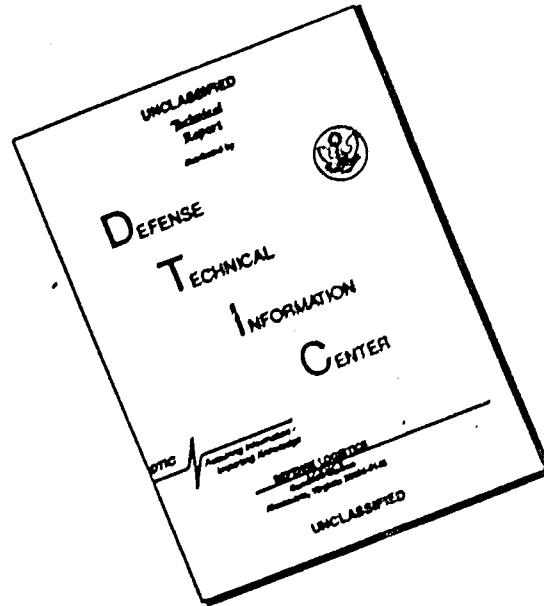OCT 30 1974

D

Defense Mapping Agency
Aerospace Center
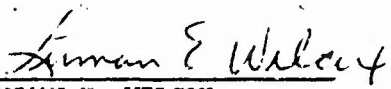St. Louis AFS, Missouri 63118

308

DISCLAIMER NOTICE

THIS DOCUMENT IS BEST QUALITY AVAILABLE. THE COPY FURNISHED TO DTIC CONTAINED A SIGNIFICANT NUMBER OF PAGES WHICH DO NOT REPRODUCE LEGIBLY.
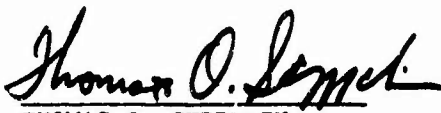
ia

AN ANALYSIS
OF GRAVITY PREDICTION METHODS
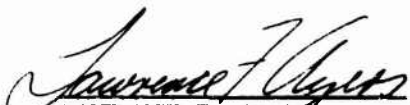# FOR CONTINENTAL AREAS

PREPARED:

Luman E Wilcox

LUMAN E. WILCOX
Chief, DOD Gravity Correlation Branch
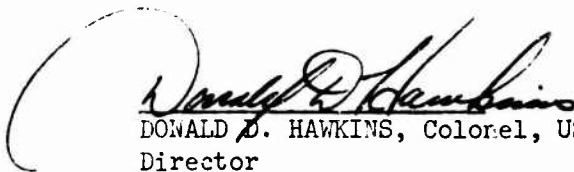
SUBMITTED:

Thomas O. Seppelin

THOMAS O. SEPPELIN
Chief, Research Department

REVIEWED:

Lawrence F. Ayers

LAWRENCE F. AYERS
Technical Director

APPROVED:

Donald D. Hawkins

DONALD D. HAWKINS, Colonel, USAF
Director

Defense Mapping Agency
Aerospace Center
St. Louis AFS, Missouri 63118

ii

NOTICES

This report is issued to provide a manual of gravity
correlation methods for the prediction of 1° x 1° mean gravity
anomaly values for continental areas. It is intended for use by
organizations and individuals interested in the geophysical
accountability and prediction of gravity anomalies. Nothing
herein is to be construed as Defense Mapping Agency Doctrine.

This report is a dissertation submitted to the Graduate
Division of the University of Hawaii in partial fulfillment of
the requirements for the degree of Doctor of Philosophy in
Geology and Geophysics.

This publication does not contain information or material of
a copyrighted nature, nor is a copyright pending on any portion
thereof. Reproduction in whole or part is permitted for any
purpose of the United States Government.

ACKNOWLEDGEMENTS

PREFACE

The intent of this study is to establish an understanding of geophysical gravity prediction. The study, however, is oriented as much to applied as to theoretical aspects of gravity correlations. The writer has endeavored throughout to provide a simple picture of the central ideas underlying gravity correlation, prediction, theory, and practice.

The first three sections provide an introduction and discussion of some gravity anomaly principles of importance to geophysical gravity prediction. In this regard, no attempt is made to discuss all of the ideas of George P. Woollard whose extensive work in geophysical gravity analysis forms the backbone of gravity correlations. Rather, a complete bibliography of previous work is included. The remainder of the report is a comprehensive examination of geophysical prediction methods and their reliability.

ABSTRACT

Mean gravity anomaly values which represent 1° x 1° surface
areas can be predicted on the continents by geophysical gravity
correlation methods whether or not measured gravity data exists
within those 1° x 1° areas. These methods take into consideration
the earth's structure, composition, and response to changes in
surficial mass distribution by means of observed or computed
correlations between gravity and other geophysical parameters within
geologic/tectonic provinces. Linear basic prediction functions,
used to describe and predict the relationships between gravity and
elevation, are shown to be a natural consequence of the properties of
gravity reduction procedures and the observed behavior of gravity
anomalies within structurally homogenous regions. The effects of
local structural variations can be computed using simple attraction
formulas or derived from systematic observation of gravity anomaly
variations which characterize different types of local structures.
With little or no measured gravity data, geophysical gravity
predictions have an accuracy range of $\pm$ 5 to $\pm$ 20 milligals. With
more adequate amounts of measured data, accuracies of $\pm$ 1 to $\pm$ 2
milligals can be achieved easily.

TABLE OF CONTENTS

viii

LIST OF TABLES

xiv

LIST OF ILLUSTRATIONS

LIST OF FREQUENTLY USED

SYMBOLS AND ABBREVIATIONS

SYMBOL	DESCRIPTION
A	Cross Sectional Area
BP	Basic Predictor
BPA	Average Basic Predictor
BPF	Free Air Basic Predictor
CC	Curvature Correction
D	Depth of Compensation
E	Standard Error (generally used with subscripts)
EXGAP	Extended Gravity Anomaly Prediction Method
F	Height of Freeboard; Force
GAIN	Geologic Attraction Interpolation Method
GAPFREE	Normal Gravity Anomaly Prediction--Free Air Version
GC	Geologic Correction
GRADE	Gravity Densification and Extension Method
$\overline{H}$	Mean Elevation
H_S	Height of Standard Crustal Column
ME	Weighted 3° x 3° Mean Elevation
N	Gravimetric Geoid Height
NOGAP	Normal Gravity Anomaly Prediction Method
ODM	1° x 1° Mean Elevation
P	Pressure
R	Height of Crustal Root

TC	Terrain Correction
TC_P	Terrain Correction at P
TC_Q	Terrain Correction at Q
UNGAP	Unreduced Gravity Anomaly Prediction Method
V	Volume
$\bar{a}_{nm}, \bar{b}_{nm}$	Fully Normalized Harmonic Coefficients
d	Depth to Basement
e	Standard Error (generally used with subscripts)
g	Gravitational Acceleration
g_B	Bouguer Correction
$(g_B)_P$	Bouguer Correction at P
$(g_P)_Q$	Bouguer Correction at Q
$\bar{g}_{DC}$	Distant Compensation Correction
$\bar{g}_E$	Local Elevation Correction
$\bar{g}_{EF}$	Local Free Air Elevation Correction
g_F	Free Air Correction
$(g_F)_P$	Free Air Correction at P
$(g_F)_Q$	Free Air Correction at Q
g_H	Gravitational Attraction of Mass Within a Hill
g_I	Isostatic Correction
$(g_I)_P$	Isostatic Correction at P
$(g_I)_Q$	Isostatic Correction at Q
g_{IC}	Isostatic-Crustal Correction

$(\Delta g_B)_Q$	Bouguer Anomaly at Q
$\overline{\Delta g_B}$	Mean Bouguer Anomaly
Δg_F	Free Air Anomaly
$(\Delta g_F)_P$	Free Air Anomaly at P
$(\Delta g_F)_Q$	Free Air Anomaly at Q
$\overline{\Delta g_F}$	Mean Free Air Anomaly
Δg_I	Isostatic Anomaly
$(\Delta g_I)_P$	Isostatic Anomaly at P
$(\Delta g_I)_Q$	Isostatic Anomaly at Q
Δg_S	Unreduced Surface Anomaly
$(\Delta g_S)_P$	Unreduced Surface Anomaly at P
$(\Delta g_S)_Q$	Unreduced Surface Anomaly at Q
Δg_Y	Free Air Anomaly with Terrain Correction
ΔR	Height of Crustal Root Increment
α, β	Regression Constants for Regional Bouguer Anomaly--Regional Elevation Relation; Regression Constants for Regional Free Air Anomaly--Regional Elevation Relation
γ	Normal Gravity
γ_P	Normal Gravity at P
γ_Q	Normal Gravity at Q
δg_0	Reduction Applied to Reduce Observed Gravity to an Equivalent Value at Sea Level
$(\delta g_0)_B$	Bouguer Reduction
$(\delta g_0)_F$	Free Air Reduction
$(\delta g_0)_I$	Isostatic Reduction

ε_L	Local Geologic Effect at a Surface Point
$\overline{g}_L$	Local Geologic Correction
g_O	Observed Gravity
$(g_O)_P$	Observed Gravity at P
$(g_O)_Q$	Observed Gravity at Q
g_P	Gravity on Earth's Surface
ε_Q	Gravity at Sea Level
$\overline{g}_R$	Regional Correction
g_S	Gravitational Attraction of Topography as a Surface Mass
g_v	Gravitational Attraction of Topography as a Volume Mass
g_Z	Vertical Component of Gravitational Attraction
h	Orthometric Height Above Sea Level
h_P	Height at P
h_Q	Height at Q
δh	$h_P - h_Q$
$\overline{h}$	Mean Elevation
k	Gravitational Constant
m	Mass of the Earth
r	Radius of Geometric Figure
Δg	Gravity Anomaly
Δg_B	Bouguer Anomaly
$(\Delta g_B)_P$	Bouguer Anomaly at P

$\delta\Delta g_B$	Gravity "Anomaly" Caused by Local Density Contrasts
ζ, θ	Regression Constants for Local Unreduced Surface Anomaly--Local Elevation Relation
ξ, η	Regression Constants for Regional Unreduced Surface Anomaly--Regional Elevation Relation; Gravimetric Deflection of the Vertical components
κ	Surface Density
π	$3.14159...$
σ	Volume Density
σ_A	Average Density of Basement Rock
σ_B	Density of Rock in the Bouguer Plate
σ_C	Actual Mean Density of the Crust
σ_m	Density of the Standard Upper Mantle
σ_M	Actual Mean Density of the Upper Mantle
σ_S	Mean Density of the Standard Crust
ψ, ω	Regression Constants for the Local Free Air Anomaly--Local Elevation Relation

AN ANALYSIS

OF GRAVITY PREDICTION METHODS

FOR CONTINENTAL AREAS

1. INTRODUCTION

1.1 The Need for Mean Gravity Anomaly Data and the Nature of the Problem in Gravity Prediction

The input data required for applications of the integral formulas of physical geodesy to compute gravimetric geoid undulations, deflection of the vertical components, and similar parameters includes a detailed global representation of the earth's gravity anomaly field. The same global representation may be used to derive an earth gravity model, e.g., a spherical harmonic expression of global gravity variations.

For both purposes, it is convenient to express the global gravity anomaly field in terms of mean or average values which represent surface areas of $1° \times 1°$ in dimension. When needed, mean gravity anomaly values representing larger sized surface areas, e.g., $5° \times 5°$, $10° \times 10°$, can be obtained readily by averaging the basic $1° \times 1°$ "building blocks."

The $1° \times 1°$ mean gravity anomaly field also is useful for geophysically analyzing semi-regional changes in gravity which reflect the effects of all major topographic and geologic changes associated with mass inequalities in the lithosphere. The $5° \times 5°$ and $10° \times 10°$ average values can be used to study gross mass and geoidal changes.

Global representations of the earth's geoid and gravity anomaly field have been deduced from satellite orbital data considered alone (Anderle, 1966; Guier and Newton, 1965; Köhnlein, 1966;

Khan and Woollard, 1968) as well as in combination with surface gravity data (Uotila, 1962; Kaula, 1963, 1966c, 1967; Khan, 1969, 1972; Beers, 1971). These global gravity representations, however, provide only very generalized gravity anomaly expressions (equivalent to mean anomalies for 15° x 15° or larger areas) and, hence, have limited geodetic and geophysical application.

The best way to obtain 1° x 1° mean gravity anomaly values is by using the gravity measurements which exist within the 1° x 1° areas together with conventional, statistical, or geophysical averaging techniques. This can be done only in those portions of the world where gravity surveys have provided a reasonably dense and well distributed network of gravity measurements.

A considerable body of measured gravity data is now available-- the DOD Gravity Library, for example, holds more than ten million measurements. Most of the continental data is based on the same gravity standard and datum as a result of the international gravity standardization program initiated in 1948 (Woollard 1950; Woollard and Rose, 1963).

However, measured gravity coverage is by no means complete. There are many large regions on the continents where gravity measurements are lacking or available only in sparse quantities. In the oceans, the situation is even worse because of the great areas involved, the fact that few ships are equipped with gravimeters, and the relatively few years in which it has been possible to have accurate navigation at sea as well as reliable gyrostablized shipboard gravimetric systems.

Obviously, 1° x 1° mean gravity anomalies cannot be obtained by averaging gravity measurements for the many large regions of the earth's surface where an insufficient number of gravity measurements are available. Some other approach must be used to obtain the best possible estimate of average gravity anomaly values for such regions.

Statistical extrapolations and the methods of satellite geodesy can be used to obtain approximate mean values for the gravimetrically unsurveyed areas. Since these methods have been discussed by other authors (see, for example, Kaula, 1966a, 1966b; Rapp, 1966) they will not be reviewed here.

Geophysical prediction using gravity correlation methods provides an attractive alternative to the statistical-satellite methods. With the geophysical methods, 1° x 1° mean gravity anomalies can be determined for any continental area whether or not gravity measurements have been made in that area. More specifically, the geophysical methods can improve predictions made by other methods where some gravity measurements are available, and can provide usable evaluated predictions where no gravity measurements exist. A unique feature of the geophysical approach is that the actual geological and geophysical causes of gravity anomalies are taken into account.

The fundamental premise of the geophysical methods is that gravity anomalies can be predicted using correlations with some combinations of earth parameter values which either are known or can

be readily determined. Parameters such as regional surface
elevation and age of the crust, for example, are related to
regional changes in gravity anomaly values. Local changes in
gravity anomalies are related to local changes in geology and
topography. Both types of relationships can be established
analytically or empirically and combined to predict gravity
anomalies which have considerable geodetic value.

The geophysical prediction methods are based on the concept
that the lithosphere, on a regional basis, is inherently weak and
in isostatic equilibrium with the underlying aesthenosphere.
However, these methods do not assume that zero isostatic and free
air gravity anomalies are associated with equilibrium conditions.
Indeed, Woollard and Strange (1966) have shown that zero free
air and isostatic anomalies are not to be expected, given a crust
of variable density and thickness, even under conditions of
perfect isostatic equilibrium. The recognition of these
constraints, which are a consequence of the proximity effect
obvious in the Newtonian expression for gravitational attraction,
makes it necessary to consider lithospheric structure and
composition either directly, as revealed by seismic refraction
and reflection deep soundings, or indirectly in the absence of
such data through standardized relations observed between
averaged gravity and regional elevation values in different
continental areas.

It must be recognized that the problem of mean gravity
anomaly prediction is not a simple one. The complex structure
and composition of the lithosphere which exists today has evolved
over a time span of a billion years or longer. Changing patterns
and locations of orogenic events have resulted in the creation of a
more heterogeneous mass distribution rather than a more homogeneous
one. Consider, for example, the effects of lithospheric subduction
and obduction at crustal plate boundaries. The resulting
mechanical displacements in plate mass, the selective melting of
mobile components in a deeper, hotter environment with the
subsequent intrusion, volcanism, thermal and pressure metamorphism
have led to uplift in the orogenic belts. Many such belts have
been eroded away and then buried under the detrital material of
younger orogenic belts. Yet, the root effects of the older belts
persist as mass anomalies in the crust. Consider also that the
spreading centers have shifted in location, have been displaced
along major transform faults, and even have been overridden by
migrating continental blocks, thereby generating abnormal crustal
and gravity relations.

In addition to the above effects, there have been prolonged
periods of worldwide volcanic activity (for example, during
Triassic-Jurassic time), periods of worldwide continental flooding
by the oceans (for example, during Cretacious time), and periods
of extensive worldwide glaciation and de-glaciation. In each
case, the resulting changes in surface mass distribution have
resulted in a differential vertical displacement of the

lithosphere and its boundary with respect to the underlying
aesthenosphere. The earth's crust does adjust for these
changes in mass distribution through the isostatic mechanism.
Such an adjustment, subsequent to the removal of the Pleistocene
ice caps in Europe and North America, can be observed in even the
short period of a decade by the rising of Fenno-Scandanavia and
eastern Canada as measured by repeated levelling. There is, thus,
a time lag between changes in surface mass distributions and the
achievement of isostatic equilibrium.

The effects of the time lag are also evident in the case of
the Rocky Mountains. Although the Rockies were base levelled in
Eocene to Miocene time, 17-40 million years before present time
(MYBP), they now stand 6000 feet or more above the surrounding
terrane. The much older Appalachian Mountains show remnant
peneplains of at least two such cycles of base levelling and
rejuvenation caused by the time lag in the isostatic adjustment
cycle.

The mechanism involved in isostatic adjustment is plastic
flow and viscous creep. This process is much slower than surface
erosion. Furthermore, isostatic adjustment involves total crustal
mass movement and momentum and not just surficial mass removal
and transfer as with surface erosion.

The combination of the earth responding differentially at
its surface to internal dynamic forces, with the attendant tectonic
and compositional changes in its outer layer, and adjusting
isostatically (but with an out of phase time lag) for changes in

surficial mass distribution causes isostatic equilibrium to be
only an average condition for the earth as a whole. Isostatic
equilibrium, thus, is not realized on a semi-continental or even
continental sized basis, and certainly not on a 1° x 1° sized basis.
Even where there is local isostatic equilibrium, it does not follow
that there will be zero free air and isostatic gravity anomalies.

Because of the above considerations, statistical approaches
to the prediction of gravity on a global basis do not have general
applicability. Rather, it has been necessary to use empirical
relations determined for application to specific regions. These
relations, in effect, take into account the complexity of the
underlying lithospheric structure and composition as well as the
geologic history of regions comprising the domains in which a
given empirical relation has general application. The present
study, therefore, incorporates a tacit recognition of the
complexities of lithospheric structure, composition, and response
to changes in surficial mass distribution. It is evident that
all these factors must be considered if gravity is to be predicted
with any degree of reliability.

Included in the present study are: (1) a review of the
geophysical methods which have proven to be the most effective in
predicting gravity anomaly values; (2) the writer's analysis as
to why these methods are effective; and (3) the writer's contributions
towards making these methods more reliable and exact.

Some recent studies have suggested that a combined statistical--geophysical approach to gravity prediction is highly desirable (Wilcox, 1971) especially if a single "best" prediction method can be developed (Lebart, 1972). However, because of the complexities of earth structure and geologic history, it is quite unlikely that a single "best" prediction method really exists. Indeed, there are a number of rather different geophysical prediction methods, each of which works well in some situations, poorly in others. Thus, it seems better to inject statistical rigor into each of the geophysical methods. This has been done insofar as possible.

The prediction of mean gravity anomaly values for areas smaller than $1° \times 1°$, e.g., $1' \times 1'$, $5' \times 5'$, is not considered in this study. Geophysical prediction of mean values for such small sized areas, in general, cannot be justified in terms of increased precision for the $1° \times 1°$ values obtained as averages of the smaller sized means. Prediction of the smaller sized means, per se, presents an entirely different and more complex set of problems than does prediction of $1° \times 1°$ means. The smaller sized means, for example, are extremely sensitive to very local topographic and geologic changes. Further, these changes seldom conform to any fixed grid system such as is generally used in $1° \times 1°$ prediction. Thus, each prediction for a small sized area has to be handled on an individual basis--a time consuming and costly process. Geophysical predictions certainly can be and are made for the small sized areas, when required, but the methods used are other than those contained in this study.

1.2 Gravity Correlations

Gravity correlations is the study and application of numerical interrelationships (i.e., correlations) between variations in the gravity anomaly field and corresponding variations in geological, crustal, and upper mantle structure, regional and local topography, and various other types of related geophysical data. Examples of well known gravity correlations are (1) the inverse relationship between regional elevation and regional Bouguer gravity anomalies, and (2) the association of local minimums in the gravity anomaly field with certain types of sedimentary basins.

Geophysical correlations, a term having a somewhat broader meaning than gravity correlations, is the study and application of numerical interrelationships between any set of geophysical parameters.

Gravity correlations draw upon many branches of earth science. Geology provides data pertaining to local geologic structure, rock density, and geotectonics. Geodesy provides methods for gravity reduction and analysis plus the theories of isostasy. Celestial mechanics, applied to artificial earth satellites, provides an indication of global scale density anomalies in the upper portions of the earth. Seismology provides knowledge of crustal and upper mantle structure. Cartography provides topographic maps giving elevation data. Magnetic anomaly data assists in the interpretation of geologic and crustal structure. Analysis of heat flow data provides additional insight into the intricacies of crustal and upper mantle structure.

Although the term, gravity correlations, is relatively new, gravity correlations relationships have been studied and used for

many years. Geologists, for example, have used variations in the
gravity anomaly field to assist in the interpretation of geologic
structure. Similarly, geophysicists have used the gravity anomaly
field as a tool in the interpretation of crustal and upper mantle
structure. The application of gravity correlations discussed in this
study are the reverse of these "classical" uses. Here, known geologic
and crustal structure is used to predict the gravity anomaly field.

1.3 Gravity Prediction

The term, gravity prediction, has been used in the literature
to denote any process which enables the estimation of a gravity anomaly
value (1) for any point (i.e., site) at which the acceleration of
gravity has not been measured, or (2) which represents the average
gravity anomaly value within a given surface area--whether or not
the acceleration of gravity has been measured at points within
that surface area. Thus, gravity prediction may involve interpolation,
extrapolation, or both.

As used in this study, gravity prediction refers to the
application of gravity correlation methods to estimate $1^\circ \times 1^\circ$ mean
gravity anomaly values for continental regions of the earth's surface,
especially those regions which contain a few or no gravity measurements.

Gravity prediction using gravity correlations generally involves
(1) an analysis of the numerical interrelationships between the gravity
anomaly field and geological, geophysical, and topographic data within
regions of the earth's surface where variations in the gravity anomaly
field are well defined by gravity observations, and (2) application

of appropriate correlations determined by (1) to predict gravity anomaly
values for 1° x 1° areas within regions of the earth's surface where
gravity measurements are lacking or available only in sparse
quantities. Geologic, geophysical, and topographic data is generally
available in sufficient quality and quantity to support gravity
predictions using gravity correlations in most continental areas.

Gravity correlation technology has advanced steadily over the
past few years, and gravity predictions now can be made for any
continental 1° x 1° area. Remarkably accurate results are obtained
in many instances, although uniformly reliable predictions cannot be
made in all situations where gravity measurements are lacking. In
the latter case, however, gravity correlation produced 1° x 1° mean
anomaly predictions always provide a usable approximation of the true
value--probably the best estimate of the 1° x 1° mean gravity anomaly
field for regions in which gravity measurements are not available.

1.4 Gravity Interpolation

Gravity interpolation is any process which enables the estimation
of gravity anomaly values for points or areas located between or
among sites of gravity observations. Gravity interpolation by gravity
correlations is most often used to densify a field of existing gravity
anomaly values during a gravity prediction operation.

2. HISTORICAL BACKGROUND

The basic principles of gravity correlations have been used for
many years in geophysical exploration studies and in the interpretation
of geologic structure. Paving the way for later gravity prediction
applications was the work of George P. Woollard who, in the
1930-1960 time period, published many careful and extensive
analyses of the geological and geophysical accountability of gravity
anomaly variations.

The specific application of gravity correlations to gravity
prediction is a comparatively recent development. Pioneering
the geophysical gravity prediction movement was William P. Durbin, Jr.
(1961a, 1961b, 1966) who first suggested the possibility of
estimating gravity anomaly values using gravity--geology
correlations, then demonstrated the feasibility of the idea by
constructing gravity anomaly maps based upon geologic evidence
for the south central United States.

The earliest known application of geologic data to evaluate
and predict $1^\circ \times 1^\circ$ mean gravity anomalies is the work of
Pothermel et al. (1963).

Geophysical data was added to geologic data as a basis for
gravity prediction by George P. Woollard (1962) who published
a document which has come to be regarded as a fundamental gravity
correlations reference manual. Since then, Woollard and his
associates at the University of Hawaii have published several

additional works giving further development to gravity correlations as a method of gravity analysis, interpolation, and prediction (Strange and Woollard, 1964a; Woollard, 1966, 1968b, 1968c, 1969a).

Practical methods for prediction of 1° x 1° mean gravity anomalies using gravity correlations first appeared in 1964. At the USAF Aeronautical Chart & Information Center (ACIC), now the Defense Mapping Agency Aerospace Center (DMAAC), Rothermel (1964) developed a number of methods including the original version of the GRADE interpolation and prediction technique. At the University of Hawaii, Strange and Woollard (1964b) proposed a method which was to be the forerunner of the NOGAP prediction technique and demonstrated its reliability in the United States. A modified version of the technique (GAPFREE) was published two years later (Woollard and Strange, 1966). The original version of the GAIN interpolation method was described by Strange and Woollard (1964a) and applied in Wyoming with good success.

The NOGAP prediction method has been applied with modifications by Woollard and his associates to geophysically predict and evaluate mean gravity anomalies for East Asia (Woollard and Fan, 1967), Mexico (Woollard, 1968a), and Europe (Woollard, 1969b). Much of the gravity correlation research and mean anomaly prediction work of the University of Hawaii has been done under contract to ACIC and DMAAC.

In 1966, a gravity correlations working group was established at ACIC. This group under the direction of the writer further developed and refined the geophysical prediction methods, and

began a program to use these methods to systematically predict
1° x 1° mean gravity anomalies for all continental and oceanic
areas which contain few or no gravity measurements. The group
also investigated the use of geophysical methods for gravity
interpolation (Wilcox, 1967) and for prediction of mean anomalies
to represent large sized surface areas (Wilcox, 1966). Other
major contributions of the group include the standardization of
geophysical gravity prediction techniques (Wilcox, 1968), the
development of the EXGAP prediction procedure by L. E. Wilcox in
1968 (revised in 1973), and the development of the UNGAP method
by J. T. Voss in 1972.

By 1971, the ACIC group had completed predictions for the
entire Eurasian continent. This work was published in the form
of a Bouguer gravity anomaly map (USAF ACIC, 1971a; Wilcox et al.,
1972) and a geoid (Durbin et al., 1972). The mean anomalies
were also made available in the form of a mean gravity anomaly
tabulation (USAF ACIC, 1971b). Predictions for all of Africa
and South America were completed in 1973 and published in the
form of Bouguer anomaly maps (Slettene et al., 1973; Breville
et al., 1973). Work is continuing at DMAAC to complete 1° x 1°
mean anomaly predictions for other continental areas and, in
conjunction with the University of Hawaii, to develop geophysical
prediction techniques suitable for application in oceanic areas
(Woollard and Daugherty, 1970, 1973; Khan et al., 1971; Woollard
and Khan, 1972; Daugherty, 1973; Woollard, 1974).

A multiple regression approach, in which several geophysical correlations are combined to predict gravity anomalies, has been tested successfully in the United States, Western Europe, and Australia by Vincent and Strange (1970).

Free air anomaly maps compiled using observed and geophysically predicted anomalies have been published by Strange (1972).

It is especially gratifying to note that in the past two or three years, there has been a general birth of interest among geodesists in the geophysical accountability of gravity variations. In fact, no less than cne-third of the sessions at the International Symposium on Earth Gravity Models, held at St. Louis on August 16-18, 1972, were devoted to geophysical problems. A portion of the new interest in "geophysical geodesy" has been generated, no doubt, by the new theory of plate tectonics--which has had an overall unifying effect on the earth sciences. However, part of the interest must be attributed to the gravity correlation pioneers of the early 1960's who paved the way for making geophysics an integral part of geodesy.

3. THEORETICAL BACKGROUND

3.1 Observed Gravity

The acceleration of gravity at any discrete point on the physical surface of the earth is generated by all of the masses contained within the real earth. The value for the acceleration of gravity at any surface point, obtained by suitably adjusted and corrected gravity measurements, is known as "observed gravity," g_o. For the purposes of gravity prediction, observed gravity, as obtained by modern land gravity measurements, may be considered to be error free.

The existence of mountains, ocean basins, and other topographic structures is direct evidence that the masses within the earth are irregularly distributed at the surface, and interpretations of seismic data have provided indirect evidence of the existence of irregularities in mass distribution within the earth's interior. These mass distribution irregularities must be the source of the irregular variations which are found in the earth's observed gravity field.

3.2 Normal Gravity

Normal gravity is a computed value which refers to the surface of the normal earth, i.e., the normal ellipsoid chosen to represent the earth. Values of normal gravity vary as a regular function of latitude only. The overall magnitude of the normal gravity field depends upon constants which express the size, shape, and rate of rotation of the normal ellipsoid.

The normal gravity field represents the attraction of an idealized fluid earth whose masses are assumed to be in complete equilibrium and symmetrically distributed with respect to the rotation axis and equator. The mass of the normal earth is, by definition, equal to the mass of the real earth. Such a model is geophysically reasonable and will generate the regular normal gravity field. An exact structure-density model of the normal earth is of no great interest either to geodesy or geophysics and, in fact, an exact geophysically reasonable model of the normal earth has never been derived.

3.3 Gravity Anomaly

3.3.1 Geodetic Definition

A gravity anomaly is the difference between the observed gravity and normal gravity at a given location. In classical geodetic applications, the point of comparison is the point on the geoid directly below the point where gravity is observed. The method used to reduce the observed value of gravity to an equivalent value at sea level (on the geoid) determines the type of gravity anomaly obtained.

$$\Delta g = (g_o + \delta g_o) - \gamma \qquad (3.3\text{-}1)$$

where

Δg = gravity anomaly

g_o = observed gravity on the physical surface of the earth at elevation $h = h_o$

h = the orthometric height above sea level

γ = normal gravity computed on the ellipsoid directly below

the point at which gravity is observed

δg_O = reduction applied to gravity observed at elevation

$h = h_O$, to obtain an equivalent value at sea level,

$h = 0$

Note that observed gravity is reduced to a point on the geoid and normal gravity is computed at a point on the ellipsoid. In general, the two points do not coincide and this fact is of some importance to geodesy. However, for geophysical analysis purposes, the point of comparison for both quantities is assumed to be located on the geoid.

Application of the reduction, δg_O, actually accomplishes two physical operations by the computation: (1) all earth mass above sea level is either moved inside of the geoid (e.g., free-air reduction, isostatic reduction) or removed entirely (e.g., Bouguer reduction), and (2) the observed gravity value is lowered from the physical surface to sea level. The physical significance of this two step operation is that no mass remains outside of the point of comparison after δg_O is applied, i.e., there is no gravitational component directed upward.

3.3.2 Geophysical Definition

Being the difference between the observed and normal values of gravity, a gravity anomaly must reflect the difference between the true and normal mass distributions within the earth.

$$\Delta g = M_T - M_N \qquad (3.3-2)$$

where

M_T = the anomalous mass distribution within the real earth

M_N = the regular mass distribution within the normal earth

When the regular normal gravity field is subtracted from the irregular observed gravity field, the remainder--the gravity anomalies--are essentially just the irregularities in the observed gravity field caused by the anomalous mass distribution within the real earth. Application of the reduction, δg_o, in computing the gravity anomalies superimposes certain additional effects onto those caused by the mass distribution irregularities. One effect of the Bouguer reduction, for example, is that the irregularities in observed gravity caused by local topographic variations are filtered out. The nature of the superimposed effects depends upon the properties of the type of reduction used.

3.4 Global, Regional, and Local Gravity Anomaly Variations

Analysis of the gravity anomaly field with respect to its regional and residual components, a technique used extensively in geophysical exploration (geophysical prospecting) work, has proven to be very convenient for gravity correlation studies and, thus, has been adopted in the NOGAP and other geophysical gravity anomaly prediction methods. Because of a basic difference in definition, however, the term "local" replaces the term "residual" for gravity prediction application.

The purpose of regional-local (or regional-residual) separation always is to isolate elements of the gravity anomaly field which can be interpreted with respect to particular geological

or geophysical elements. In the case of geophysical exploration applications, only the residual gravity anomaly variations are of practical interest. Both components are important for geophysical gravity prediction.

The many methods of regional-residual separation which have been proposed for geophysical prospecting purposes (see, for example, Agocs, 1951; Nettleton, 1954; and Simpson, 1954) all involve a smoothing of the gravity anomaly field according to some mathematical or graphical criteria. The smoothed field is interpreted as the regional component and the difference (i.e., residual) between the gravity anomaly field and the smoothed field is taken as the residual component. The degree of smoothing applied varies depending upon the criteria chosen and, as a result, the process of regional-residual separation is highly subjective.

For gravity prediction purposes, regional gravity anomaly variations are defined to be that portion of the gravity anomaly variations caused by mass distribution irregularities in the crust and by regional topography and the degree of its isostatic compensation. Prediction of regional gravity effects, therefore, is based upon correlation between regional topography and regional gravity with due consideration being given to isostatic effects, and by analysis of the gravitational effects of regional changes in crustal structure.

Superimposed upon the regional variations are the local variations defined to be that portion of the gravity anomaly variations caused by mass distribution irregularities in nearby (local) surface geologic structure and by local topography.

Prediction of the local gravity effects, then, is a function of changes in surface geology as well as correlations between local topography and local gravity.

Although the boundary between regional and local gravity anomaly variations is defined carefully for geophysical prediction methods, some logical decisions are still necessary with respect to whether a particular structure contributes to the gravity anomaly field in a regional or local sense. It can be argued, for example, that a large sedimentary basin which extends over several $1^\circ \times 1^\circ$ areas is, in fact, a regional structure. However, in some prediction methods the gravitational effect of such basins is most conveniently predicted in terms of its local perturbations on a regional field defined by a basic predictor. Hence, the gravity anomaly effect of sedimentary basins is considered to be local for such methods.

In addition to the local and regional gravity anomaly variations discussed in the preceding paragraphs, there are also longer period or global variations. A gravity anomaly representation obtained by harmonic analysis of the perturbations of artificial earth satellites shows only the longer period or global variations. To date, these global variations have been correlated with known structural variations only in a qualitative sense. Kaula (1969, 1970), for example, suggests that, with some exceptions, global positives tend to be correlated with active tectonic departures from equilibrium which, in turn, are correlated with areas of current dynamic activity at the earth's surface and reflect internal

dynamic activity. At present, these internal processes are not sufficiently understood to enable their use for prediction of global gravity variations. Fortunately, it hardly seems necessary to develop a geophysical method to predict the longer period variations _per se_ since the global gravity fields derived from satellite perturbation analysis can be used for this purpose.

Woollard and Khan (1972) have confirmed the desirability of analyzing the gravity anomaly field in terms of three components: (1) a short wavelength component depending upon local topography, local geology, and their mode of emplacement; (2) an intermediate wavelength component depending upon regional topographic and tectonic patterns and their isostatic compensation, and (3) a long wavelength component depending upon global scale morphological and tectonic patterns. Table 3-1 compares this three component scheme to the classical two component scheme, the latter being modified to include the global component. The two schemes are seen to be completely compatible. In current geophysical prediction methodology, however, the global and regional contributions to the gravity anomaly are predicted as a single component.

3.5 Mean Gravity Anomalies

3.5.1 Geodetic Uses

Gravity is measured and gravity anomalies are computed at discrete points on the surface of the earth. Yet, the integral formulas used for most geodetic applications require a knowledge of

TABLE 3-1

COMPARISON OF GRAVITY CORRELATION

ANOMALY ANALYSIS SCHEMES

Expanded Classical Gravity Analysis System	Woollard-Khan Gravity Analysis System
Local - near surface geologic structure - local topography	Short Wavelength - local topography - local geology - mode of emplacement
Regional - crustal structure - regional topography - degree of isostatic compensation	Intermediate Wavelength - regional topography - regional tectonic patterns - isostatic compensation
Global - geodynamic processes - mantle structure	Long Wavelength - global morphology - global tectonic patterns

gravity anomaly data continuously over the whole earth. Examples of these integral formulas are (Heiskanen and Moritz, 1967)

$$N = \frac{R}{4\pi G} \int\!\!\int_{\sigma} \Delta g \; S(\psi) \; d\sigma$$

$$\left.\begin{array}{c} \xi \\ \\ \\ \eta \end{array}\right\} = \frac{1}{4\pi G} \int\!\!\int_{\sigma} \Delta g \; \frac{dS}{d\psi} \left\{\begin{array}{c} \cos\alpha \\ \\ \\ \sin\alpha \end{array}\right\} \; d\sigma \qquad (3.5\text{-}1)$$

$$\left.\begin{array}{c} \overline{a}_{nm} \\ \\ \\ \overline{b}_{nm} \end{array}\right\} = \frac{1}{4\pi} \int\!\!\int_{\sigma} \Delta g \; \overline{P}_{nm} \; (\sin\phi) \left\{\begin{array}{c} \cos m\lambda \\ \\ \\ \sin m\lambda \end{array}\right\} \; d\sigma$$

where

N = gravimetric geoid height

ξ, η = gravimetric deflection of the vertical components

$\overline{a}_{nm}, \overline{b}_{nm}$ = fully normalized harmonic coefficients of degree, n, and order, m, for an earth gravity model

Δg = gravity anomaly representing the differential surface element, $d\sigma$

$S(\psi)$ = Stokes' function

$\overline{P}_{nm} (\sin\phi)$ = fully normalized Legendre's associated function

α, ψ = Spherical polar coordinates

ϕ, λ = Geodetic latitude and longitude

R, G = constants

$\int\!\!\int_{\sigma}$ denotes integration over the whole earth

For practical evaluation of the integral formulas (3.5-1) summation over finite surface elements replaces the integration over differential elements. Therefore, in the practical case, the gravity anomaly input must be in the form of values which represent finite surface areas, e.g., 5' x 5', 1° x 1°, etc Mean gravity anomalies, predicted as a function of the gravity anomalies computed from measurements at discrete points over the surface, serve as the required input data.

3.5.2 Definition: Comments on Prediction Methods

A mean gravity anomaly is defined as the mean value of the gravity anomaly field within a specified surface area. A 1° x 1° mean Bouguer anomaly, for example, is the average value of an infinite number of Bouguer anomalies computed at measurement sites which are evenly distributed throughout the 1° x 1° area.

The rigorous formula for 1° x 1° mean gravity anomaly, $\overline{\Delta g}$, which represents a rectangular 1° x 1° surface area with dimensions a and b is (Heiskanen and Moritz, 1967)

$$\overline{\Delta g} = \frac{1}{ab} \int_{x=0}^{a} \int_{y=0}^{b} \Delta g\,(x,\,y)\,dxdy \qquad (3.5\text{-}2)$$

where the gravity anomaly, $\overline{\Delta g}$, must be known at every point $(x,\,y)$ within the 1° x 1° area. If the $\Delta g\,(x,\,y)$ are free air anomalies, $\overline{\Delta g}$ is a 1° x 1° mean free air anomaly. If the $\Delta g\,(x,\,y)$ are Bouguer anomalies, $\overline{\Delta g}$ is a 1° x 1° mean Bouguer anomaly.

Since gravity is measured at only a finite number of discrete points within any surface area, equation (3.5-2) never can be evaluated in the given form. Instead, the $1° \times 1°$ mean anomaly, $\overline{\Delta g}$, can be approximated by a linear combination of the measured values, Δg_i (Heiskanen and Moritz, 1967)

$$\overline{\Delta g} = \sum_{i=1}^{n} \alpha_i \Delta g_i \qquad (3.5-3)$$

The coefficients, α_i, which depend only upon the relative positions of the gravity measurements and mean anomaly value, may be chosen in several ways. In least squares (statistical) prediction, for example, the α_i are determined so that the standard error of prediction is minimized. With a large value of n for gravity measurements well distributed throughout the $1° \times 1°$ area, setting all values of $\alpha_i = 1/n$ gives the required mean value.

$$\overline{\Delta g} = \frac{1}{n} \sum_{i=1}^{n} \Delta g_i \qquad (3.5-4)$$

Formula (3.5-4) applies to Bouguer anomalies in continental areas. If free air anomalies are used within the continents, a correction must be added to (3.5-4) to account for the difference between the mean elevation, $\overline{H}$, of the area and the average, $\overline{h}$, of the elevations at the points where Δg_i is observed. The correction is computed using equation (3.6-25) where $(\Delta g_F)_Q$ represents the average of the observed free air anomaly values, $(\Delta g_F)_P$ represents the true $1° \times 1°$ mean free air anomaly, and $\delta h = \overline{H} - \overline{h}$.

With fewer measurements and/or uneven distribution of measurements within a surface area, an isoanomaly map can be constructed using linear interpolation, modified by geological considerations, of the Bouguer anomalies. Then the integration (3.5-2) can be performed graphically with reference to the Bouguer anomaly map. Some additional Bouguer anomaly values may be obtained by gravity correlation interpolation between measurement sites to supplement the measured values used to construct the gravity anomaly contours. The GRADE prediction method uses this approach.

The $1^\circ \times 1^\circ$ mean gravity anomalies also may be predicted with direct reference to correlations between variations in geological/geophysical/topographic parameters and the corresponding variations in mean gravity anomaly values. In this case

$$d\overline{\Delta g} = f(d\overline{h}, d\overline{S}) \qquad (3.5-5)$$

where $f(d\overline{h}, d\overline{S})$ is some function of topographic and structural changes, respectively. If, for example, the changes in the regional part of the $1^\circ \times 1^\circ$ mean gravity anomalies are constant with respect to changes in mean elevations, which is true for $1^\circ \times 1^\circ$ mean Bouguer anomalies and mean elevations in many regions, then

$$\frac{d\overline{\Delta g}}{d\overline{h}} = \beta \qquad (3.5-6)$$

or, in a slightly modified form,

$$d\overline{\Delta g} = \beta \, d\overline{h} \qquad (3.5-7)$$

Integration of the above gives, immediately,

$$\overline{\Delta g} = \beta\ \overline{h} + \alpha \qquad (3.5\text{-}8)$$

which is the equation for the basic predictor in the NOGAP
prediction method. Equations such as $(3.5\text{-}5)$ and $(3.5\text{-}8)$ can
be defined in portions of an area having uniform regional structure
and adequate gravity measurements, and used as prediction functions
in other portions of the same area which contain little or no
measured gravity data.

Although geophysical constraints are sometimes
included in the formulations, statistical mean anomaly prediction
procedures, using equations such as $(3.5\text{-}3)$ typically are based
primarily upon an expression of the manner in which the gravity
anomaly field varies with respect to itself within a given region.
To simplify the mathematical expressions involved, such variations
are assumed to be isotropic when, in reality, they usually are
not. The invalidity of this assumption appears to place a severe
constraint on the applicability of statistical prediction.

By contrast, although statistical procedures are often
used in the fomulations, geophysical mean anomaly predictions, using
equations such as $(3.5\text{-}8)$, are based primarily on expressions of
the manner in which the gravity anomaly field varies with respect
to some other physical parameter within a structurally homogeneous
region.   Such variations usually _are_ isotropic, and this fact
strengthens the validity of the geophysical prediction methods.

3.5.3   Mean vs. Point Anomalies

Point gravity anomalies fully reflect all effects of regional and local variations in earth structure. Mean gravity anomalies which represent surface areas of 1° x 1° or larger, on the other hand, are essentially regional anomalies since much (but not all) of the effect of local structural variations is lost in the averaging process which produces the mean anomaly. A local mass anomaly of small areal extent, such as an ultra-basic dike, may have a pronounced local effect upon a point anomaly, but virtually no effect upon a 1° x 1° mean anomaly. Larger local geologic features, such as sedimentary basins, will affect both point and mean anomalies in a similar (but not identical) way. Local anomaly effects, therefore, must be analyzed specifically with respect to the type of anomaly, point or mean, which is being considered.

Thus, the details of local gravity anomaly variations must be studied in terms of point anomalies, whereas the regional gravity variations are conveniently analyzed in terms of the mean gravity anomalies. In fact, the regional anomaly field reflected in 1° x 1° mean anomaly values is contaminated only by the effects of fairly broad local structural variations. It is the gravitational effects of these broad local variations which must be determined in 1° x 1° mean anomaly predictions.

3.5.4 Mean Elevation

The elevation value corresponding to the mean gravity
anomaly (3.5-2) is the mean elevation, $\overline{H}$, given by

$$\overline{H} = \frac{1}{ab} \int_{x=0}^{a} \int_{y=0}^{b} h(x, y) \, dxdy \qquad (3.5-9)$$

where h is the elevation at every point (x, y) within the area.
Mean elevations are determined by graphical integration from
topographic maps.

3.6 Free Air Anomaly

3.6.1 Complete Free Air Reduction*; Simple Free Air Reduction

Two steps are necessary to obtain a theoretically
correct free air gravity anomaly, Figure 3-1. Firstly, all masses
above sea level are "condensed" vertically to form an infinitesimally
thin surface mass which is placed just underneath the geoid. The
density, κ, of this surface mass at any point, Q, vertically
beneath the point, P, on the physical surface, is given by

$$\kappa = \sigma h \qquad (3.6-1)$$

---

*The non-standard terminology, "complete free air reduction," is
used for descriptive clarity. The type of complete free air
reduction described here is attributed to Helmert and is usually
called Helmert's condensation reduction.

where

h is the elevation of P above sea level

σ is the average density of the topographic masses between

P and Q.

At the completion of the first step, the topographic masses have been removed, an equivalent mass has been inserted at elevation h=0 in the form of a surface layer, and a gravity observation at point P is now situated "in free air" at an elevation, h, above sea level. In the second step of the complete free air reduction, the gravity observation is lowered "through free air" to sea level.

The gravitational effects of both steps are determined computationally and combined to obtain the complete free air reduction, $(\delta g_0)_F$.

$$(\delta g_0)_F = - g_T + g_S + g_F \qquad (3.6-2)$$

where

g_T = gravitational attraction at P of the volume mass constituting the topography which is removed in step 1.

g_S = gravitational attraction at P of the surface mass which is inserted just under the geoid in step 1.

g_F = free air correction, step 2, which lowers the observation from P to sea level at Q.

Except for areas of very rugged topography, the gravitational effect of the surface layer is very nearly equal to the gravitational attraction of the topography. Therefore, with good approximation

FIGURE 3-1

ILLUSTRATION OF COMPUTATIONAL STEPS NECESSARY

TO OBTAIN THEORETICALLY CORRECT

FREE AIR ANOMALY

TOPOGRAPHIC MASSES SHADED

Point, P, on physical surface
Point, Q, vertically below P on geoid surface

STEP 1. Remove topographic masses completely.
Point, P, now situated in free air at elevation, h, above geoid.

STEP 2. Lower observed gravity value through free air to sea level.
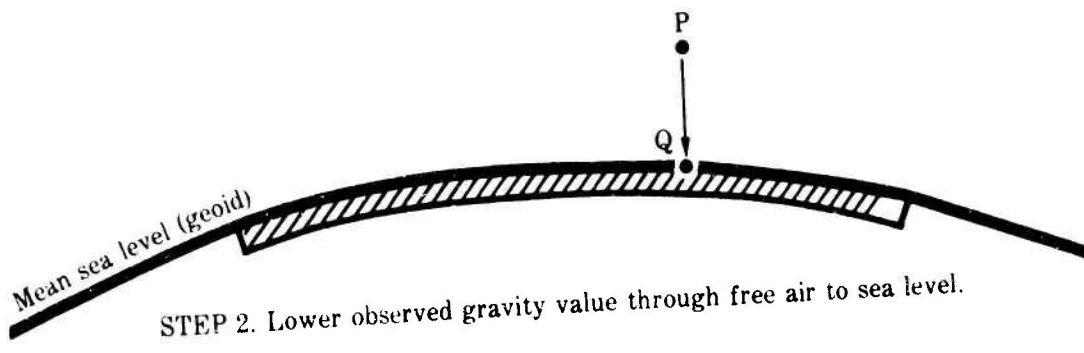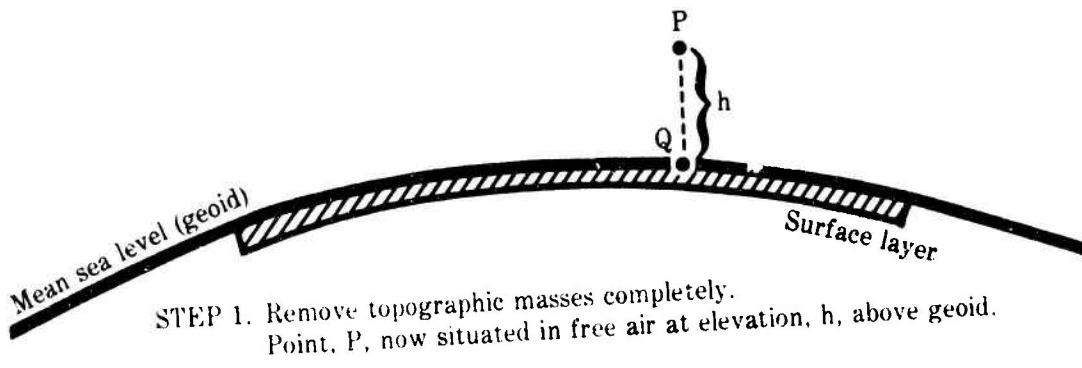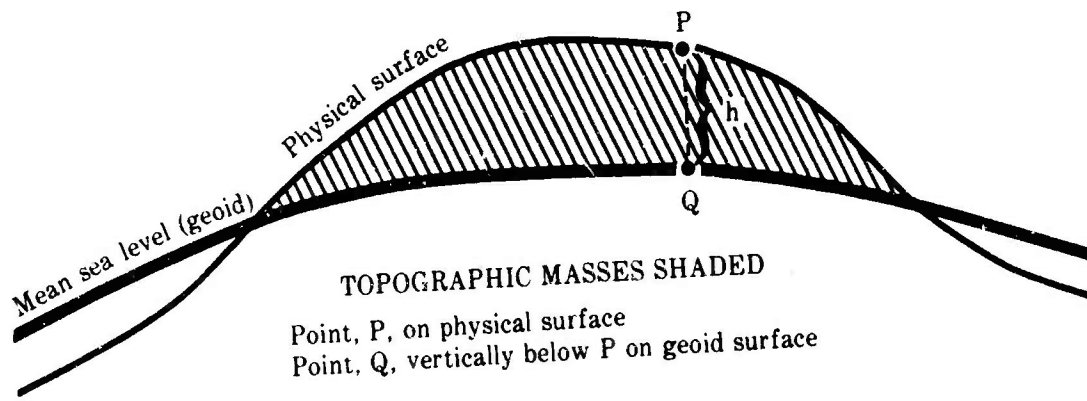
for most cases, the assumption

$$g_P = g_Q \qquad (3.6-3)$$

is made and equation (3.6-2) reduces to the simple free air reduction

$$(\delta g_0)_F = g_F \qquad (3.6-4)$$

and inserting (3.6-4) into (3.3-1), the simple free air gravity anomaly, Δg_F, is given by

$$\Delta g_F = g_0 + g_F - \gamma \qquad (3.6-5)$$

3.6.2 Free Air Correction

The free air correction gives the difference between gravity at the point P on the earth's physical surface where gravity is observed and at the point Q on the geoid, where Q lies vertically beneath P at a distance, h. It is assumed that no rock matter exists between P and Q, Figure 3-1, step 2.

Under the condition that no matter lies between P and Q, gravity and its derivatives of all orders exist and vary as continuous functions of elevation between these points. Therefore, the necessary conditions are fulfilled for application of the Taylor (Maclaurin) Series

$$g (z) = g (0) + g' (0) z + \tfrac{1}{2} g'' (0) z^2 + \ldots \qquad (3.6-6)$$

where the primes indicate differentiation.

In the present case, $g (z) = g_P$, gravity observed at elevation h; $g (0) = g_Q$, gravity at sea level, $h = 0$; and $z = -h$ where the negative sign is required because elevation increases outward while gravity increases inward. With these definitions

the series (3.6-6) becomes

$$g_P = g_Q - \frac{\partial g}{\partial h} h + \frac{1}{2} \frac{\partial^2 g}{\partial h^2} h^2 - \cdots \qquad (3.6-7)$$

or, solving for gravity at the geoid

$$g_Q = g_P + \frac{\partial g}{\partial h} h - \frac{1}{2} \frac{\partial^2 g}{\partial h^2} h^2 + \cdots \qquad (3.6-8)$$

The quadratic term of (3.6-8) contributes 726×10^{-10} h^2 mgals/meter. This amounts to less than one mgal unless gravity is observed at elevations in excess of 12,000 feet above sea level. Therefore, the quadratic term is always omitted except when gravity is observed in the highest mountains.

Evaluation of the linear term of (3.6-8) requires a knowledge of the vertical gradient of gravity, $\partial g/\partial h$, which varies as a function of latitude, height, and near surface mass distribution. However, the variation is sufficiently small to enable the use of a constant value for $\partial g/\partial h$ for many practical purposes (Heiskanen and Moritz, 1967). To obtain this constant, consider Newton's law of gravitation for a normal spherical earth

$$\gamma = \frac{km}{r^2} \qquad (3.6-9)$$

where

γ = normal gravity

k = gravitational constant

m = mass of the earth

r = radius of curvature of the normal earth

The vertical derivative of (3.6-9) is

$$\frac{\partial \gamma}{\partial h} \approx \frac{\partial \gamma}{\partial r} = -\frac{\partial}{\partial r}\left(\frac{km}{r^2}\right) = \frac{2km}{r^3} \qquad (3.6\text{-}10)$$

where the negative derivative is used because elevation, h, is positive outward while normal gravity is positive inward. Substituting (3.6-9) into (3.6-10) leaves

$$\frac{\partial \gamma}{\partial h} = \frac{2\gamma}{r} \qquad (3.6\text{-}11)$$

Insertion of average values for γ and r into (3.6-11) gives the constant value

$$\frac{\partial \gamma}{\partial h} \approx \frac{\partial g}{\partial h} = + 0.3086 \text{ mgal/meter} \qquad (3.6\text{-}12)$$

Detailed discussions of more exact expressions for $\partial g/\partial h$, and of the approximations involved in obtaining the constant value (3.6-12) may be found in Heiskanen and Moritz, 1967, and Bomford, 1971.

The final form for the free air correction, using only linear terms of (3.6-8) with (3.6-12) is

$$g_F = g_Q - g_P = \frac{\partial g}{\partial h} h = 0.3086 \text{ h} \qquad (3.6\text{-}13)$$

where h is in meters. Insertion of (3.6-13) into (3.6-5) gives, for the simple free air anomaly

$$\Delta g_F = g_0 + 0.3086 \text{ h} - \gamma \qquad (3.6\text{-}14)$$

3.6.3 Geophysical Properties of the Free Air Anomaly

Observed gravity corrected to sea level by the free air reduction, $(g_0 + g_F)$, measures the force of gravity generated by the real earth and includes all gravitational effects of (1) the

topographic masses and (2) the other lateral density variations within the real earth. Normal gravity, γ, measures the force of gravity generated by the normal earth which has neither topographic masses nor irregular density variations. Yet the total mass of the normal earth which generates γ is defined as being equal to the total mass of the real earth which generatec $(g_0 + g_F)$. Therefore, the free air anomaly computed according to (3.6-5)

$$\Delta g_F = (g_0 + g_F) - \gamma$$

is simply a measure of all gravitational differences between the irregular mass distribution within the real earth and the regular mass distribution within the normal earth.

3.6.3.1 Isostasy and the Free Air Anomaly

The topographic masses, condensed onto the geoid sufface of the real earth by the free air reduction, unquestionably represent a gross excess of mass with respect to the normal sea level earth which has no mass above sea level. Consequently, there ought to be a strong direct correlation between elevation and the free air gravity anomaly and in fact, such a correlation does exist in most areas--but only on a local basis. On a regional basis there is, at best, only a mild correlation between elevation and free air anomaly. In fact, free air anomaly values for gravity observations located on broad regional topographic features, such as plateaus, tend to average near zero and, on a global basis, the most probable free air anomaly value is zero.

The lack of any strong regional correlation
between elevation and free air anomaly means that, on a regional
basis, the mass excess due to topography must be nearly cancelled
out, i.e., isostatically balanced, by some compensating mass
deficiency within the real earth.

On a global basis, isostatic compensation
of the topographic masses is nearly complete. Regionally, however,
the gravitational balance usually is not exact. Since regional
departures from isostatic balance are fully reflected in regional
free air anomaly values, the effects of regional structures on the
free air gravity anomaly field always must be considered with
respect to the degree of isostatic compensation which exists
within the region.

The existence of a strong local correlation
between free air anomaly and elevation suggests that local topographic
variations and, hence, local density variations of any type are
either very poorly compensated or not compensated at all. In other
words the full gravitational effects of local topographic and
structural variations are reflected in local free air anomaly
variations without reference to compensation effects.

The wisdom of analyzing free air gravity
anomalies with respect to their regional and local components
should be immediately evident from the foregoing paragraphs.

Note, incidentally, that computation of the
free air anomaly using (3.6-14) involves no assumptions about
either rock density or the nature of the isostatic mechanism.

Therefore, use of the free air anomaly provides substantial freedom
in the interpretation of geological and geophysical structures
which produce the anomaly. Such freedom is not possible with the
isostatic anomaly forms which are computed with respect to rock
density assumptions and tied to earth structural models both
of which are now known to be incorrect.

The foregoing advantage of free air anomalies
is, to a major degree, offset by a disadvantage which is particularly
troublesome in mountainous areas, namely, the extreme sensitivity
of free air anomalies to local elevation changes and the consequent
masking of local geologic effects.

3.6.3.2 Local Variations in the Free Air Anomaly

The specific nature of the variations of
the free air anomalies within a local area depends largely upon
the topographic characteristics of that area.

With flat to low surface relief, the free
air anomalies tend to have small magnitudes and are as likely to
be positive as negative. Any local variations in the free air
anomalies within such localities are caused by uncompensated
local geologic variations. Local positives, for example, may
reflect higher density rocks or structural uplifts which bring
higher density rocks nearer to the surface. Conversely, local
negatives may reflect lower density rocks or structural depressions
which cause higher density rocks to be a greater distance from
the surface and/or which are filled with low density sediments.

With moderate to high surface relief, the
free air anomalies are directly correlated with uncompensated local
topographic variations, being highly positive on mountain peaks
and strongly negative in deep valleys. The dominant topographic
effects in such localities mask any free air gravity anomaly
variations caused by local geologic variations.

Consider Figure 3-2. If (1) the topographic
rise under point P is completely compensated, i.e., the positive
gravitational effect of the mass excess due to the hill is
cancelled out by the negative gravitational effect of some
compensating mass deficiency at depth, and (2) there are no other
lateral mass distribution variations between the points, P and Q,
then the free air anomaly at P should equal that at Q

$$(\Delta g_F)_P = (\Delta g_F)_Q \qquad (3.6\text{-}15)$$

or, using (3.6-14)

$$(g_0)_P - \gamma_P + 0.3086\, h_P = (g_0)_Q - \gamma_Q + 0.3086\, h_Q \quad (3.6\text{-}16)$$

Define the unreduced surface gravity anomaly,
Δg_S, to be given by

$$\Delta g_S = g_0 - \gamma \qquad (3.6\text{-}17)$$

where γ is interpreted to function merely as a latitude correction
term to remove the systematic effects of the earth's flattening
from observed gravity. Thus, Δg_S applies at the point on the
physical surface where g_0 is measured, and variations in Δg_S
are tantamount to variations in observed gravity.

Using the above definition of Δg_S, equation (3.6-16) becomes

$$(\Delta g_S)_P = (\Delta g_S)_Q - 0.3086 \; \delta h \qquad (3.6-18)$$

where

$(\Delta g_S)_P = (g_0)_P - \gamma_P$ = unreduced surface anomaly at P

$(\Delta g_S)_Q = (g_0)_Q - \gamma_Q$ = unreduced surface anomaly at Q

h_P = elevation at P

h_Q = elevation at Q

$\delta h = h_P - h_Q$

Equation (3.6-18) can hold only if the topographic feature at P is a regional structure such as a broad plateau. Woollard (1962) maintains that topographic features must be about $3^\circ \times 3^\circ$ or larger in lateral extent in order to be completely compensated--as was assumed in deriving (3.6-18).

If the hill under point P is a local topographic feature, it must be treated as being totally uncompensated or nearly so. This is true because, as shown by Woollard (1962) and Strange and Woollard (1964), the gravitational effect of the topography always greatly exceeds that for the compensation for local features. This is confirmed by Jeffreys (1970) who states that a topographic variation of small areal extent will have the same effect on free air gravity whether the variation is compensated or not, namely, approximately the simple Bouguer plate effect. This relation will now be derived.

42

FIGURE 3-2

TOPOGRAPHIC VARIATION

SIMPLE MODEL FOR FORMULA DERIVATION

$\delta h = h_P - h_Q$

Physical (ground) surface

h_P

h_Q

P

Q

Mean sea level
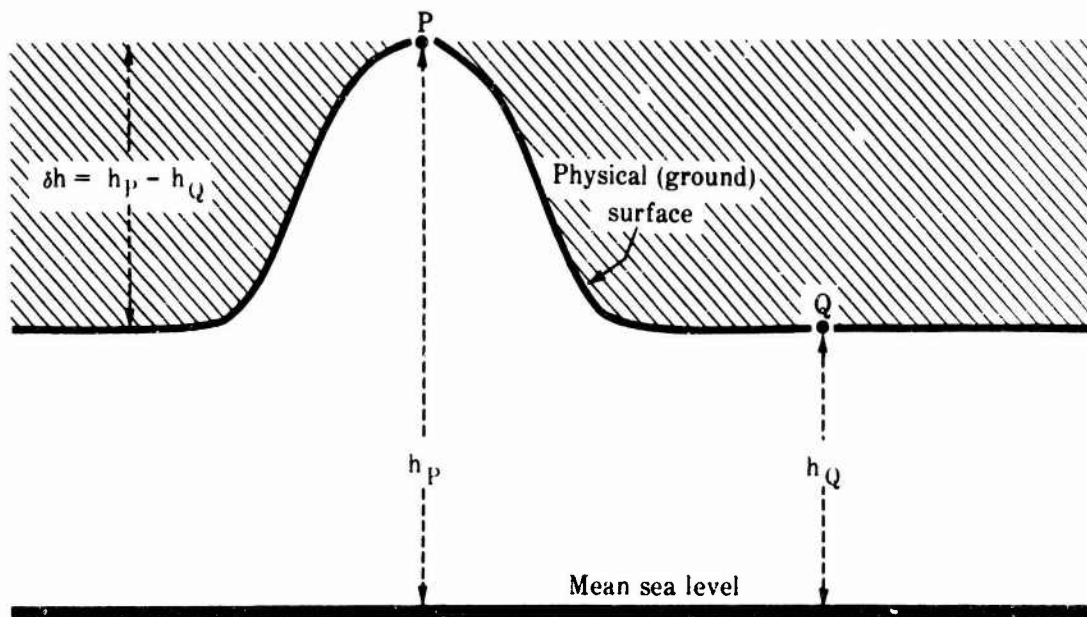
If the hill at P (Figure 3-2) is treated as being wholly uncompensated, then the gravitational attraction of the mass within the hill must be removed from observed gravity at P and Q in order to maintain the equality (3.6-18). Thus,

$$(\Delta g_S)_P - (g_H)_P = (\Delta g_S)_Q + (g_H)_Q - 0.3086 \, \delta h \qquad (3.6\text{-}19)$$

where

$(g_H)_P$ = gravitational attraction at P of the mass within the hill (Figure 3-2)

$(g_H)_Q$ = gravitational attraction at Q of the mass within the hill (Figure 3-2)

The sign of $(g_H)_P$ in (3.6-19) is negative since the removal of mass in the hill beneath P will reduce the value of gravity measured at P. The sign of $(g_H)_Q$ in (3.6-19) is positive because the removal of mass in the hill which is situated above Q will increase the value of gravity measured at Q.

As a first approximation, the hill under P can be replaced by a right circular cylinder of infinite radius and height equal to δh, i.e., the Bouguer plate of height, δh. The attraction at P of the rock mass contained within the Bouguer plate is given by

$$g_{BP} = 2 \, \pi \, k \, \sigma \, \delta h \qquad (3.6\text{-}20)$$

where

g_{BP} = attraction of the Bouguer plate

k = gravitational constant

σ = volume density of the rock matter within the Bouguer plate

Now the attractive force computed by (3.6-20)
includes not only that of the topographic mass under P, but also
that of the adjacent area shaded in Figure 3-2. In reality, the
shaded area is void of rock mass. Therefore, it is necessary to
subtract the gravitational attraction of the shaded area from
the Bouguer plate attraction given by (3.6-20) to obtain just
the attractive force of the hill.

The attractive force at P of the shaded area,
Figure 3-2, is given by the terrain correction at P, TC_P. Thus,
the attraction of the hill under P, Figure 3-2, is given exactly
by

$$(g_H)_P = 2 \pi k \sigma \delta h - TC_P \qquad (3.6-21)$$

Within the context of the simple relationship
shown in Figure 3-2, it is obvious that the gravitational attraction
of the hill at Q is given exactly by the terrain correction at Q, TC_Q.

$$(g_H)_Q = TC_Q \qquad (3.6-22)$$

The value of the terrain correction approaches
a minimum of zero in areas of gentle relief, a maximum of 0.05
milligals per meter in areas of very rugged relief, and averages
0.0316 milligals per meter of elevation difference (δh) for point
gravity anomalies (Voss, 1972b).

Now putting (3.6-21) and (3.6-22) into (3.6-19)

$$(\Delta g_S)_P = (\Delta g_S)_Q - 0.3086 \delta h + 2 \pi k \sigma \delta h - TC_P + TC_Q \qquad (3.6-23)$$

Converting (3.6-23) to the free air anomaly
by (3.6-14) and the definition, $\Delta g_S = g_0 - \gamma$, gives

$$- \gamma_P + (\Delta g_F)_P - 0.3086 \, h_P + \gamma_P = - \gamma_Q + (\Delta g_F)_Q - 0.3086 \, h_Q$$

$$+ \gamma_Q - 0.3086 \, (h_P - h_Q) + 2 \, \pi \, k \, \sigma \, (h_P - h_Q) - TC_P + TC_Q$$

Simplification of the preceding equation
leaves

$$(\Delta g_F)_P = (\Delta g_F)_Q + 2 \, \pi \, k \, \sigma \, \delta h - TC_P + TC_Q \qquad (3.6\text{-}24)$$

The density value generally used in equations
of the type (3.6-24) is 2.67 grams per cubic centimeter (gm/cm^3).
This value is " . . . a reasonable approximation for the density
of continental topographic features" (Woollard and Khan, 1972).
Actual values, however, may vary between about 2.2 and 2.9 gm/cm^3
(Strange and Woollard, 1964).

Using $\sigma = 2.67 \, gm/cm^3$ and the generally
accepted value for the gravitational constant, $k = 6.67 \times 10^{-8}$
$cm^3/gm \, sec^2$, then (3.6-24) becomes

$$(\Delta g_F)_P = (\Delta g_F)_Q + 0.1119 \, \delta h - TC_P + TC_Q \qquad (3.6\text{-}25)$$

Although the general equations (3.6-24) and
(3.6-25) were derived specifically for the simple topographic
model of Figure 3-2, Appendix C shows that these equations, in
fact, have general application to all topographic settings.

The general relations (3.6-24) and (3.6-25)
hold for local topographic variations, i.e., for topographic
variations within a radius of about 10 kilometers. Within such a

small area, these equations show that the free air anomaly varies

largely as a linear function of elevation difference between points

where gravity is observed. Since local elevation, of course, does

not vary as a linear function of position, then it follows that

linear interpolation between free air anomaly values is an

invalid procedure and, for this reason, free air anomaly maps are

very difficult to draw accurately in continental areas. Indeed,

the property of free air anomaly values to be closely associated

with elevation variations within a local area makes the free air

anomaly an undesirable form for interpolation and extrapolation

purposes within the continents particularly in mountainous areas.

The general validity of (3.6-25) can be

illustrated by a numerical example for a physical setting which

closely approximates Figure 3-2. Suppose the point, P, of Figure

3-2 lies at the summit of Pikes Peak and the point, Q, lies on the

nearby plain at Colorado Springs. Gravity and elevation data for

these two stations are given in Table 3-2. Then,

$$(\Delta g_F)_{\text{PIKES PK}} = (\Delta g_F)_{\text{COLO SPG}} + 0.1119 \, \delta h$$

$$- TC_{\text{PIKES PK}} + TC_{\text{COLO SPG}}$$

$$(\Delta g_F)_{\text{PIKES PK}} = -17 + 0.1119 \, (4293 - 1842) - 57 + 0$$

$$(\Delta g_F)_{\text{PIKES PK}} = +200 \text{ mgal}$$

which checks closely with the free air anomaly value of + 203 mgal

(Table 3-2) which was computed from observed gravity at Pikes Peak.

TABLE 3-2

DATA FOR GRAVITY OBSERVATIONS

AT PIKES PEAK AND COLORADO SPRINGS

STATION LOCATION	Δg_F (mgal)	h (meters)	TC (mgal)	Complete Δg_B (mgal)
PIKES PEAK	+203	4293	+57	−220
COLORADO SPRINGS	− 17	1842	0	−223

SOURCE: Woollard (1962)

Now suppose that the point, Q, in Figure 3-2 is located at sea level. Then, $h_Q = 0$, $\delta h = h_P$, and equation (3.6-25) becomes

$$(\Delta g_F)_{h=h_P} = (\Delta g_F)_{h=0} + 0.1119 \, h_P - TC_P + TC_Q \quad (3.6-26)$$

Equation (3.6-26) shows that, within a local area, the free air anomaly at any point above sea level, $(\Delta g_F)_{h=h_P}$, is given by a constant sea level free air anomaly value, $(\Delta g_F)_{h=0}$, plus about one milligal per nine meters of elevation. In a more general form, (3.6-26) may be written

$$\Delta g_F = \psi + \omega h \quad (3.6-27)$$

where

Δg_F = free air anomaly computed from observed gravity by

(3.6-14) for a point within a local area

h = elevation of that point

ψ and ω are constants which may be determined empirically by a linear least squares data fit according to (3.6-27).

Note that only free air anomaly values are involved in (3.6-26) and (3.6-27) even though these expressions resemble the Bouguer--free air anomaly relation, cp. (3.7-15).

The sea level free air anomaly value, ψ, though nearly constant within a very local area, will vary from place to place mainly as a function of local topographic characteristics, although it is also sensitive to other locally and regionally varying factors.

The value of ω within any local area depends primarily upon the average magnitude of the terrain corrections, the density of the rock matter composing the topography, and the degree of local compensation actually afforded to the local topographic features. Using equation (3.6-25) some logical limits can be place upon the magnitude of ω with reference to the normal limits of the rock density, σ, and terrain corrections. With the limits 2.2 and 2.9 for density, the value of $2 \pi k \sigma h$ will vary between 0.092 h and 0.122 h, where h is in meters. Adding the limits 0 and 0.05 mgal/meter for the terrain corrections, then the limits on ω in milligals per meter are

$$0.042 \le \omega \le 0.172 \qquad (3.6-28)$$

The limits (3.6-28) assume a total lack of local compensation. As the local features become increasingly broader in extent, however, an increasing amount of compensation is afforded. Since, for complete compensation, $\omega = 0$, a more inclusive limits statement is

$$0 \le \omega \le 0.172 \qquad (3.6-29)$$

Extensive empirical tests in the United States and Europe suggests that a good overall average value for point data is (Voss, 1972b)

$$\omega = 0.080 \qquad (3.6-30)$$

which, interestingly, lies about midway in the range given by (3.6-29).

It is also interesting to note that using
the "normal" values of 2.67 for σ and 0.0316 mgal/meter for TC_P,
assuming TC_Q to be zero, yields the value $\omega = 0.080$.

The existence of the local free air anomaly
relationship (3.6-27) suggests that a $1° \times 1°$ mean free air anomaly
can be predicted by

$$\overline{\Delta g_F} = \psi + \omega \overline{h} \qquad (3.6-31)$$

where

$\overline{\Delta g_F}$ = predicted $1° \times 1°$ mean free air anomaly

$\overline{h}$ = mean elevation of the $1° \times 1°$ area for which the mean
free air anomaly is to be predicted

The constants, ψ and ω, are determined by a
least squares fit of equation (3.6-27) at many well distributed
measurement sites within the $1° \times 1°$ area. In regions of locally
homogeneous structure and topography, the constants ψ and ω will
vary uniformly from one $1° \times 1°$ area to the next, and linear
interpolation is possible. However, very rapid variations in
ψ and ω are encountered across breaks in local structure or where
local topographic characteristics change. Consequently, considerable
care must be exercised when using (3.6-31) for $1° \times 1°$ mean anomaly
prediction.

3.6.3.3 Regional Variations in the Free Air Anomaly

The free air anomaly varies as a linear
function of elevation within a local area because local topographic
variations of up to about 10 kilometers in width can be treated as
wholly or nearly uncompensated features. Regional topographic

variations greater than about $3° \times 3°$ in extent, on the other hand,
may be treated as nearly compensated features. Consequently,
free air anomalies will not necessarily be positive over an
extensive area with high average height, but rather, should have
an average value of near zero in such regions.

The behavior of free air anomalies with
respect to topographic features varying in lateral extent between
about 10 km x 10 km and about $3° \times 3°$ is transitional. Relatively
positive free air anomalies are generally associated with relatively
high topographic features whose lateral extent lies within the
transitional range. As the topographic high becomes narrower,
the positive free air anomaly associated with it becomes more
intense. The limiting cases are no correlation (except at the
edges) as the feature becomes increasingly broad on the one hand,
and the relation (3.6-25) as the feature becomes narrower on
the other hand.

Woollard (1969a) has determined the regional
relations which exist between free air anomalies and elevations
within the United States. These relations, given in terms of
$1° \times 1°$ mean values are:

$$\overline{\Delta g_F} = -\ 0.103\ \overline{H} + 18 \qquad 0 \leq \overline{H} \leq 200 \qquad (3.6\text{-}32)$$

$$\overline{\Delta g_F} = \quad 0.009\ \overline{H} - 3 \qquad 200 \leq \overline{H} \leq 1800 \qquad (3.6\text{-}33)$$

$$\overline{\Delta g_F} = \quad 0.047\ \overline{H} - 74 \qquad \overline{H} > 1800 \qquad (3.6\text{-}34)$$

where

$\overline{\Delta g_F}$ = $1° \times 1°$ mean free air anomaly in milligals

$\overline{H}$ = $1° \times 1°$ mean elevation in meters

The first relation (3.6-32) applies to coastal and interior lowlands where surface relief is slight. The relation is actually very poorly defined which suggests that, in fact, there is virtually no regional correlation between free air anomaly and elevation in the flat lowlands (Strange and Woollard, 1964a).

The second relation (3.6-33) applies to moderately elevated areas in the interior where relief is typically low to moderate. Insertion of the limiting elevation values into (3.6-33) shows that, on the average, the $1° \times 1°$ mean free air anomaly increases only by about 10 mgal over the mean elevation range of 200 to 1800 meters. This is a very mild correlation.

The third relation (3.6-34) shows that the $1° \times 1°$ mean free air anomaly values tend to increase somewhat more rapidly with elevation in the highly mountainous areas of the United States whose $1° \times 1°$ mean elevations exceed 1800 meters. This is due to the smaller width of topographic features in the mountains as compared to those at lower elevations. However, note that the slope constant of (3.6-34) is still only about half that normally expected for the local free air anomaly elevation correlation, relation (3.6-30).

Relations of the type (3.6-33) and (3.6-34) have been suggested for prediction $1° \times 1°$ mean anomalies in unsurveyed areas (see Woollard and Strange, 1966). However, experience has shown that prediction with the Bouguer anomaly generally gives superior results, i.e., more definitive correlations than that provided by, e.g., (3.6-33).

Superimposed upon the regional elevation effects,
if any, are the effects of regional geology, crustal structure, and
regional isostatic imbalances. Woollard (1962) states the factors,
other than elevation, which can affect the regional part of the
free air anomaly:

(1) Regional departures from isostatic
balance due to (a) variations in crust or upper mantle strength,
(b) external stresses such as compression at the edges of crustal
plates, or (c) a time lag in establishing equilibrium conditions
for changes in surface mass caused by erosion, deposition,
glaciation, or deglaciation.

(2) Lateral gradational density changes
within the crust and/or upper mantle due to compositional variations,
and

(3) Regional variations in depth to
basement or other intra-crustal boundaries across which a density
contrast exists.

These non-elevation dependent factors affect
all of the common gravity anomaly types in a similar manner and to
a similar degree.

3.7 Bouguer Anomaly

3.7.1 Elements of the Bouguer Anomaly

Analagously to the free air anomaly, two steps are
necessary to obtain a theoretically correct Bouguer gravity anomaly
value, Figure 3-3. Firstly, all masses above sea level are removed
completely leaving a gravity observation at point P situated in free

air at an elevation h above sea level. Secondly, the gravity observation is lowered through free air to sea level. In a mathematical sense, the topographic masses are moved to infinity.

The gravitational effects of each step are determined computationally and combined to obtain the Bouguer reduction, $(\delta g_0)_B$

$$(\delta g_0)_B = - g_T + g_F \qquad (3.7-1)$$

where g_T and g_F are as defined for equation (3.6-2).

The term, g_F, is the free air correction given by equation (3.6-13). The term, g_T, includes the following mandatory and/or optional elements:

Mandatory element

Bouguer correction, g_B

Optional elements

Terrain correction, TC

Curvature correction, CC

Geologic correction, GC

Different terminology applies depending upon which, if any, of the optional elements are used. With the omission of all optional elements, the relation

$$g_T = g_B \qquad (3.7-2)$$

FIGURE 3-3

ILLUSTRATION OF COMPUTATIONAL STEPS NECESSARY

TO OBTAIN THEORETICALLY CORRECT

BOUGUER ANOMALY

TOPOGRAPHIC MASSES SHADED

Point, P, on physical surface
Point, Q, vertically below P on geoid surface

STEP 1. Remove topographic masses completely.
Point, P, now situated in free air at elevation, h, above geoid.

STEP 2. Lower observed gravity value through free air to sea level.
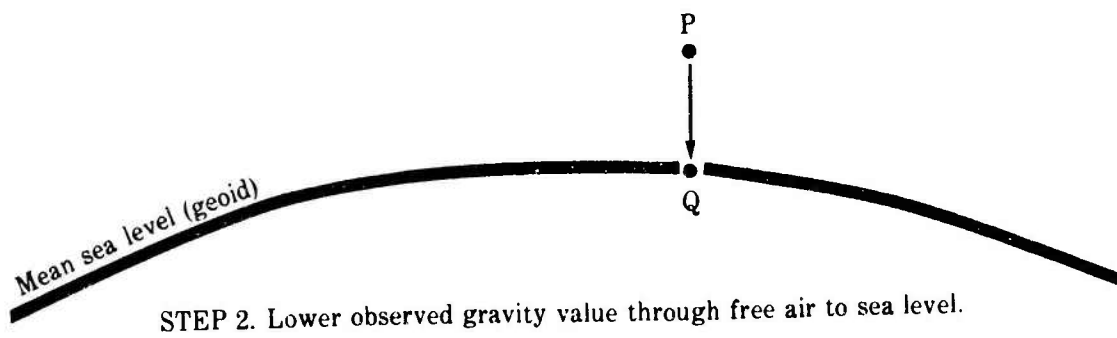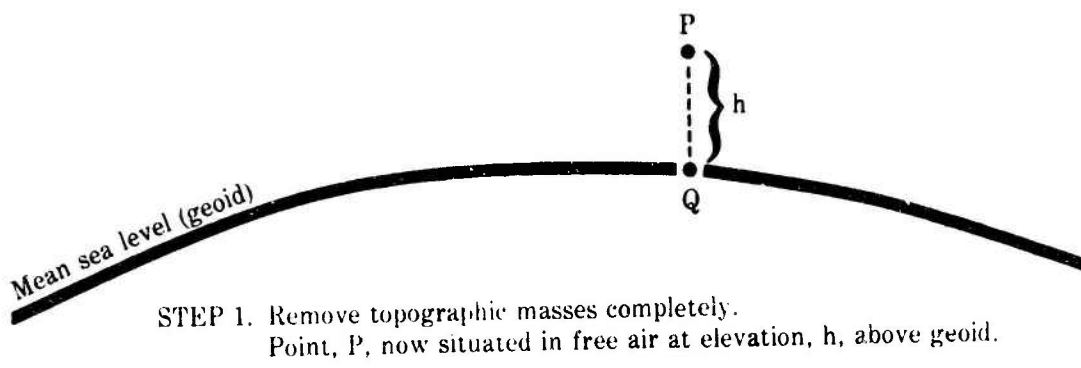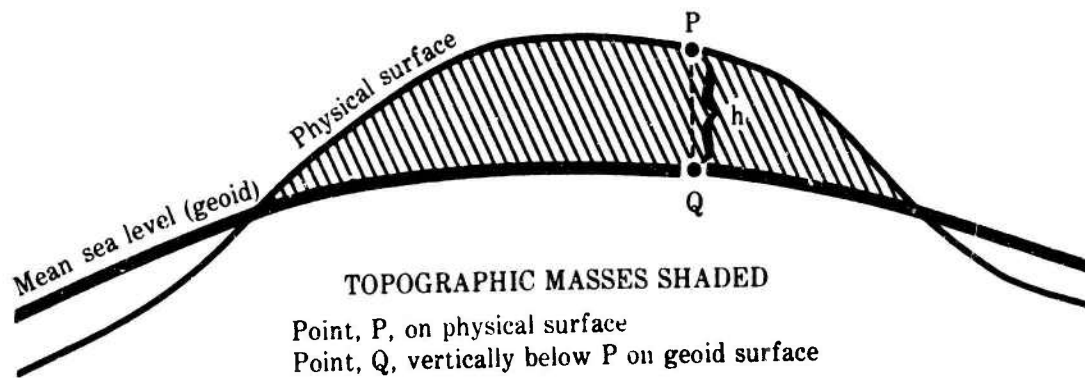
when inserted into equation (3.7-1) defines the simple Bouguer reduction*

$$(\delta g_0)_B = - g_p + g_F \qquad (3.7-3)$$

such that, by (3.3-1), the simple Bouguer anomaly is given by

$$\Delta g_B = g_0 - g_B + g_F - \gamma \qquad (3.7-4)$$

The relation

$$g_T = g_B - TC \qquad (3.7-5)$$

defines the complete Bouguer reduction

$$(\delta g_0)_B = - g_B + TC + g_F \qquad (3.7-6)$$

such that the complete Bouguer anomaly is given by

$$\Delta g_B = g_0 - g_B + TC + g_F - \gamma \qquad (3.7-7)$$

The curvature correction is an optional addition to (3.7-7) and the geologically corrected forms which follow.

Geologically corrected Bouguer anomalies may or may not contain the terrain correction and, hence, are of two forms. The geologically corrected simple Bouguer anomaly is

$$\Delta g_B = g_0 - g_B + GC + g_F - \gamma \qquad (3.7-8)$$

---

*Regrettably, there is no consistency in Bouguer anomaly terminology in the literature. The form identified here as the simple Bouguer reduction is sometimes termed the complete Bouguer reduction; also the form identified later as the complete Bouguer reduction is sometimes called the refined Bouguer reduction. Other variants are also found.

and the geologically corrected complete Bouguer anomaly is

$$\Delta g_B = g_0 - g_B + TC + GC + g_F - \gamma \qquad (3.7\text{-}9)$$

Comparison of (3.6-5) and (3.7-4) shows that the relation between the simple free air anomaly and simple Bouguer anomaly is

$$\Delta g_F = \Delta g_B + g_B \qquad (3.7\text{-}10)$$

Similarly, comparison of (3.6-5) and (3.7-7) shows that the relation between the simple free air anomaly and complete Bouguer anomaly is

$$\Delta g_F = \Delta g_B + g_B - TC \qquad (3.7\text{-}11)$$

Relations (3.7-10) and (3.7-11) apply to both point and mean gravity anomaly values.

3.7.2 Bouguer Correction, g_B

Assume that the physical surface of the earth which passes through the point where gravity is observed is flat (planar) and horizontal and that the surface of the geoid is parallel to it. These two assumed surfaces, when extended infinitely far in all horizontal directions, enclose and define the Bouguer plate (Figure 3-4).

Mathematically, the Bouguer plate is a right circular cylinder of height, h, and infinite radius where h corresponds to the elevation of the gravity observation site above sea level. The observation site is assumed to be situated at the intersection of the axis and upper surface of the cylinder.

60

FIGURE 3-4

THE BOUGUER PLATE

(Bouguer plate is shaded)

Physical surface →

P

h

Mean sea level (geoid)
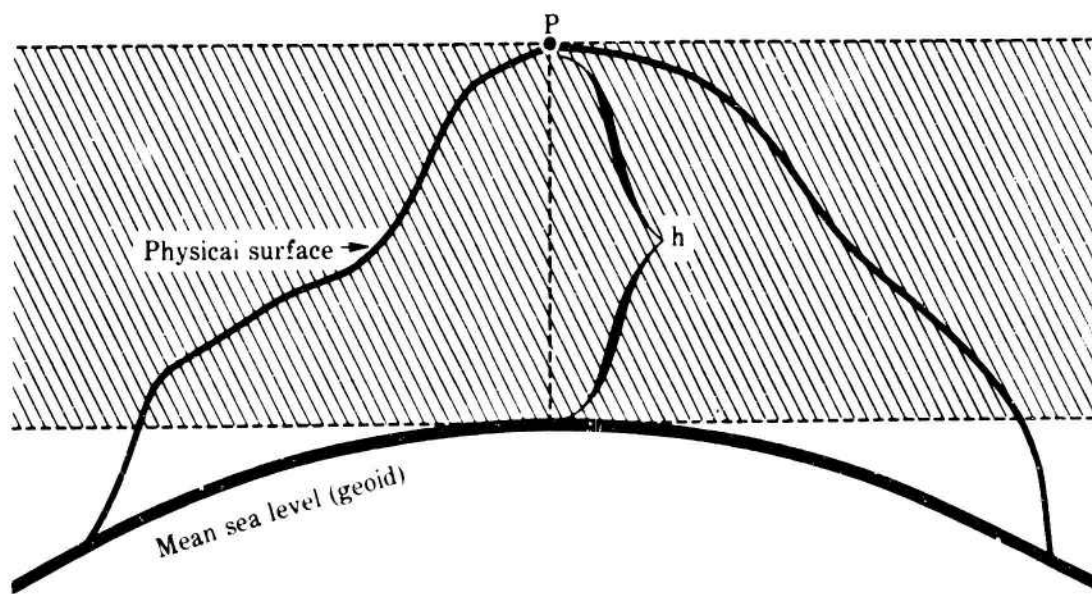
A complete derivation of the gravitational attraction of the infinite Bouguer plate is given in Appendix A with the result appearing there as equation (A-16). It is written here as

$$g_B = 2 \pi k \sigma n \qquad (3.7\text{-}12)$$

where

k = gravitational constant

σ = volume density of the rock matter within the Bouguer plate

h = elevation of the gravity observation above sea level.

The most commonly used value for the density factor in the Bouguer correction is 2.67 gm/cm^3. This value, when used for gravity reduction purposes, represents the average density of the sedimentary and crystalline rocks lying between the ground surface and sea level; a value of about 2.9 gm/cm^3 is needed to represent the mean density of the crust as a whole (see Woollard and Khan, 1972). With the value of 2.67 gm/cm^3 for density and the commonly accepted value for the gravitational constant, equation (3.7-12) is obtained in its usual form

$$g_B = 0.1119\ h \qquad (3.7\text{-}13)$$

where h is in meters. Using (3.7-13), the equations (3.7-10) and (3.7-11) now read

$$\Delta g_F = \Delta g_B + 0.1119\ h \qquad (3.7\text{-}14)$$

$$\Delta g_F = \Delta g_B + 0.1119\ h - TC \qquad (3.7\text{-}15)$$

which are the forms in which these relations are usually stated.

Note that three basic approximations are made when the Bouguer correction (3.7-13) is used to compute the gravitational effect of the masses above sea level. Namely, these topographic masses are assumed to be (1) perfectly flat, (2) of infinite horizontal extent, and (3) composed of rock whose density is 2.67 gm/cm^3 throughout.

The first approximation does not cause appreciable error in computation of the topographic gravitational effect for areas which are, in fact, essentially flat and planar, e.g.. coastal and interior lowlands, platforms, etc., Figure 3-5B. In mountainous terrain, however, where the topographic profile is not well approximated by the Bouguer plate, Figure 3-5A, the terrain correction must be applied in order to obtain a theoretically correct Bouguer anomaly value, i.e., a value from which the gravitational effects of the topographic masses have been eliminated completely.

The second approximation, while having significant consequences for the geophysical interpretation of the meaning of the Bouguer anomaly, causes only negligible error in the computation of the topographic gravitational effect. If desired, the error can be eliminated by application of the small curvature correction.

The third approximation is actually a strength of the Bouguer anomaly since it provides a foundation for analysis of the effects of local geologic structure on gravity anomaly variations. The analysis is done with reference to the geologic correction.

64

FIGURE 3-5A .

TERRAIN CORRECTION NEEDED

FIGURE 3-5B

TERRAIN CORRECTION NOT NEEDED

TERRAIN CORRECTION NEEDED
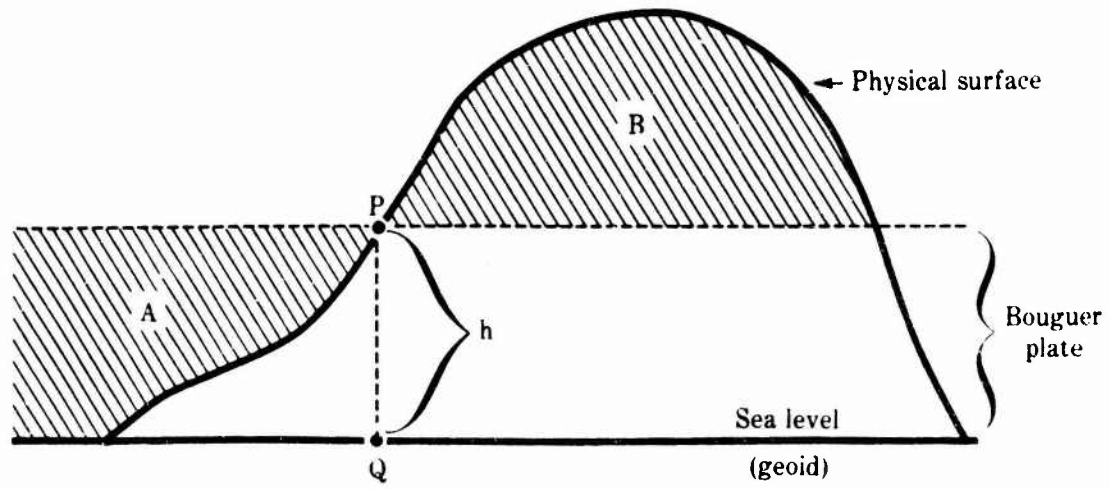
TERRAIN CORRECTION NOT NEEDED
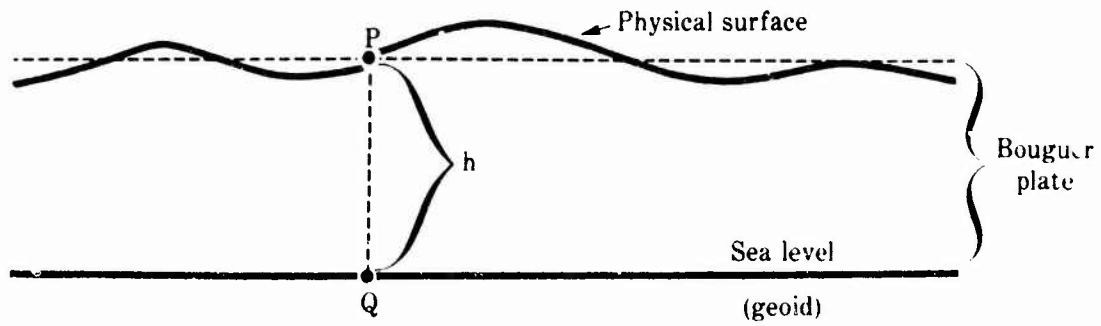
3.7.3 Terrain Correction

The terrain correction should be used in Bouguer anomaly computations whenever the topographic relief in the vicinity of the gravity observation point differs markedly from the flat planar model implied by the Bouguer plate.

There are two situations to be considered as shown in Figure 3-5A. Area A, included within the Bouguer plate, is above the physical surface of the earth and, therefore, contains no rock mass. On the other hand, the mass contained within area B lies entirely above the upper surface of the Bouguer plate. Thus, when the attraction of the Bouguer plate is subtracted from observed gravity as an approximation of the attraction of the actual topography, too much mass is subtracted at A, too little mass is subtracted at B, and the resulting anomaly form will not be free of topographic effects.

The terrain correction, when applied, (1) restores the attraction of the mass mistakenly removed at A when the attraction of the Bouguer plate is subtracted, the restoration of mass beneath the point P causing gravity observed at P to increase, and (2) eliminates the attraction of the mass remaining at B after the Bouguer plate has been removed. Since the mass at B exerts an upward or diminishing effect on gravity observed at P, its removal will cause observed gravity at P to increase. The terrain correction, thus, is always positive in the context of equations

(3.7-6) and (3.7-7) for continental areas, i.e., when the terrain correction is interpreted as a correction to observed gravity in the Bouguer reduction.

For practical computation of the terrain correction, the physical surface of the earth in the vicinity of the gravity observation point is approximated by a series of horizontal plane segments which, together with the upper surface of the Bouguer plate, define the upper and lower surface of a series of cylindrical compartments radiating outward from the observation point. Cylindrical formulas such as (A-16) of Appendix A, modified for application to cylindrical compartments, are used to compute the attraction of the mass within each compartment where the elevation argument in the formulas is the difference between the elevation of the horizontal plane segment and the elevation of the upper surface of the Bouguer plate. The gravitational effects of all compartments are summed to obtain the final terrain correction value.

The gravitational attraction of the topographic masses attenuates rapidly as the horizontal distance from the gravity observation point increases. Consequently, the terrain correction computation need be carried only a maximum distance of 166 km from the gravity observation point. Masses beyond 166 km in horizontal distance, being on the horizon* exert practically no gravitational

---

*The attraction of mass on the horizon is predominately horizontal (rather than vertical, i.e., gravitational).

attraction of the computation point. In many cases, it is

unnecessary to carry the computation beyond a 20 km radius from

the station. Woollard (1962) shows that in general, 95% of the

terrain correction value is generated by the masses contained

within an inner 20 km radius of the observation. Thus, if the

contribution to the terrain correction from the inner 20 km is

found to be 20 mgal or less, omission of the area between 20

and 166 km will cause an error of less than 1 mgal.

3.7.4 Curvature Correction

Because of the earth's curvature, the outer portion

of the Bouguer plate departs from the earth's surface. In fact,

at a distance of 166 kilometers from the gravity observation

point, the lower surface of the Bouguer plate is more than a

kilometer above sea level.

Since topographic mass is actually situated somewhat

below the outer regions of the Bouguer plate, the vertical

attraction of that mass is somewhat greater than that predicted

by the Bouguer plate. The curvature correction accounts for this

small difference.

In addition to eliminating the effects of curvature,

the curvature correction also removes the attraction of that

part of the Bouguer plate beyond 166 kilometers from the

observation point.

The maximum curvature correction value, less than 2 mgal,

occurs when the gravity observation station lies at an altitude of about

2300 meters. The correction is smaller for lesser or greater elevations.

3.7.5 Geologic Correction

The geologic correction generally is used to obtain some insight into local lateral density variations in the upper part of the crust--especially those within the sedimentary column.

Consider first the case of lateral density variations within the topographic masses. Figure 3-6 shows a sedimentary sequence where the average rock density varies from 2.8 gm/cm^3 within region A through 2.67 gm/cm^3 within region B to 2.6 gm/cm^3 within region C. For simplicity, the upper topographic surface is assumed to be flat and planar.

Now examine the result of computing Bouguer gravity anomaly values over areas A, B, and C using the usual density factor of 2.67 gm/cm^3 in the Bouguer correction. Within area B, the correct amount of topographic mass is subtracted in the Bouguer plate and the Bouguer anomaly profile will be level--assuming, of course, that there are no lateral density variations below the geoid. Within area A, an insufficient amount of mass is subtracted in the Bouguer plate since the actual density of the rock matter within A exceeds the density of the Bouguer plate. The attraction of the unsubtracted mass remaining within area A after the Bouguer correction is made must cause a positive deflection or "anomaly" in the Bouguer anomaly profile over area A.

Looking again at this relation from a slightly different viewpoint, the greater mass per unit area within A as compared to area B means that observed gravity over A must exceed that over B.

FIGURE 3-6

THE GEOLOGIC CORRECTION:

LATERAL DENSITY VARIATIONS

ABOVE SEA LEVEL
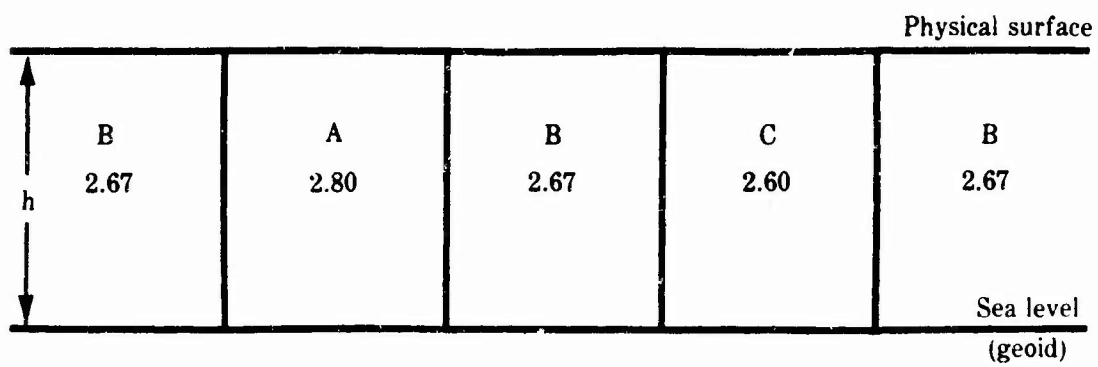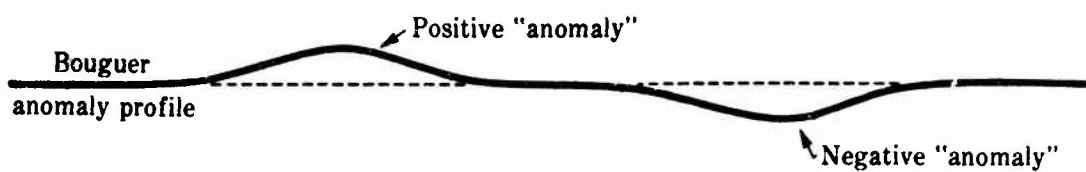
$$(g_0)_A > (g_0)_B$$

Since there are no lateral density variations in the normal earth, then*

$$Y_A = Y_B$$

And, since the elevation of area A is the same as that of area B

$$(g_B)_A = (g_B)_B$$

$$(g_F)_A = (g_F)_B$$

According to the above and equation (3.7-4), therefore, it must be true that

$$(\Delta g_B)_A > (\Delta g_B)_B$$

The magnitude of the "anomaly," $\delta \Delta g_B$, over A and C is given by

$$\delta \Delta g_B = 2\pi k\ (\sigma - \sigma_B)h \qquad (3.7\text{-}16)$$

where

σ = actual density of the rock within A or C

σ_B = density of rock in the Bouguer plate

Equation (3.7-16) should be recognized as a form appropriate to computing the attraction of a cylindrical disk of infinite radius, height, h, and density, $\sigma - \sigma_B$.

---

*Assuming, of course, that the latitude of A is not greatly different from that of B.

Equation (3.7-16) shows that the magnitude of the "anomaly" over A and C is a function of not only the density difference, $\sigma - \sigma_B$, but also of the elevation, h. That is, the magnitude of the "anomaly" over A or C is correlated with elevation. The correlation is direct when $\sigma - \sigma_B$ is positive, inverse when $\sigma - \sigma_B$ is negative. Suppose the physical surface of Figure 3-6 is a normal topographic profile instead of a flat plane. Then, if $\sigma - \sigma_B \neq 0$, the local Bouguer anomaly profile will be a direct or inverse reflection of that local topographic profile. This fact is of importance to the GRADE prediction method.

With the limits 2.2 and 2.9 gm/cm^3 for actual rock density, then the factor, $\sigma - \sigma_B$, has the limits

$$- 0.47 \leq (\sigma - \sigma_B) \leq + 0.23$$

Insertion of these limits into (3.7-16) gives, as approximate limiting values

$$- 0.020 \ h \leq \delta \Delta g_B \leq + 0.010 \ h \qquad (3.7-17)$$

The magnitude of the dependence of local Bouguer anomaly variations upon local elevation variations (3.7-17) is thus much smaller than the magnitude of the dependence of local free air anomaly variations upon local elevation variations (3.6-30). Further, if $\sigma - \sigma_B = 0$, the Bouguer anomaly is independent of local elevation variations. This fact is demonstrated further in Section 3.7.6.

The condition, $\sigma - \sigma_B = 0$, can be simulated by use of
the geologic correction which is given by (3.7-16) with reversed
sign.

$$GC = 2\pi k \ (\sigma_B - \sigma)h \qquad\qquad (3.7\text{-}18)$$

For area A the geologic correction, with h in meters, is

$$GC_A = 2\pi k \ (2.67 - 2.8)h$$
$$= 0.04191 \ (- \ 0.13)h$$
$$= - \ 0.005h$$

And, for area C

$$GC_C = 2\pi k \ (2.67 - 2.6)h$$
$$= 0.04191 \ (+ \ 0.07)h$$
$$= + \ 0.003h$$

The negative correction, GC_A, added to observed gravity
over area A and the positive correction, GC_C, added to observed
gravity over area C will cause the Bouguer anomaly profile to be
level over the entire sedimentary sequence (dashed line, Figure 3-6)
again assuming that there are no lateral density variations below
the geoid. In the case of the real earth, there are density
variations below the geoid which will cause the Bouguer anomaly
profile to fluctuate. In this case, application of the proper
geologic corrections will still remove all correlations between the
local Bouguer anomaly profile and the local topographic profile.

Consider next the case of lateral density variations
just below sea level. Since no mass below sea level is subtracted
in the Bouguer reduction, the density value used in the Bouguer
correction is not a factor here. What is important is the density

structure implied by normal gravity, namely an average density basement rock with no lateral density variations. On the other hand, normal gravity is not a factor in analyzing the topographic column because the normal earth lacks topographic mass.

Figure 3-7 shows a sedimentary sequence extending from sea level downward a depth, d, to the top of the basement complex. The average rock density within this sedimentary sequence varies from 2.79 gm/cm^3 within region D through 2.74 gm/cm^3 within region E to 2.63 gm/cm^3 within region F. These values reflect the study of Woollard (1962) which shows that the value of 2.74 gm/cm^3 is close to the average density for all basement rocks encountered in North America.

Now examine the result of deducting normal gravity when the Bouguer anomaly is computed over each of these regions. Within areas E, the correct amount of mass is deducted; within D too little mass is subtracted causing a positive "anomaly"; and within F too much mass is deducted causing a negative "anomaly."

The magnitude of the "anomaly" over D and F is given by

$$\delta \Delta g_B = 2\pi k \ (\sigma - \sigma_A)d \qquad (3.7\text{-}19)$$

where

σ = actual rock density within D or F

σ_A = average density of basement rock as implied by normal gravity

FIGURE 3-7

THE GEOLOGIC CORRECTION:

LATERAL DENSITY VARIATIONS

BELOW SEA LEVEL

Positive "anomaly"

Bouguer
anomaly profile

Negative "anomaly"

Sea level
(geoid)

| E | D | E | F | E |
| 2.74 | 2.79 | 2.74 | 2.63 | 2.74 |

d

Top of basement
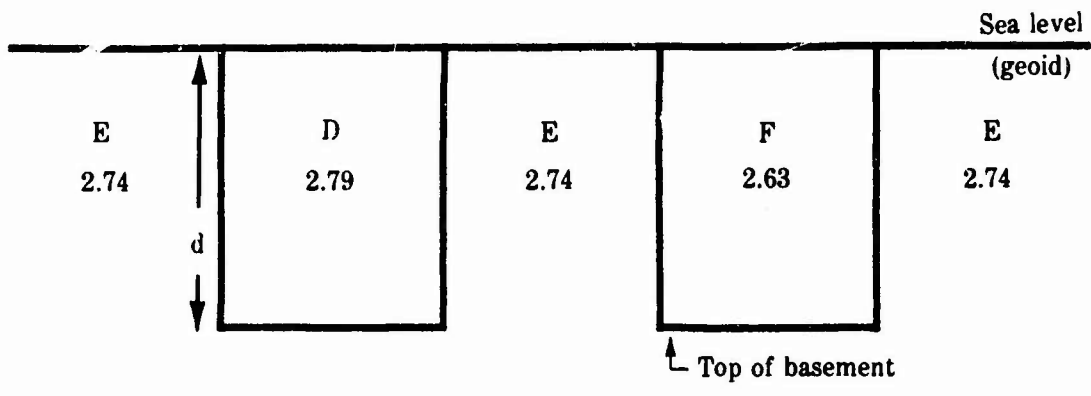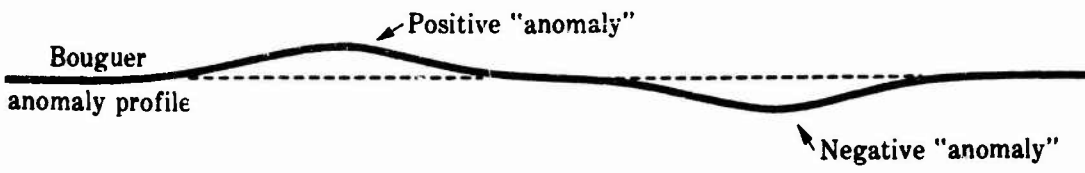
Equation (3.7-19) shows that the "anomaly" is a function of both the density difference, $\sigma - \sigma_A$, and the depth to basement, d. The correlation between anomaly and depth to basement is direct when $\sigma - \sigma_A$ is positive, and inverse when $\sigma - \sigma_A$ is negative. Figure 3-7 shows that the local Bouguer anomaly profile is a direct or inverse reflection of the buried basement topography. This fact, again, is of importance in the GRADE prediction method.

The factor, $\sigma - \sigma_A$, also may be interpreted as the density contrast between rocks within the sedimentary sequence and the underlying basement rock. In fact, this interpretation is desirable when more complex geologic structures are being gravimetrically analyzed.

The geologic correction for the below sea level case is given by

$$GC = 2\pi k\ (\sigma_A - \sigma)d \qquad\qquad (3.7-20)$$

For area D, the geologic correction, with d in meters, is

$$GC_D = 2\pi k\ (2.74 - 2.79)d$$
$$= 0.04191\ (- 0.05)d$$
$$= - 0.002d$$

And for area F

$$GC_F = 2\pi k\ (2.74 - 2.63)d$$
$$= 0.04191\ (+ 0.11)d$$
$$= + 0.005d$$

Application of these corrections to observed gravity will eliminate the correlation between depth to basement and Bouguer anomaly in the case of an undulating basement surface.

Two different methods have been used for determining the geologic correction. One was developed by Woollard (1937, 1938) and the other by Nettleton (1939).

In Woollard's method, subsurface geologic information is used to determine the actual mean density for each compartment of the Hayford and Bowie (1912) terrain correction zones. The density is determined down to sea level or the top of the crystalline basement complex. Examples are given by Woollard (1937, 1938) in his study of the Big Horn Mountain-Black Hills area.

In the density profiling method of Nettleton (1939) trial density values are used along a profile across topographic features to determine which density value gives no correlation between terrain corrected gravity anomalies and topographic elevations.

Woollard's method is preferred in areas where the topography is of tectonic or igneous intrusion origin. Nettleton's method is applicable in areas where the topography is of erosional origin except when there is a considerable amount of relief in the basement surface underlying the sedimentary strata. Woollard's method is better in the latter case.

More complex geological correction computations are often attempted. For example, a hypothetical model of rock structure can be set up, stratified if desired, and exact attraction formulas appropriate to the shape of the structure can

be used to compute the attraction effects of the density contrasts. The computed anomaly profiles can be compared to observed Bouguer anomaly profiles, and then the structure and density of the model can be adjusted within logical bounds until a best fit is obtained between the two profiles. The result is a most probable model of subsurface rock structure. The remaining unexplained differences between the Bouguer anomaly profile and the computed profile can be ascribed to lateral density variations deeper within the crust and upper mantle.

With a knowledge of local Bouguer gravity anomaly variations, then, the local subsurface geologic structures which generate these variations can be deduced. Other information, e.g., seismic, geological survey, well logs, etc., is always necessary as input to enable construction of a first approximation and to put logical limits on solutions because the problem has no unique solution. In fact, there are an infinite number of subsurface geologic structure arrangements which can generate any given Bouguer anomaly profile.

On the other hand, if the subsurface geologic structure is known with reasonable accuracy, the gravity variations generated by said structures can be predicted. This problem _does_ have a unique solution and is the basis for the local geologic correction term used in the NOGAP prediction scheme.

3.7.6 Geophysical Properties of the Bouguer Anomaly

The Bouguer gravity anomaly is a useful, easy to compute tool for geophysical and geological interpretation as well as for gravity interpolation and prediction. Yet, at the same time, it is wholly unsuitable for most geodetic applications. This seemingly schizophrenic nature of the Bouguer anomaly is due to its peculiar geophysical properties.

Consider, for example, the equation obtained by inserting the Bouguer reduction, equation (3.7-1), into the basic gravity anomaly relation (3.3-1). The result may be written

$$\Delta g_B = (g_O + g_F) - (\gamma \cdot g_T) \qquad (3.7\text{-}21)$$

As was pointed out at the outset of Section 3.6.3 on the free air anomaly, the total mass of the earth generates the term, $(g_O + g_F)$, the total mass of the normal earth generates the value, γ, and these two masses are defined to be equal. Therefore, the term, $(\gamma + g_T)$ implies the existence of more mass than the total mass of the earth. In consideration of the foregoing and equation (3.7-21), it is not at all surprising that the Bouguer anomaly is generally negative approximately in proportion to the amount of mass subtracted in the Bouguer reduction*; nor is it surprising that an anomaly form which is not conservative of earth mass should be of little value in applying the integral formulas of physical geodesy. On the other hand, subtraction of the Bouguer

---

*A more convenient geophysical interpretation of this phenomenon will be discussed in Section 3.7.6.1.

reduction is a necessary prerequisite to application of the geologic correction--whose value to structural interpretation has been discussed in Section 3.7.5.

Next, consider a highly instructive interpretation of the Bouguer gravity anomaly suggested by Bomford (Bomford, 1971). Recall that, in the Bouguer reduction, the topography is approximated by a circular cylinder of infinite radius which is tangent to the geoid at the gravity anomaly computation point and whose thickness is equal to the elevation of the point where gravity is observed. Note that the curvature of the earth is totally neglected in the Bouguer model.

In the immediate vicinity of the gravity observation station, say within a radius of 50 km--about $1^{\circ} \times 1^{\circ}$--the terrain corrected Bouguer plate gives an excellent approximation of the actual topography such that the gravitational attraction of the nearby topographic masses can be accurately removed by the Bouguer reduction if the correct density factor is used.

The inner zone grades outward into an intermediate belt in which the gravitational effect of the topography becomes small both for the real earth and for the Bouguer plate model because all masses in both cases are near the horizon.

Outside of the intermediate belt the gravitational effect of the topography again becomes significant because the curvature of the earth causes the topography to be significantly below the horizon of the gravity computation point. On the real earth, the gravitational effect of distant topography is nearly

cancelled by isostatic compensation. In the Bouguer model, neglect of curvature means that all distant topography is on the horizon and, hence, exerts no vertical attraction component at the point where gravity is observed. In other words, in the Bouguer model, the effect of the distant topography is cancelled by neglect of curvature.

It is evident, therefore, that the regional character of the Bouguer anomaly differs markedly from the local character. Locally, the Bouguer anomaly is a sensitive indicator of lateral density variations within nearby masses. Regionally, the Bouguer anomaly is an indicator of the degree of regional isostatic balance. However, since masses located at intermediate distances have little effect on the Bouguer anomaly, there is no sharp boundary between the local and regional effects.

The Bouguer gravity anomaly thus is well suited to analysis and prediction in t rms of regional and local components.

3.7.6.1 Isostasy and the Bouguer Anomaly

Consider again the geophysical consequences of computing a geologically corrected complete Bouguer gravity anomaly. The Bouguer and terrain corrections subtract the gravitational effects of the masses above sea level. Then, if the density factors are chosen properly, all local gravitational effects of density variations within the topographic masses and sub geoid rocks can be eliminated by the geologic correction. Addition of the free air correction and subtraction of normal gravity now give a Bouguer gravity anomaly referenced to the geoid which is free of near surface geologic effects.

Yet, it is an observed fact that no matter what "reasonable" density factors are used to compute Bouguer anomalies, these anomalies almost always resemble a smoothed mirror image of the topography--the higher the regional elevation, the more negative the Bouguer anomaly. Note especially that the inverse relation between elevation and Bouguer anomaly is a smooth regional effect. Complete Bouguer anomalies do not reflect local topographic variations when the proper density factor is chosen for use in the Bouguer reduction.

The strong inverse correlation between regional elevation and Bouguer anomaly, evidently, cannot be related to near surface density variations--the effects of these were eliminated when the geologic correction was applied. The only possible explanation is that the negative Bouguer anomalies are caused by a regional mass deficiency which exists under the continents in proportion to the regional elevation of the overlying land mass. This mass deficit is called "compensation."

Regional Bouguer anomalies can serve as a kind of indicator of the degree of compensation extant in an area. If the regional Bouguer anomaly is more negative than expected for a given regional elevation level, then a condition of overcompensation* is indicated. Conversely, if the regional Bouguer anomaly is more positive than expected for a regional elevation level, then a condition of undercompensation is indicated. The

---

*That is, the gravitational effect of the mass deficit at depth exceeds the gravitational attraction of the topographic mass.

picture can be complicated by the presence of regional abnormalities in crustal and upper mantle structure or density. For example, an abnormally dense crustal block can be in complete isostatic equilibrium, yet still generate a relatively positive gravity anomaly indication which suggests a condition of undercompensation (Golizdra, 1972; Woollard, 1969a).

Now, if the strong inverse correlation between regional elevation and regional Bouguer gravity anomaly is generated by compensating mass, then the lack of such a strong correlation must signal a lack of compensating mass. And, since it is observed that local topographic variations are not correlated with the geologically corrected Bouguer anomaly, it follows that local topographic variations are uncompensated. This same conclusion was deduced with respect to local free air anomaly-- elevation correlations.

3.7.6.2 Local Variations in the Bouguer Anomaly

Local variations in the complete Bouguer gravity anomaly field are very nearly free of correlation with local topographic variations. Only a relatively small amount of elevation dependence exists because of local geologic influences.

Note, however, that simple Bouguer anomalies contain a negative bias due to omission of the terrain correction and, to this degree, do depend upon local topography.

Consider Figure 3-2. If the hill is of local extent, it may be treated as an uncompensated feature and equation (3.6-24) applies for the case of no lateral density or geological

structure variations. For the case where lateral density and
structural variations do exist, equations such as (3.7-16) and
(3.7-19) must be considered in addition to equation (3.6-24).

$$(\Delta g_F)_P = (\Delta g_F)_Q + 2 \pi k \sigma \delta h - TC_P + TC_Q$$

Conversion of the above to an expression
involving the complete Bouguer anomaly is accomplished by
substitution of (3.7-11) and (3.7-12) which gives

$$(\Delta g_B)_P + 2 \pi k \sigma h_P - TC_P$$

$$= (\Delta g_B)_Q + 2 \pi k \sigma h_Q - TC_Q + 2 \pi k \sigma \delta h - TC_P + TC_Q$$

Since $\delta h = h_P - h_Q$, the above immediately
reduces to the form

$$(\Delta g_B)_P = (\Delta g_B)_Q \qquad (3.7-22)$$

The general validity of the remarkable result
expressed by equation (3.7-22) is illustrated by the numerical
example of Table 3-2.

Thus, the derivation of (3.7-22) shows that
the pronounced non-linear variations in the free air gravity
anomalies due to local topographic variations can be eliminated
entirely by application of the complete Bouguer reduction.

It is evident from the foregoing that any
local variations in the complete Bouguer gravity anomaly field
must be caused solely by lateral mass variations due to changes in
density and/or local structural pattern. Since (1) observed gravity

is the integrated effect of mass attraction over a wide area,
(2) lateral mass variations are mostly gradational, and (3) really
sharp anomalies in mass distribution are of limited occurrence in
sub-geoid local continental geologic structure, it follows that the
continental Bouguer gravity anomaly field, in general, is continuous
and smoothly varying. Thus, Bouguer anomaly values are well suited
for linear interpolation and for this reason most gravity anomaly
maps of continental areas depict Bouguer anomalies. Another
reason for the latter is the simplicity of Bouguer anomaly
computation as compared to, e.g., isostatic anomaly computation.

3.7.6.3 Regional Variations in the Bouguer Anomaly

The gravitational effect of the compensating
mass distributions generates the observed inverse relationship
between regional elevation levels and Bouguer anomaly values. A
useful mathematical expression will now be derived for this
relationship.

If the topographic feature of Figure 3-2
is of regional extent, then this feature may be treated as being
wholly compensated and equation (3.6-15) applies.

$$(\Delta g_F)_P = (\Delta g_F)_Q$$

This equation assumes a lack of lateral
density variations between points P and Q other than those associated
with the topography and its isostatic compensation.

88

Conversion of the above expression to a form involving complete Bouguer anomalies is accomplished by substitution of equations (3.7-11) and (3.7-12), giving

$$(\Delta g_B)_P + 2\pi k \sigma h_P - TC_P$$

$$= (\Delta g_B)_Q + 2\pi k \sigma h_Q - TC_Q$$

Or, solving for $(\Delta g_B)_P$

$$(\Delta g_B)_P = (\Delta g_B)_Q - 2\pi k \sigma (h_P - h_Q) + (TC_P - TC_Q)$$

Under most conditions, the regional terrain correction terms, TC_P and TC_Q, are nearly equal in magnitude and the term $(TC_P - TC_Q)$ will tend to zero. Then, letting $\delta h = h_P - h_Q$, the above reduces to

$$(\Delta g_B)_P = (\Delta g_B)_Q - 2\pi k \sigma \, \delta h \qquad (3.7\text{-}23)$$

Considerable care must be exercised in interpreting equation (3.7-23) because, although the difference between $(\Delta g_B)_P$ and $(\Delta g_B)_Q$ is actually a function of the differing amounts of <u>compensating</u> <u>mass</u> deficiency under P and Q, only the <u>topography</u> related quantities σ and δh actually appear in the equation itself. Recall the three stated conditions for (3.7-23) to hold, namely, (1) the anomaly and elevation values are regional values, (2) isostatic compensation is complete under P and Q, and (3) there are no lateral mass abnormalities. Under these conditions, equation (3.7-23) merely expresses the evident fact that the gravity effect of the difference in compensation between P and Q is equal (but opposite in sign) to the gravity effect of the difference in

topographic mass between P and Q.

For complete compensation to exist, the regional values Δg_B and δh must represent surface areas of $3° \times 3°$ or larger in dimension (Woollard, 1969a). The "normal" value of (3.7-23) in such cases is found by inserting the density factor used to compute the Bouguer anomalies $(\Delta g_B)_P$ and $(\Delta g_B)_Q$. For the usual factor, $\sigma = 2.67$ gm/cm^3, equation (3.7-23) becomes

$$(\Delta g_P)_P = (\Delta g_B)_Q - 0.1119 \, \delta h$$

If the regional values, $(\Delta g_B)_P$, $(\Delta g_B)_Q$. and δh, represent areas smaller than $3° \times 3°$, isostatic compensation cannot be assumed to be complete. Also, lateral mass abnormalities may exist. Then (3.7-23) cannot be evaluated in its present form because the gravity effects of the topography and compensation, in general, will not be equivalent. Thus, it appears that an equation involving quantities related to the amount of compensation present must replace (3.7-23). Unfortunately, such an equation can be derived only with reference to an assumed isostatic model.

In order to avoid the use of an assumed isostatic model, consider converting (3.7-23) to a more general form which eliminates specific reference to the topographic quantity, σ, which may have no simple relationship to the amount of compensation present in an area.

Let Q be located at sea level. Then $h_Q = 0$, $\delta h = h_P$, and (3.7-23) becomes

$$(\Delta g_B)_{h=h_P} = (\Delta g_B)_{h=0} - 2 \pi k \sigma h_P \qquad (3.7-24)$$

Then, arbitrarily rewrite (3.7-24) in the more

general form

$$\overline{\Delta g_B} = \alpha + \beta \overline{h} \qquad (3.7\text{-}25)$$

where

$\overline{\Delta g_B} \rightarrow (\Delta g_B)_{h=h_P}$ = regional Bouguer anomaly

for any continental area, P, whose regional elevation above sea level
is $\overline{h} = h_P$,

$\alpha \rightarrow (\Delta g_B)_{h=0}$ = a sea level regional Bouguer anomaly value

representing the region PQ

β = a coefficient representing the regional Bouguer

anomaly gradient with respect to elevation

within the region PQ

The topographic quantity, $\overline{h}$, still appears in
equation (3.7-25). However, it is very reasonable to suppose that
the regional compensation can be expressed as a linear function
of regional elevation level.

If (1) the degree of isostatic compensation and
(2) any regionally anomalous lateral mass distribution structure
of the crust remain essentially constant over a particular regional
geologic or tectonic entity, then it follows that the values, α and
β, must also remain essentially constant over that regional structural
entity. Then values for α and β can be determined empirically by a
linear regression of $\overline{\Delta g_B}$ and $\overline{h}$ over the region covered by that structural
entity.

It is a unique property of the Bouguer anomaly
that, within most areas of homogeneous structural characteristics,
the value of the constant, β_R, determined with reference to regional

$\overline{\Delta g_B}$ and $\overline{h}$ values is very similar to the value of the constant, β_P, determined with reference to point Δg_B and h values. (Note that this similarity is not a property of the corresponding free air anomaly relationships.) However, the interpretation of (3.7-25) is slightly different depending upon which type of data, point or mean, is regressed to obtain the α and β constants.

In one case, (3.7-25) may be written

$$\overline{\Delta g_B} = \alpha_P + \beta_P \overline{h} \qquad (3.7-26)$$

where

$\overline{\Delta g_B}$ = a 1° x 1° mean Bouguer anomaly

$\overline{h}$ = the 1° x 1° mean elevation corresponding to $\overline{\Delta g_B}$

α_P and β_P are determined by a linear regression of point elevation and point Bouguer anomalies within the 1° x 1° area represented by $\overline{\Delta g_B}$ and $\overline{h}$.

Since the correlation between Bouguer anomalies and elevation defined by (3.7-25) is a regional one, then (3.7-26) is a valid relation between the regional values $\overline{\Delta g_B}$ and $\overline{h}$ even though the constants α_P and β_P are determined from point data. In fact, (3.7-26) can be used to predict valid 1° x 1° mean anomalies when h, α_P, and β_P are known for the 1° x 1° area in question.

The constants, α_P and β_P, will vary somewhat from one 1° x 1° area to the next. The variation will be small when both 1° x 1° areas are similar in regional structure, larger when the regional structure is dissimilar. These variations are regional with respect to the point anomalies--but local with respect to the 1° x 1° mean anomalies.

In the other case, (3.7-25) may be written

$$\overline{\Delta g_B} = \alpha_R + \beta_R \, \overline{h} \qquad\qquad (3.7\text{-}27)$$

where

$\overline{\Delta g_B}$ and $\overline{h}$ are the same as in (3.7-26)

α_R and β_R are determined by a linear regression of mean elevation vs. $1° \times 1°$ mean Bouguer anomalies within areas whose regional structure is similar to and which are continuous with the $1° \times 1°$ area corresponding to $\overline{\Delta g_B}$ and $\overline{h}$.

The constants, α_R and β_R, can be evaluated for most areas of uniform regional structure within the continents. Recently determined examples, written in the form of equation (3.7-27), include:

AREA	EQUATION
Alpine Geosyncline, Europe	$\overline{\Delta g_B} = -\,0.104 \, \overline{h} + 21.4$
Cordillera, W. Canada	$\overline{\Delta g_B} = -\,0.078 \, \overline{h} - 7.1$
Red Sea	$\overline{\Delta g_B} = -\,0.114 \, \overline{h} - 7.0$
Trans Urals	$\overline{\Delta g_B} = -\,0.090 \, \overline{h} - 2.4$

In the above equations which, incidentally, can be used to predict the regional part of valid $1° \times 1°$ mean anomalies within each area, $\overline{\Delta g_B}$ is the regional Bouguer anomaly (milligals) represented by the $1° \times 1°$ mean value and $\overline{h}$ is the regional elevation (meters) represented in some cases by the $1° \times 1°$ mean value, in other cases by the $3° \times 3°$ mean value. Other examples, similar to the above, are given by Woollard (1969a, 1968b).

93

Application of (3.7-26) for 1° x 1° mean
gravity anomaly prediction is essentially an interpolation
process which may be used when the 1° x 1° area for which the
prediction is to be made contains a fair to good density and
distribution of observed gravity data. The method fails when
elevation differences within the 1° x 1° area are too small to
enable definition of the regional elevation-anomaly relationship,
or when the gravitational effects of local structural variations
within the 1° x 1° mask the regional elevation-anomaly relationship.
In fact, the constants, α_p and β_p, of equation (3.7-26) will
always be less well defined than the constants, α_R and β_R, of
equation (3.7-27) because of the larger gravitational effects
of local structural variations on point anomalies as compared to
mean anomalies.

Application of (3.7-27) for 1° x 1° mean
anomaly prediction is essentially an extrapolation process
which may be used when the 1° x 1° area for which the prediction
is to be made contains few or no gravity observations. However,
sufficient gravity data must be available in adjacent 1° x 1° areas
with similar structure to enable definition of the α_R and β_R
values. Corrections for some kinds of local and regional
structural variations must be made when (3.7-27) is used for
gravity anomaly prediction. Such corrections are unnecessary
when (3.7-26) is applied for 1° x 1° mean anomaly prediction.

In addition to the elevation dependent
regional variations discussed above, Bouguer anomalies are also
subject to regional variations in geologic and crustal structure.
Examples of factors causing such variations were mentioned in
connection with the discussion on regional variations in the
free air anomaly.

3.8 Isostatic Anomaly

3.8.1 Elements of the Isostatic Anomaly

As was the case with the free air and Bouguer anomalies,
computation of an isostatic gravity anomaly is essentially a two
step process. In the first step, all masses above sea level
(the topographic masses) are removed and then redistributed beneath
the geoid in such a manner as to eliminate the negative gravitational
effects of the compensating mass deficiencies. The mass
redistribution is carried out with reference to (1) an assumed
model of earth structure and (2) a specific concept of the nature
of the isostatic mechanism.

At the completion of the first step, which removes
both the topography and its compensation, the gravity observation
site is situated in free air at an elevation, h, above sea level.
In the second step, gravity is lowered through free air to sea
level.

The gravitational effects of each of the two steps are
determined computationally and combined to obtain the isostatic
reduction, $(\delta g_0)_I$

$$(\delta g_0)_I = - g_T + g_I + g_F \qquad (3.8\text{-}1)$$

where

g_I = isostatic correction

g_T and g_F are the same as defined for equation (3.6-2)

For the isostatic reduction, the term g_T includes the complete Bouguer correction given by equation (3.7-5) to which the curvature correction, CC, has been added. The term, g_F, is the free air correction given by (3.6-13). Insertion of these relations into (3.8-1) gives for the isostatic reduction

$$(\delta g_0)_I = - g_B + TC + CC + g_I + g_F \qquad (3.8\text{-}2)$$

such that, by (3.3-1), the isostatic anomaly, Δg_I, is

$$\Delta g_I = g_0 - g_B + TC + CC + g_I + g_F - \gamma \qquad (3.8\text{-}3)$$

Comparison of (3.7-7) to (3.8-3) shows that the relation between the complete Bouguer anomaly and the isostatic anomaly is

$$\Delta g_I = \Delta g_B + g_I \qquad (3.8\text{-}4)$$

where the small curvature correction term has been dropped. Equation (3.8-4) shows that the Bouguer anomaly is actually one limiting case of the isostatic anomaly because, when the topographic mass is moved to infinity in the Bouguer reduction, then $g_I = 0$ and $\Delta g_I = \Delta g_B$. Incidentally, the free air anomaly is another limiting case of the isostatic anomaly. In this case, the topographic mass, moved just underneath the geoid, is essentially still topographic mass in its gravitational effects. Then,

$$g_I = g_T, \text{ and } \Delta g_I = \Delta g_B + g_T = \Delta g_F$$

Insertion of (3.7-11) and (3.7-12) into (3.8-4) gives
the relation between the free air anomaly and the isostatic anomaly

$$\Delta g_I = \Delta g_F - 2 \pi k \sigma h + TC + g_I \qquad (3.8\text{-}5)$$

3.8.2 Isostatic Correction

The isostatic correction includes (1) the gravitational
attraction at the observation site, P, of the volume mass placed
beneath the geoid in accordance with a particular earth model and
isostatic theory, said mass being equivalent to the topographic
masses removed by the Bouguer reduction; plus (2) the gravitational
attraction at P of distant topography and its compensation.

The basic purpose of any isostatic correction is to
redistribute all topographic mass removed by the Bouguer
reduction in order to (1) cancel the negative gravitational
effects of the mass deficiencies which compensate the topography,
and (2) eliminate any correlation between the resulting isostatic
anomalies and elevation variations. Actually, the second of the
foregoing is a consequence of the first.

There are several varieties of isostatic correction
in common or occasional use, each depending upon a different earth
model and/or isostatic concept, but all purporting to accomplish
the same purpose. The problem here is that the exact nature of
the isostatic mechanism and structure of the earth's interior is
still a matter of conjecture. Therefore, any earth model and
isostatic concept used is, at best, only an idealized approximation
of the truth. Moreover, each variety of isostatic anomaly must

have a somewhat different geophysical meaning, and any detailed

geophysical interpretation of isostatic gravity anomalies must

be made within the context of a given model and mechanism

assumption. Fortunately, a general discussion of isostatic

anomaly properties can be made without specific reference to a

particular model or isostatic concept.

Most geodesists feel that, for geodetic purposes, it

does not matter which variety of isostatic correction is used.

However, the same kind of isostatic correction must be used in a

mathematically precise and self-consistent manner to reduce all

gravity data to be applied in deriving the geodetic products

desired.

The most commonly used concepts of the isostatic

mechanism are the Pratt-Hayford and Airy-Heiskanen systems. Some

geophysical properties peculiar to each of these systems, as well

as the idealized structural models associated with them, are

discussed in Section 3.10. A discussion of the rather complex

formulas and reduction procedures for these systems is given in

Heiskanen and Vening Meinesz (1958), Heiskanen and Moritz (1967),

and other sources.

Both Pratt-Hayford and Airy-Heiskanen isostatic

systems require the topographic masses to be moved to considerable

depths beneath sea level. (The masses in their new location

may be called compensating masses In the most commonly used

Airy-Heiskanen model, all such masses are relocated at depths

greater than 30 kilometers and up to about 60 kilometers below

sea level, the maximum depth being proportional to the regional

elevation levels. In the most commonly used Pratt-Hayford

models, the masses are evenly distributed between sea level

and depths of 56.9, 96, or 113.7 kilometers.

The much greater depth of the topographic masses

after redistribution as compared to these masses in their

original above sea level location means that the nature of the

gravitational effect of the deep seated compensating masses on

a surface gravity observation must be greatly different than

that of the topographic masses in their original near surface

location. In fact, the gravitational effect of the topography

is local and immediate, while the gravitational effect of the

compensation is regional and distant.

Consider Figure 3-8. The vertical component of the

gravitational attraction, g_Z, of any mass element, M, varies in

inverse proportion to the square of the distance between M and

the observation site P, and in direct proportion to the cosine

of the angle, θ, subtended at the observation point by the vector,

g_Z, and the line connecting the observation site to the mass

element.

$$g_Z \propto \frac{\cos \theta}{D^2} \qquad (3.8\text{-}6)$$

Now, the topographic masses directly beneath P have

a very small θ and D, hence, a large vertical gravitational

effect at P. But θ becomes very large for topographic mass

elements only a small horizontal distance from P, and as M_T

approaches the horizon, θ rapidly approaches $90°$ and the vertical

gravitational effect of M_T rapidly approaches zero. Thus,
topographic masses nearby P have a large gravitational effect
at P, but topographic masses even a relatively small horizontal
distance away from P have only a minor gravitational effect at P.

Compensating masses directly beneath P, although also
having a small G, have a much larger D than the topographic masses.
Hence the gravitational effect of compensating mass nearby P is
small. As the horizontal distance between M_C and P increases, θ
increases more slowly than for topographic masses at the same
horizontal distances (and cos θ does not become vanishingly
small). Hence the gravitational effect of compensation can be
expected to accumulate slowly over a rather wide range of
distance from P. (A detailed discussion of this effect is given
by Hayford and Bowie, 1912).

Table 3-3, based on graphs in Woollard (1959) shows
the relative gravitational effects of topography and compensation
which exists at various distances away from the point of observation.
For example, the table shows that 90 percent of the total
gravitational attraction (vertical component) at P of the
topographic masses is generated by those masses within 10
kilometers of the observation point (but only 4% of the total
gravitational attraction [vertical component] at P of the
compensating masses is generated by such masses within a
horizontal distance of 10 kilometers from the observation point).
This means that local topographic variations can, in fact, be
treated as being virtually uncompensated locally--as was done
during the discussions of the free air and Bouguer anomalies.

FIGURE 3-8

COMPARISON OF GRAVITATIONAL EFFECTS

TOPOGRAPHY VS. COMPENSATION

M_T = Element of topographic mass

M_C = Element of compensating mass

D_T = Distance from observation point, P, to topographic mass element,
M_T

D_C = Distance from observation point, P, to compensating mass element,
M_C

θ_T = Angle between vertical gravity component, g_Z, and line connecting
observation point, P, with topographic mass element, M_T

θ_C = Angle between vertical gravity component, g_Z, and line connecting
observation point, P, with compensating mass element, M_C
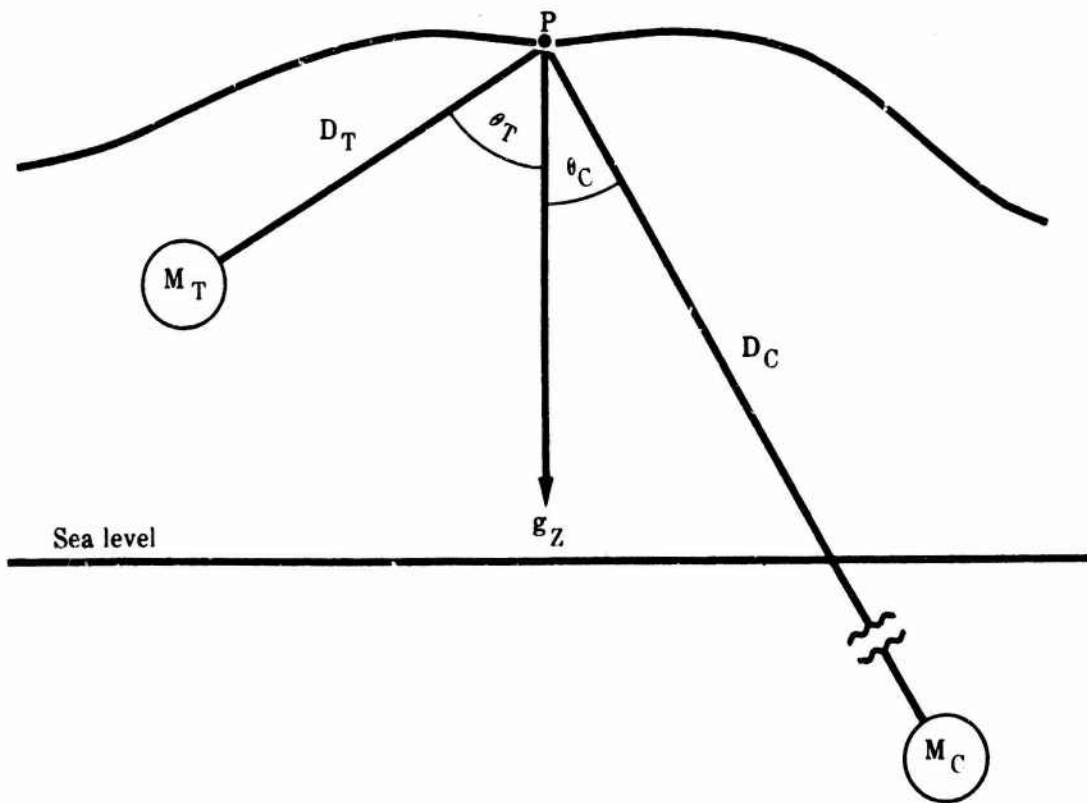
TABLE 3-3

RELATIVE GRAVITATIONAL EFFECTS

OF TOPOGRAPHY AND COMPENSATION

AT VARIOUS DISTANCES FROM GRAVITY OBSERVATION POINT

D_H = horizontal distance from the point of observation in Km

T = percent of total topographic gravitational attraction (vertical component) generated by topographic masses within the indicated zone

C = percent of total compensation gravitational attraction (vertical component) generated by compensating masses within the indicated zone

ΣT = cumulative percentages of T

ΣC = cumulative percentages of C

sm = small

D_H	T	ΣT	C	ΣC	$\dfrac{\Sigma C}{\Sigma T}$	$1 - \dfrac{\Sigma C}{\Sigma T}$
0-10	90	90	4	4	.04	.96
10-20	05	95	9	13	.14	.86
20-30	02	97	11	24	.25	.75
30-40	01	98	10	34	.35	.65
40-50	01	99	9	43	.43	.57
50-60	sm	99	7	50	.51	.49
60-70	sm	99	6	56	.57	.43
70-80	sm	99	5	61	.62	.38
80-90	sm	99	4	65	.66	.34
90-100	sm	100	3	68	.68	.32
100-110	sm	100	2	70	.70	.30
110-120	sm	100	2	72	.72	.28
120-130	sm	100	2	74	.74	.26
130-140	sm	100	2	76	.76	.24
140-166	sm	100	3	79	.79	.21
Distant	0	100	21	100	1.00	

The table also shows that nearly 100 percent of the topographic gravitational effect is generated by masses within 50 kilometers distance (about a 1° x 1° area) from the observation point--but only 50 percent of the total compensation effect. Even at a distance of 166 kilometers (about a 3° x 3° area), only 79 percent of the total compensation effect has been accounted for. This means that about 21% of the compensation is due to distant masses, and that a 3° x 3° area is about the smallest area within which the topography can be considered to be about 80 percent compensated locally.

Because of the fact that the gravitational effects of the compensation are generated by masses which are mostly rather far from the observation point and consist of an integration of small components over the whole earth, it follows that the isostatic correction, g_I, is a comparatively slowly varying quantity. Indeed, the difference between two g_I values at two points fairly close together (within a local area) will be close to zero. This is true because most of the components largely overlap for the two computations.

3.8.3 Geophysical Properties of the Isostatic Anomaly

Isostatic gravity anomalies can be a useful tool for geophysical and geological interpretation. They interpolate well and are also suitable for geodetic applications. However, computation of isostatic anomalies is difficult and time consuming, and isostatic anomalies cannot be predicted easily using geophysical methods. The latter is true because isostatic anomalies, in general,

tend to be uncorrelated with elevation variations. The isostatic

anomalies are discussed here mainly because of the insight they

provide to the types of anomalies which more readily can be

predicted using geophysical methods.

Among the advantages of the isostatic anomaly form is

that it is conservative of mass. Consider equation (3.8-3)

written in the form

$$\Delta g_I = (g_0 + g_F) - \gamma - (g_B - TC - CC) + g_I$$

Recall that the term, $(g_0 + g_F)$, is generated by the

total mass of the real earth and that the term, γ, arises from

the total mass of the normal earth, these two masses being equal

by definition. The topographic masses within 166 kilometers from

the point P, for which Δg_I is being calculated, generate the term

$(g_B - TC - CC)$, and these masses moved to locations beneath the

geoid to counteract the compensating mass deficiencies generate the

major portion of g_I, the moved masses being equal to the topographic

masses removed in the Bouguer reduction. The balance of g_I is

generated by the effects of distant topography and its compensation,

i.e., all topography and compensation mass deficiencies located

more than 166 kilometers from P. Thus, the isostatic anomaly,

like free air anomaly, is conservative of mass and useful for

geodetic as well as geophysical purposes.

3.8.3.1 Isostasy and the Isostatic Anomaly

The topographic masses, removed in the

Bouguer reduction, are replaced beneath the geoid by the isostatic

correction in such a way that the negative gravitational effec s

of the compensating mass deficiencies, as reflected in the regionally
negative Bouguer anomalies, are cancelled. Note carefully that
all of the mass removed by the Bouguer reduction is fully restored
by the isostatic correction. Thus, if a topographic feature is, in
fact, completely compensated, the positive effect of the mass
restored by the isostatic correction will exactly cancel the
negative effect of the compensating mass deficiencies, and the
resulting isostatic anomaly will be equal to the free air anomaly
less local topographic effects. A positive isostatic anomaly
suggests an excess of topographic mass over compensating mass
deficiency, and a negative isostatic anomaly suggests an excess
of compensating mass deficiency over topographic mass. The
actual situation is complicated by differences between reality
and the isostatic concept and earth model used in a particular
isostatic reduction.

3.8.3.2 Properties of Free Air and Bouguer Anomalies as Derived from Isostatic Anomaly Relationships

Once again, consider Figure 3-2. If the
degree of compensation under both the topographic rise and adjacent
lower areas is the same, and there are no lateral density variations
between P and Q other than those due to topography and its
compensation, then it must be true that

$$(\Delta g_I)_P = (\Delta g_I)_Q \qquad (3.8\text{-}7)$$

Expanding by (3.8-3)

$$(g_0)_P - (g_B)_P + TC_P + CC_P + (g_I)_P + (g_F)_P - \gamma_P$$

$$= (g_0)_Q - (g_B)_Q + TC_Q + CC_Q + (g_I)_Q + (g_F)_Q - \gamma_Q \qquad (3.8\text{-}8)$$

Since $\Delta g_F = g_0 + g_F - \gamma$, then

$$(\Delta g_F)_P - (g_B)_P + TC_P + CC_P + (g_I)_P$$

$$= (\Delta g_F)_Q - (g_B)_Q + TC_Q + CC_Q + (g_I)_Q$$

And, since $g_B = 2 \pi k \sigma h$, $\delta h = h_P - h_Q$; and dropping the small CC terms,

$$(\Delta g_F)_P - (\Delta g_F)_Q = 2 \pi k \sigma \delta h - TC_P + TC_Q \qquad (3.8\text{-}9)$$

$$- [(g_I)_P - (g_I)_Q]$$

Note that equation (3.8-9) can also be written in the more general form

$$(\Delta g_F)_P - (\Delta g_F)_Q = (g_T)_P - (g_T)_Q - [(g_I)_P - (g_I)_Q] \qquad (3.8\text{-}10)$$

Equation (3.8-9) is the general form for the specific regional relations (3.6-32), (3.6-33), and (3.6-34).

Equation (3.8-9) shows that for the condition (3.6-15)

$$(\Delta g_F)_P = (\Delta g_F)_Q$$

to hold, it is necessary that the difference between the attraction of the topography at P and Q must be equal to the difference between the attraction of the compensation at P and Q, that

$$2 \pi k \sigma \delta h - TC_P + TC_Q = (g_I)_P - (g_I)_Q \qquad (3.8\text{-}11)$$

Equation (3.8-11) is a most reasonable condition for the existence of a constant degree of isostatic compensation at P and Q.

Equation (3.8-9), although derived for regional gravity relations, can be used to illustrate why local free air gravity relations depend heavily on local elevation variations. Within a local area, the topography related term, $2 \pi k \sigma \delta h$, varies as rapidly as the topography varies. However, the compensation related term, $(g_I)_P - (g_I)_Q$, varies rather slowly and is close to zero when P and Q are nearby. Thus, it is mathematically impossible for local topographic variations to be locally compensated. In fact, as

$$(\Delta g_I)_P - (\Delta g_I)_Q \rightarrow 0$$

then (3.8-9) reverts to the relation (3.6-24) previously derived for the local free air anomaly relationship

$$(\Delta g_F)_P - (\Delta g_F)_Q = 2 \pi k \sigma \delta h - TC_P + TC_Q$$

Thus, the local free air anomaly relationship is actually just a special case of the general free air anomaly equation (3.8-9). Next, insert the relation

$$\Delta g_B = g_0 - g_B + TC + CC + g_F - \gamma$$

into (3.8-8) to obtain

$$(\Delta g_B)_P - (\Delta g_B)_Q = - [(g_I)_P - (g_I)_Q] \qquad (3.8-12)$$

Equation (3.8-12) is a more precise version of (3.7-23), and shows that the regional Bouguer anomaly is, in fact, a measure of compensation. Again, (3.8-12) applies for the regional case. For local Bouguer anomaly relations, the right side of (3.8-12) approaches zero, and the equation reduces to the local relation (3.7-22)

$$(\Delta g_B)_P = (\Delta g_B)_Q$$

Hence, the local Bouguer anomaly relation is also just a special case of the general Bouguer anomaly equation (3.8-12).

Now, insert (3.8-5) into (3.6-15) which gives the regional relation

$$(\Delta g_I)_P + 2 \pi k \sigma h_P - TC_P - (g_I)_P$$
$$= (\Delta g_I)_Q + 2 \pi k \sigma h_Q - TC_Q - (g_I)_Q$$

As before, $\delta h = h_P - h_Q$, and after some rearrangement,

$$(\Delta g_I)_P - (\Delta g_I)_Q = - 2 \pi k \sigma \delta h + TC_P - TC_Q + [(g_I)_P - (g_I)_Q] \quad (3.8-13)$$

Note that the right side of (3.8-13) for the isostatic anomaly is the negative equivalent of the right side of (3.8-9) for the free air anomaly. In the case of the free air anomaly, the topography is condensed into a surface layer on the geoid where it still has a positive effect on the observed gravity, whereas the negative gravity effect of the compensating mass deficiency remains unaltered. In the case of the isostatic anomaly,

110

the topographic mass is removed by the Bouguer reduction causing
a negative effect on observed gravity, and restored beneath the
geoid to cancel the compensating mass deficiency, causing a
positive effect on observed gravity.

Note also that, since the Bouguer reduction
is applied to compute the isostatic anomaly, the geologic correction
applies equally to both anomaly types.

In (3.8-13), suppose the point Q is at sea level.
Then, $h_Q = 0$, and $\delta h = h_P$. Also, there is no topographic mass above
Q to be redistributed beneath the geoid. Therefore, $(g_I)_Q$ can only
contain the effects of distant topography and its compensation. Thus,

$$(\Delta g_I)_{h=h_P} = (\Delta g_I)_{h=0} - 2 \pi k \sigma h_P + TC_P - TC_Q + [(g_I)_P - DTC_Q] \quad (3.8\text{-}14)$$

The relative complexity of the above and the fact
that the compensation related terms tend to cancel the elevation
related terms suggest that no simple relationship of the form $\Delta g_I =$
$\alpha + \beta h$ can be used to represent isostatic anomaly variations.

A slight rearrangement of (3.8-14) gives the form

$$(\Delta g_I)_{h=h_P} - (g_I)_P = [(\Delta g_I)_{h=0} - DTC] - 2 \pi k \sigma h_P + TC_P - TC_Q$$

By (3.8-4), the above reduces to

$$(\Delta g_B)_{h=h_P} = [(\Delta g_I)_{h=0} - DTC] - 2 \pi k \sigma h_P + TC_P - TC_Q \quad (3.8\text{-}15)$$

Comparison of (3.8-15), (3.7-24), and (3.7-25)
shows that the α constant in the relation

$$\overline{\Delta g_B} = \alpha + \beta h$$

is a form of sea level isostatic anomaly which lacks distant
topography and compensation effects.

Next, insert (3.8-5) into the local
relationship (3.6-24) to obtain

$$(\Delta g_I)_P + 2 \pi k \sigma h_P - TC_P - (g_I)_P = (\Delta g_I)_Q + 2 \pi k \sigma h_Q$$

$$- TC_Q - (g_I)_Q + 2 \pi k \sigma (h_P - h_Q) - TC_P + TC_Q$$

The above reduces to

$$(\Delta g_I)_P - (\Delta g_I)_Q = (g_I)_P - (g_I)_Q$$

But, for the local situation, $(g_I)_P - (g_I)_Q \rightarrow 0$.

Therefore, the local isostatic anomaly relationship is, simply

$$(\Delta g_I)_P = (\Delta g_I)_Q \qquad (3.8\text{-}16)$$

Now, (3.8-16), derived for a local situation,

is an equation which guarantees that the same degree of isostatic

compensation exists at P as does at Q. Yet, in the local case,

the topographic feature at P cannot possibly be compensated

locally. The apparent contradiction can be resolved only if

isostasy is a condition with regional, not local, applicability.

In other words, (3.8-16) says only that the same degree of

regional isostatic compensation exists at both P and Q. This is

most reasonable if P and Q are close together within a local area.

3.8.3.3 Properties of the Free Air Anomaly With

Terrain Correction as Derived From Isostatic Anomaly Relationships

Equation (3.8-9) may be written in the form

$$(\Delta g_Y)_P - (\Delta g_Y)_Q = 2 \pi k \sigma \delta h - [(g_I)_P - (g_I)_Q] \qquad (3.8\text{-}17)$$

where the expressions

$$(\Delta g_Y)_P = (\Delta g_F)_P + TC_P$$

$$(\Delta g_Y)_Q = (\Delta g_F)_Q + TC_Q \qquad (3.8\text{-}18)$$

represent the free air anomaly with terrain correction at points P

112

and Q, respectively. This anomaly form, sometimes called the Faye anomaly, is often used in applications of Molodenskiy's solution to the problems of physical geodesy.

For the local situation where $(g_I)_P - (g_I)_Q \to 0$, equation (3.8-17) reduces to

$$(\Delta g_Y)_P - (\Delta g_Y)_Q = 2 \pi k \sigma \delta h \qquad (3.8-19)$$

The right side of (3.8-19) is the difference in gravitational attraction between two horizontal plateaus (Bouguer plates), one with elevation, h_P, and the other with elevation, h_Q. At first glance this peculiar anomaly form may seem to have some application for geophysical gravity prediction because, for the case of Q at sea level, (3.8-19) becomes

$$(\Delta g_Y)_{h=h_P} = (\Delta g_Y)_{h=0} + 2 \pi k \sigma h_P \qquad (3.8-20)$$

which is rigorously in the form

$$\Delta g_Y = \psi + \omega h \qquad (3.8-21)$$

From a geophysical viewpoint, however, it is difficult to understand why the free air anomaly with terrain correction has achieved ready acceptance for geodetic applications. Insertion of the definition (3.8-17) into the basic free air anomaly relation (3.6-5) gives the equation

$$\Delta g_Y = (g_0 + g_F) - (\gamma - TC) \qquad (3.8-22)$$

Recall that the total mass of the real earth generates the term, $(g_0 + g_F)$, the total mass of the normal earth generates the value, γ, and these two masses are defined to be equal. Therefore, the term, $(\gamma - TC)$, implies the existence of less mass than the total mass of the real earth! Anomaly forms

which are not mass conservative are usually avoided for geodetic application.

Equation (3.8-22) shows that the anomaly, Δg_γ, will tend to have a positive bias in areas of rugged topography where TC is large--much as the Bouguer anomaly has a negative bias in mountainous areas. Thus, the regional form (3.8-17) has no isostatic significance and is difficult to interpret from a structural standpoint since the topographic term has a positive bias and the magnitude of the bias is solely a function of the ruggedness of the local terrain. Consequently, it appears most unlikely that Δg_γ is a useful form for gravity prediction.

3.9 Unreduced Surface Anomaly

The unreduced surface anomaly, Δg_S, defined by

$$\Delta g_S = g_0 - \gamma \tag{3.9-1}$$

is not in the same class as the gravity anomaly types previously discussed because the reduction to sea level, δg_0, is omitted. It has no geodetic value on the continents, and never before has been used for geophysical analysis.

There are two ways to view the unreduced surface anomaly. One is that, since g_0 applies at the earth's surface and γ applies at sea level (technically, at the ellipsoid surface), then Δg_S is really undefined since its point of application is ambiguous. The second view, more suitable for geophysical purposes, is that the only purpose of γ in (3.9-1) is to serve as a kind of latitude correction which removes the systematic gravitational

effects of the earth's flattening from observed gravity. Using

the latter interpretation of γ, then variations in Δg_S are

tantamount to variations in observed gravity caused by mass

distribution irregularities in the real earth.

The normal regional relation for the unreduced surface anomaly

is given by equation (3.6-18)

$$(\Delta g_S)_P = (\Delta g_S)_Q - 0.3086\ \delta h \qquad (3.9\text{-}2)$$

which, if Q is taken sea level, is rigorously in the form

$$(\Delta g_S) = \xi + \eta h \qquad (3.9\text{-}3)$$

where the constants, ξ and η, may be determined by a linear

regression analysis of mean values within a region of homogeneous

structure.

Using equations (3.6-32), (3.6-33), and (3.6-34) and the

difference between (3.9-2) and (3.6-15), estimated average regional

relations between unreduced surface anomalies and elevations within

the United States, based upon $1° \times 1°$ mean values, are

$$\overline{\Delta g_S} = +\ 18 - 0.0412\ \overline{H} \qquad 0 \le \overline{H} \le 200 \qquad (3.9\text{-}4)$$

$$\overline{\Delta g_S} = -\ 3 - 0.300\ \overline{H} \qquad 200 \le \overline{H} \le 1800 \qquad (3.9\text{-}5)$$

$$\overline{\Delta g_S} = -\ 74 - 0.262\ \overline{H} \qquad \overline{H} > 1800 \qquad (3.9\text{-}6)$$

where $\overline{H} = 1° \times 1°$ mean elevation in meters.

The normal local relationship between Δg_S and elevation is

given by equation (3.6-23).

$$(\Delta g_S)_P = (\Delta g_S)_Q - 0.3086\ \delta h + 2\ \pi\ k\ \sigma\ \delta h - TC_P + TC_Q \qquad (3.9\text{-}7)$$

which, if Q is taken at sea level, can be written in the form

$$(\Delta g_S)_P = \zeta + \theta h \qquad (3.9\text{-}8)$$

Using the limits of 2.2 to 2.9 gm/cm^3 for density, 0 to 0.05 mgal per meter for the terrain corrections, and assuming the free air gradient to be constant, then the limits on θ are

$$- 0.2664 \leq \theta \leq - 0.1370 \qquad (3.9\text{-}9)$$

Since, for the case of complete compensation, $\theta = - 0.3086$, then a more comprehensive limits statement is

$$- 0.3036 \leq \theta \leq - 0.1370 \qquad (3.9\text{-}10)$$

Empirical tests in the United States suggests that a good average value for θ, using point data, is (Voss, 1972)

$$\theta = - 0.2287$$

Relation (3.9-4) gives a value for θ which lies outside of the limits (3.9-10). However, (3.9-4) is based upon the free air anomaly relation (3.6-32) which, as has been mentioned previously, was very poorly defined.

3.10 Isostatic Models, Mechanisms, and Analysis

3.10.1 Isostasy

Isostasy refers to a state of equilibrium in the outer parts of the earth in which (1) the land masses which extend above sea level are counterbalanced by a compensating mass deficiency beneath sea level, and (2) the ocean basins which contain low density

116

water are counterbalanced by a compensating mass excess beneath
the ocean floor.

The general validity of the isostatic principle
has been established conclusively using purely geodetic arguments.
For example, the fact that free air anomalies are largely
uncorrelated with regional elevation changes can be cited as
evidence of the existence of regional isostatic balance. The
reader is referred to Heiskanen and Vening Meinesz (1958) for
free air, Bouguer, and isostatic gravity anomaly statistics
which demonstrate that, on a regional basis, the mountains and
oceanic basins are very close to being in complete isostatic
equilibrium.

Some departures from regional isostatic balance do
exist, for example, recently deglaceated regions. Also, the crust
of the earth appears to have sufficient strength to maintain
local mass distribution variations such that the local density
and topographic irregularities are largely uncompensated. The
strong correlation between free air anomalies and local elevation
variations, for example, proves that local topographic irregularities
are uncompensated.

The exact physical mechanisms of isostasy are, as
yet, unknown. However, there are a number of isostatic theories
which probably provide at least a good approximation of the
isostatic mechanisms. Each of these theories specifies an exact
manner in which the compensating mass deficiencies or excesses
are distributed within the earth. One such theory must be adopted
and used as a basis for determining the isostatic correction in

isostatic anomaly computations and, in general, for estimating the gravitational effects of the compensating masses.

The two "classic" isostatic theories are those of J. B. Pratt and G. B. Airy. Both date from 1855.

3.10.2 Pratt Isostatic Theory

In the Pratt isostatic system, the deficiency of mass beneath the land areas and the excess of mass below the oceanic areas are evenly distributed between ground or sea floor level and some depth, called the depth of compensation, where isostatic equilibrium is complete. It follows that each column of matter with unit cross sectional area, extending to the earth's surface from the depth of compensation, contains equal mass.

Equal mass above the level of compensation in the unit area crustal columns means that the pressure must be equal everywhere at the level of compensation. Indeed, the meaning of isostasy is "equal pressure."

Pressure is defined as force per unit area,

$$P = \frac{F}{A} \qquad (3.10-1)$$

where

P = pressure

F = force

A = area

Force, in turn, is defined as the product of mass and acceleration; in this case, the acceleration due to gravity

$$F = mg \qquad (3.10-2)$$

118

where

m = mass

g = gravitational acceleration

and mass is the product of volume and density

$$m = V\sigma \qquad (3.10-3)$$

where

V = volume

σ = density

Therefore, combining the above equation, pressure is given by

$$P = \frac{V\sigma g}{A} \qquad (3.10-4)$$

Consider a series of columns with unit cross sectional area extending from the level of compensation up to the surface of the earth, Figure 3-9. The upper surface of column S is at sea level and its height, h_S, is equivalent to the distance from sea level to the depth of compensation. Column P stands beneath a mountain area, and the elevation of its upper surface above sea level is $\Delta h = h_P - h_S$. Column Q stands beneath an oceanic area whose water depth is $h_Q - h_S$.

Suppose the pressure is equal at the depth of compensation for all columns. Then

$$P_S = P_P = P_Q$$

or, using (3.10-4) for columns P and S

$$\frac{V_S \sigma_S g_S}{A_S} = \frac{V_P \sigma_P g_P}{A_P} \qquad (3.10-5)$$

Since the volume of each column is the product of its cross sectional area and height, h,

$$V = Ah \qquad (3.10\text{-}6)$$

then (3.10-5) becomes

$$h_S \sigma_S g_S = h_P \sigma_P g_P \qquad (3.10\text{-}7)$$

Assuming that the acceleration of gravity is constant at the level of compensation leaves

$$h_S \sigma_S = h_P \sigma_P \qquad (3.10\text{-}8)$$

Equation (3.10-8) shows that the density of a Pratt crustal column is inversely proportional to its height. Thus, column P has a lesser density, and column Q has a greater density than column S.

Now, solve (3.10-8) for σ_P and subtract σ_S from both sides.

$$\sigma_P - \sigma_S = \Delta\sigma = \frac{h_S \sigma_S}{h_P} - \sigma_S$$

Simplification leaves

$$\Delta\sigma = \frac{-(h_P - h_S)\,\sigma_S}{h_P} = -\frac{\Delta h \sigma_S}{h_P} \qquad (3.10\text{-}9)$$

Equation (3.10-9) shows that, in the Pratt isostatic system, isostatic compensation is achieved entirely by a uniform variation in density above the level of compensation.

J. F. Hayford (1909) modified Pratt isostatic theory somewhat. According to Hayford, the depth of compensation is measured from the topographic surface rather than from sea level,

FIGURE 3-9

CRUSTAL COLUMNS

FOR PRATT ISOSTASY
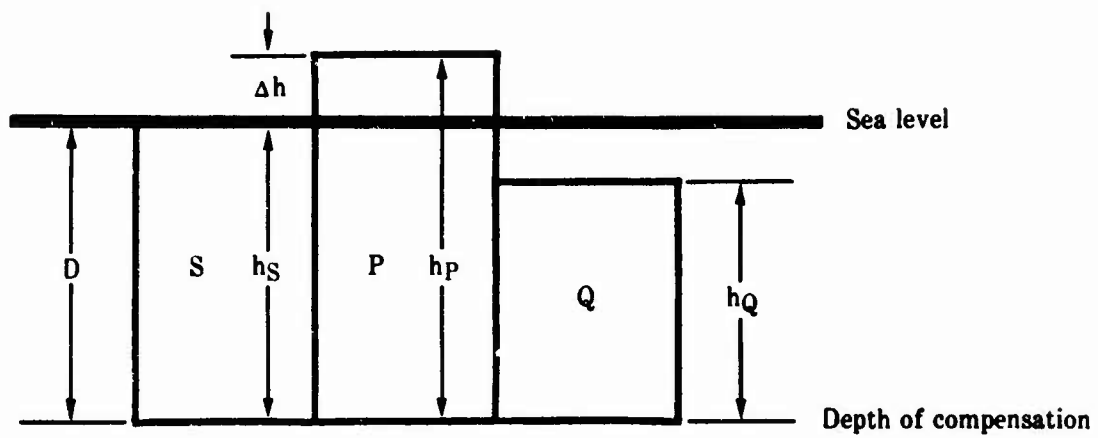
FIGURE 3-10

CRUSTAL COLUMNS

FOR PRATT-HAYFORD ISOSTASY

124
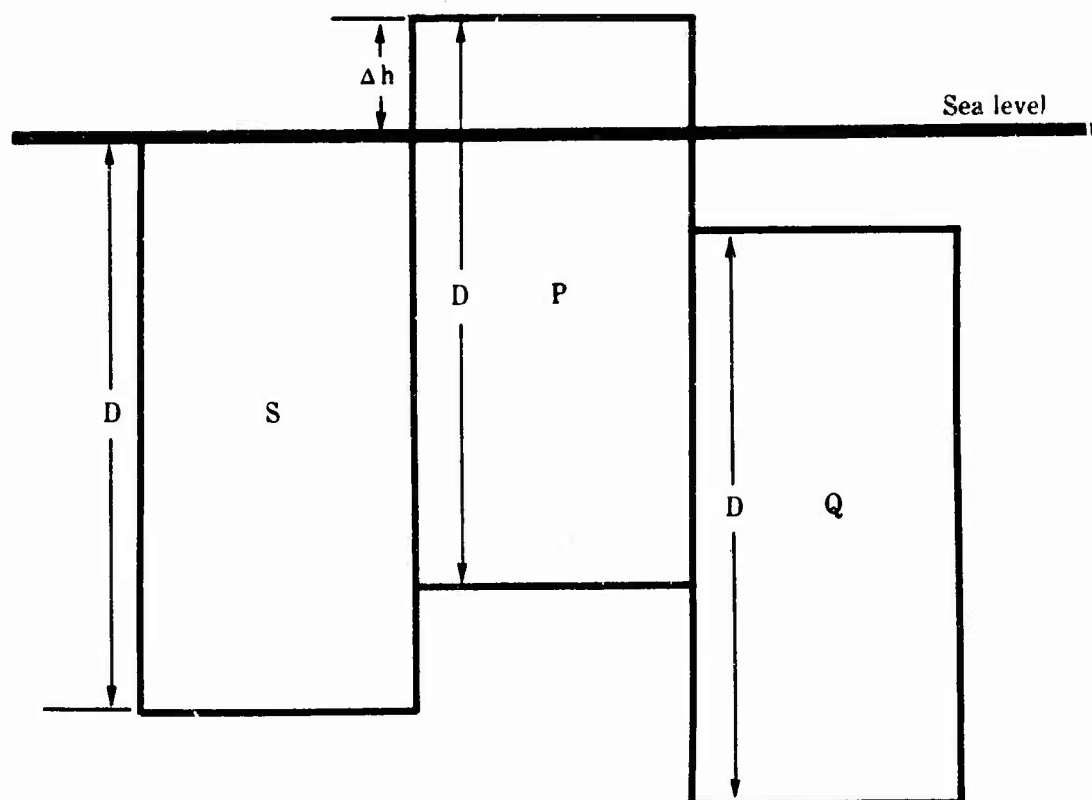
Figure 3-10. Thus, in the so-called Pratt-Hayford system, equation (3.10-9) must be modified to read

$$\Delta\sigma = \frac{-\Delta h \sigma_S}{D} \qquad (3.10\text{-}10)$$

where D = depth of compensation.

The depth of compensation producing the smallest isostatic gravity anomalies in the United States was determined to be 113.7 kilometers (Hayford and Bowie, 1912). In the Pratt-Hayford system, therefore, complete isostatic equilibrium is achieved near the top of the aesthenosphere.

Gravitational analysis of the structure of the crust and upper mantle is seldom done using Pratt-Hayford isostatic theory probably because the only information provided by this theory--changes in mean density of the earth above the level of compensation--is insufficiently diagnostic of corresponding changes in structure. Also, the infinite Bouguer plate type formula (commonly used for this type of analysis) for the gravitational attraction of Pratt-Hayford compensation,

$$\Delta g_C = -2 \pi k \Delta\sigma D \qquad (3.10\text{-}11)$$

is trivially related to the corresponding formula for attraction of the topography

$$\Delta g_F = 2 \pi k \sigma_S \Delta h \qquad (3.10\text{-}12)$$

Insert (3.10-10) into (3.10-11) and the latter reduces immediately to (3.10-12).

3.10.3 <u>Airy Isostatic Theory</u>

Airy postulated the existence of a relatively
thin crust standing above a denser rock base (the mantle). In
the Airy system, the crust beneath the continents extends downward
into the mantle and, conversely, the mantle under the oceans
projects upward into the crust such that the total mass per unit
area down to some level just beneath the deepest continental root
is everywhere equal. Essentially, Airy's system has a crust of
uniform density floating in a denser mantle material in accordance
with Archimedes Principle.

W. A. Heiskanen developed practical procedures for
computing isostatic anomalies using the Airy principle in 1938.
Also, using the geophysical knowledge of the day together with
geodetic arguments, he proposed density and thickness values
appropriate for Airy-type isostasy.

More recently, G. P. Woollard has used modern
geophysical and geochemical knowledge and evidence to deduce
the most probable density and thickness parameters for an Airy-type
isostatic system. Woollard also introduced and perfected the
"crustal column" method of gravity analysis used in this study.

Consider a pair of crustal columns floating in
the mantle in accordance with Archimedes principle, Figure 3-11.
The upper surface of column S is at sea level; the upper surface
of column P extends h kilometers above sea level. In order to
hydrostatically support the additional mass above sea level,
column P has a root increment which extends a distance ΔR kilometers

FIGURE 3-11

CRUSTAL COLUMNS

FOR AIRY ISOSTASY
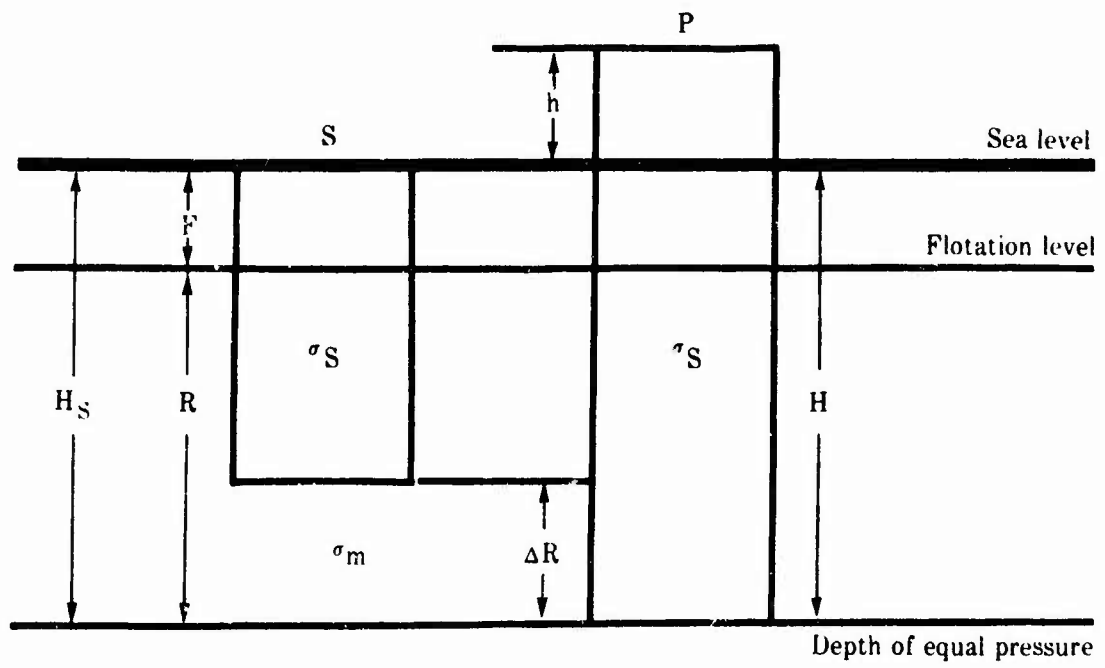
deeper into the mantle than column S. Column S is called the standard or reference sea level column. Column P represents a column of any height whose mean density is the same as the standard column.

Appropriate parameters for these Airy-type crustal columns, as determined by Heiskanen (Heiskanen and Vening Meinesz, 1958) and Woollard (1969a), are given in Table 3-4.

In Table 3-4, σ_S is the expected mean density of the standard crustal column, σ_m is the expected mean density at the top of the mantle, H_S is the expected thickness of the reference sea level crustal column, and H/R is the expected ratio of free board to root. The reader is referred to Woollard (1962) for an extensive discussion of the type of rationale used to deduce these values from geophysical, geochemical, and gravimetric evidence.

Either set of parameters may be used for isostatic anomaly computations since both enable a self-consistent determination of the gravitational effects of topography and its isostatic compensation. However, Woollard's values, being compatible with known geophysical parameters, are more appropriate for studies of crustal and upper mantle structure using gravity anomalies together with other geophysical data.

To develop the basic equations for the Airy isostatic principle note that, according to Archimedes Principle, a floating body displaces its own mass. Therefore, the mass of the standard column, column S of Figure 3-11, is equal to the mass of the mantle material displaced by its root.

TABLE 3-4

PARAMETERS FOR AIRY-HEISKANEN AND AIRY-WOOLLARD ISOSTATIC MODELS

PARAMETER	WOOLLARD	HEISKANEN
σ_S	2.93 gm/cm^3	2.67 gm/cm^3
σ_m	3.32 gm/cm^3	3.27 gm/cm^3
H_S	33 km	30 km
H/R	1/7.5	1/4.45

Since, by (3.10-3) and (3.10-6)

$$m = V\sigma$$

and,
$$V = Ah$$

then,
$$m = Ah\sigma$$

where

m = Mass

V = Volume

A = Cross sectional area

h = height

σ = density

Therefore, for the standard crustal column, it must

be true that

$$AH_S\sigma_S = AR\sigma_m$$

or, dropping the common area factor

$$H_S\sigma_S = R\sigma_m \tag{3.10-13}$$

where the symbols are defined in Figure 3-11.

Equation (3.10-13) can be used to demonstrate the

self-consistency of each parameter set in Table 3-4. From Figure 3-11,

it is evident that

$$F = H_S - R$$

Using Woollard's values

$$R = \frac{7.5}{8.5} H_S = \frac{7.5}{8.5} (33) = 29.118 \text{ km}$$

Similarly, using Heiskanen's values

$$R = 24.495 \text{ km}$$

Insertion of these and other Table 3-4 values into equation (3.10-13) shows that

$$(33) (2.93) = 96.7 = (29.118) (3.32)$$

for Woollard's values and

$$(30) (2.67) = 80.1 = (24.495) (3.27)$$

for Heiskanen's values.

Equation (3.10-13) can be modified to reflect changes in crustal root thickness due to changes in elevation. To convert from the standard sea level column, column S of Figure 3-11, to a general crustal column of elevation, h, column P of Figure 3-11, it is evident that H_S must be replaced by $h + H_S + \Delta R$ and that R must be replaced $R + \Delta R$. Putting these substitutions into equation (3.10-13) gives

$$(h + H_S + \Delta R) \sigma_S = (R + \Delta R) \sigma_m \qquad (3.10-14)$$

A simple rearrangement of terms gives

$$\sigma_S h = (\sigma_m - \sigma_S) \Delta R \qquad (3.10-15)$$

or, in another form

$$\Delta R = \frac{\sigma_S}{\sigma_m - \sigma_S} h \qquad (3.10-16)$$

Equations (3.10-15) and (3.10-16) are basic for Airy-Heiskanen isostasy and show that equilibrium is attained by variations in the depth of the crustal root but without variations in density.

132

Woollard has modified the basic Airy type equations
to allow for a variation in crustal density as well as in crustal
thickness--which is more in keeping with the situation actually
found in nature. Let

$$\sigma_C = \sigma_S + \Delta\sigma_C \qquad (3.10\text{-}17)$$

where

σ_C = actual mean crustal density

σ_S = expected mean density for the standard sea level crust

Replace σ_S by $\sigma_S + \Delta\sigma_C$ in equation (3.10-14) to
obtain

$$(h + H_S + \Delta R)\,(\sigma_S + \Delta\sigma_C) = (R + \Delta R)\,\sigma_m \qquad (3.10\text{-}18)$$

or,

$$h\,(\sigma_S + \Delta\sigma_C) + \Delta R\,(\sigma_S + \Delta\sigma_C) + H_S\sigma_S + H_S\Delta\sigma_C = R\sigma_m + \Delta R\sigma_m$$

Considering (3.10-13) and (3.10-17), the above
reduces to

$$\sigma_C h + \Delta\sigma_C H_S = (\sigma_m - \sigma_C)\,\Delta R \qquad (3.10\text{-}19)$$

or, in another form

$$\Delta R = \frac{\sigma_C h + \Delta\sigma_C H_S}{\sigma_m - \sigma_C} \qquad (3.10\text{-}20)$$

Equations (3.10-19) and (3.10-20) express Airy-
Woollard isostasy*. One further modification can be made to
allow inclusion of an anomalous mantle density. Let

———————————

*The expression, "Airy-Woollard isostasy," is used here for the first
time and connotes a variation of the Airy isostatic model which allows
density variations and uses Woollard's values for the crust/mantle
parameters of the model.

$$\sigma_M = \sigma_m + \Delta\sigma_M \qquad (3.10\text{-}21)$$

where

σ_M = actual mean density of the upper mantle

σ_m = expected mean density of the standard upper mantle

Replace σ_m by $\sigma_M + \Delta\sigma_M$ in (3.10-18) to obtain

$$(h + H_S + \Delta R)\ (\sigma_S + \Delta\sigma_C) = (R + \Delta R)\ (\sigma_M + \Delta\sigma_M)$$

or,

$$h\ (\sigma_S + \Delta\sigma_C) + \Delta R\ (\sigma_S + \Delta\sigma_C) + H_S\sigma_S + H_S\Delta\sigma_C$$

$$= R\sigma_M + R\Delta\sigma_M + \Delta R\ (\sigma_M + \Delta\sigma_M)$$

Considering (3.10-13), (3.10-17), and (3.10-21),

the above reduces to

$$\sigma_C h + \Delta\sigma_C H_S - \Delta\sigma_M R = (\sigma_M - \sigma_C)\ \Delta R \qquad (3.10\text{-}22)$$

or, in another form

$$\Delta R = \frac{\sigma_C h + \Delta\sigma_C H_S - \Delta\sigma_M R}{\sigma_M - \sigma_C} \qquad (3.10\text{-}23)$$

Since $H_S = F - R$, the two equations above also may

be written in the form

$$\sigma_C h + (\Delta\sigma_C - \Delta\sigma_M)\ H_S + \Delta\sigma_M F = (\sigma_M - \sigma_C)\ \Delta R \qquad (3.10\text{-}24)$$

$$\Delta R = \frac{\sigma_C h + (\Delta\sigma_C - \Delta\sigma_M)\ H_S + \Delta\sigma_M F}{\sigma_M - \sigma_C} \qquad (3.10\text{-}25)$$

The difference between Airy-Heisanen isostasy (no density variation) commonly used for isostatic anomaly computations and the geophysically more realistic Airy-Woollard type of isostasy (density variation possible) is given by the difference between equations (3.10-25) and (3.10-16)

$$\delta \Delta R = \frac{\sigma_C h + (\Delta\sigma_C - \Delta\sigma_M) H_S + \Delta\sigma_M F}{\sigma_M - \sigma_C} - \frac{\sigma_S h}{\sigma_M - \sigma_S} \qquad (3.10\text{-}26)$$

For the case of zero elevation (h=0), the above

reduces to

$$\delta \Delta R_{h=0} = \frac{(\Delta\sigma_C - \Delta\sigma_M) H_S + \Delta\sigma_M F}{\sigma_M - \sigma_C} \qquad (3.10\text{-}27)$$

Equation (3.10-27) shows that an increase in crustal
thickness is required to maintain isostatic equilibrium when
mean crustal density exceeds the standard value, when mean upper
mantle density is less than the standard value, or both. Conversely,
a decrease in crustal thickness is necessary to maintain isostatic
equilibrium when $\sigma_C < \sigma_S$, when $\sigma_M > \sigma_m$, or both. Since usually
$|\Delta\sigma_C| > |\Delta\sigma_M|$, the crustal effects usually are predominant.

Now a greater than normal mean density in the crust
($\Delta\sigma_C$ positive) must exert a positive influence on observed gravity
but, for this case, an insufficient amount of compensation
(ΔR too small) is predicted by Airy-Heiskanen isostatic theory
which ignores the effects of variations in mean crustal density.
As a result, the Airy-Heiskanen isostatic anomaly may be positive
even though isostatic compensation is complete. Conversely, a
lower than normal mean crustal density can yield a negative
Airy-Heiskanen isostatic anomaly even though isostatic compensation
may be complete.

In fact, all isostatic anomaly forms are subject to
and dependent upon the isostatic model chosen to compute them.
If the model is incorrect, the anomalies may give false indications
of isostatic conditions.

A summary of the effects on crustal root increment of variations in mean crustal and upper mantle density is given in Table 3-5. Numerical examples of the effects of crustal density variations on Airy-type isostasy are given by Woollard (1969).

3.10.4 Gravity Analysis Using the Airy-Heiskanen Model

The Airy isostatic model can be used in a simple gravity analysis scheme to compute the magnitude of gravitational effects generated by varying isostatic conditions. Such analyses are often useful in deducing local or regional corrections for gravity prediction.

The Airy-Heiskanen version is used here for the sake of simplicity. However, use of the Airy-Woollard version is recommended in all cases where the additional parameters ($\Delta \sigma_C$ and $\Delta \sigma_M$) required by this model are known or can be determined.

The crustal columns of Figure 3-11 are appropriate for Airy-Heiskanen isostasy. The gravitational attraction, g_T, of the topographic mass in column P can be approximated closely by using the Bouguer plate formula (3.7-12),

$$g_T = 2 \pi k \sigma_S h \qquad (3.10\text{-}28)$$

which also can be recognized as the left side of equation (3.10-15) multiplied by $2\pi k$. Similarly, the gravitational attraction, g_I, of the crustal root which compensates the topographic mass in column P can be approximated by

$$g_I = 2\pi k (\sigma_m - \sigma_S) \Delta R \qquad (3.10\text{-}29)$$

TABLE 3-5

EFFECT OF DENSITY CHANGES

ON AIRY CRUSTAL ROOT

CASE	σ_C	σ_M	$\Delta\sigma_C$	$\Delta\sigma_M$	$\delta\Delta R$	
					h = 0	h = 1
1	2.93	3.32	0	0	0	0
2	2.98	3.34	+0.06	+0.02	+3.9	+4.6
3	2.98	3.32	+0.06	0	+5.8	+7.1
1	2.98	3.30	+0.06	-0.02	+8.0	+9.8
5	2.87	3.34	-0.06	+0.02	-5.5	-6.9
6	2.87	3.32	-0.06	0	-4.4	-5.5
7	2.87	3.30	-0.06	-0.02	-3.3	-4.1
8	2.93	3.34	0	+0.02	-1.4	-1.8
9	2.93	3.30	0	-0.02	+1.6	+2.0

$\sigma_c = 2.93,\quad \sigma_m = 3.31,\quad H_S = 33,\quad R = 29.118$

which also can be recognized as the right side of (3.10-15)
multiplied by $2\pi k$.

Now recall the general difference equations for
the free air anomaly (3.8-10) and Bouguer anomaly (3.8-12)

$$(\Delta g_F)_P - (\Delta g_F)_S = (g_T)_P - (g_T)_S - [(g_I)_P - (g_I)_S]^*$$

$$(\Delta g_B)_P - (\Delta g_B)_S = - [(g_I)_P - (g_I)_S]$$

Insertion of (3.10-28) and (3.10-29) into the above
gives

$$(\Delta g_F)_P - (\Delta g_F)_S = 2 \pi k \sigma_C (h_P - h_S) - [2 \pi k (\sigma_m - \sigma_S) (\Delta R_P - \Delta R_S)]$$
$$(3.10\text{-}30)$$

$$(\Delta g_B)_P - (\Delta g_B)_S = - [2 \pi k (\sigma_m - \sigma_S) (\Delta R_P - \Delta R_S)] \quad (3.10\text{-}31)$$

Equations (3.10-30) and (3.10-31) are the fundamental
relationships for gravity anomaly analysis using the Airy-Heiskanen
isostatic model, and enable computation of actual values for the
differences in free air and Bouguer anomalies over columns S and P,
Figure 3-11.

Assume an elevation of one kilometer ($h_P = 1$ km)
for column P. The length of crustal root (ΔR_P) required to
isostatically balance one kilometer of topography is readily
determined from the free board to root ratio. Since, for the Airy-
Heiskanen system, $F/R = 1/4.45$, then $\Delta R = 4.45$ km because the

_____

*The terrain correction terms have been omitted in this approximation.
The change of subscript Q to S is obvious.

change in F is 1 km. Alternatively, the value for ΔR can be determined using equation (3.10-16) and the appropriate Airy-Heiskanen parameters. From Table 3-4

$$\Delta R = \frac{\sigma_S h}{\sigma_m - \sigma_S}$$

$$\Delta R_{F(h=1)} = \frac{(2.67)\,(1)}{3.27 - 2.67} = 4.45 \text{ km} \qquad (3.10-32)$$

The values for the standard sea level column, column S of Figure 3-11, are $h_S = 0$, and $\Delta R_S = 0$.

Putting values appropriate for columns F and S, Figure 3-11, and the Airy-Heiskanen parameters from Table 3-4 into equations (3.10-30) and (3.10-31) shows that

$$(\Delta g_F)_P - (\Delta g_F)_Q = (41.91)\,(2.67)\,(1-0)$$

$$- [(41.91)\,(3.27 - 2.67)\,(4.45 - 0)] = 0$$

and

$$(\Delta g_B)_P - (\Delta g_B)_Q = - [(41.91)\,(3.27 - 2.67)\,(4.45 - 0)] = -111.9 \text{ mgal}$$

The free air anomaly result confirms the condition (3.6-15) and the Bouguer anomaly result confirms the approximate relation (3.7-23) for the case of a constant degree of compensation in columns S and P.

The geophysical gravity prediction methods assume the existence of a constant degree of regional compensation from one 1° x 1° area to the next--which in most cases is entirely realistic. However, abnormal isostatic conditions are encountered occasionally where changes in degree of regional compensation occur

and must be included in the prediction scheme as a regional
correction. In addition, local corrections must be determined
for certain types of local structures whose local gravitational
expression is generated by isostatic effects as well as topographic
variations and near surface density contrasts. Gravity analysis
using crustal models can be a useful technique for developing
such corrections.

Consider, for example, the upper model of Figure 3-12.
Column Q is in complete isostatic equilibrium and has a topographic
mass whose elevation is one kilometer ($h_Q = 1$ km). Therefore,
the length of its crustal root increment using Airy-Heiskanen
parameters is 4.45 km ($\Delta R_Q = 4.45$ km). The topographic mass on
column P has a lower elevation than that on column Q ($h_P < h_Q$),
but the depth of its crustal root is identical to that of column Q
($\Delta R_P = \Delta R_Q$).

The upper model of Figure 3-12 is essentially a
"before" and "after" situation where column P might have been
created by rapid erosion of the topography or by rapid melting of
a glacial ice load atop column Q. There has been insufficient
time for column P to reattain isostatic balance after topographic
mass removal--this condition is simulated by assigning the same
length of crustal root to column P as to column Q. In other words,
column P is over compensated (too deep a crustal root).

Suppose the elevation of the topographic mass atop
column P (upper model) Figure 3-12 is 0.95 km, the topmost 0.05 km
of mass having been removed by rapid erosion. Using $h_P = 0.95$ and

FIGURE 3-12

AIRY ISOSTATIC MODELS

FOR RAPID EROSION,

GLACIER REMOVAL,

LOCAL UNCOMPENSATED TOPOGRAPHY,

AND MAJOR HORST

MODEL FOR RAPID EROSION
GLACIER REMOVAL
AND LOCAL UNCOMPENSATED TOPOGRAPHY
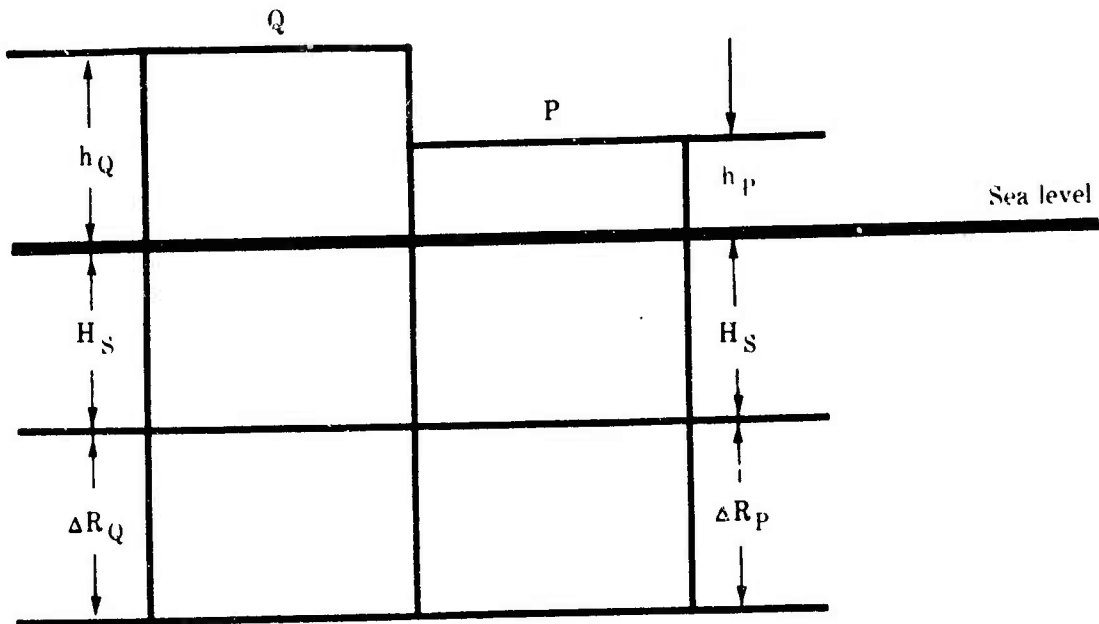
MODEL FOR MAJOR HORST
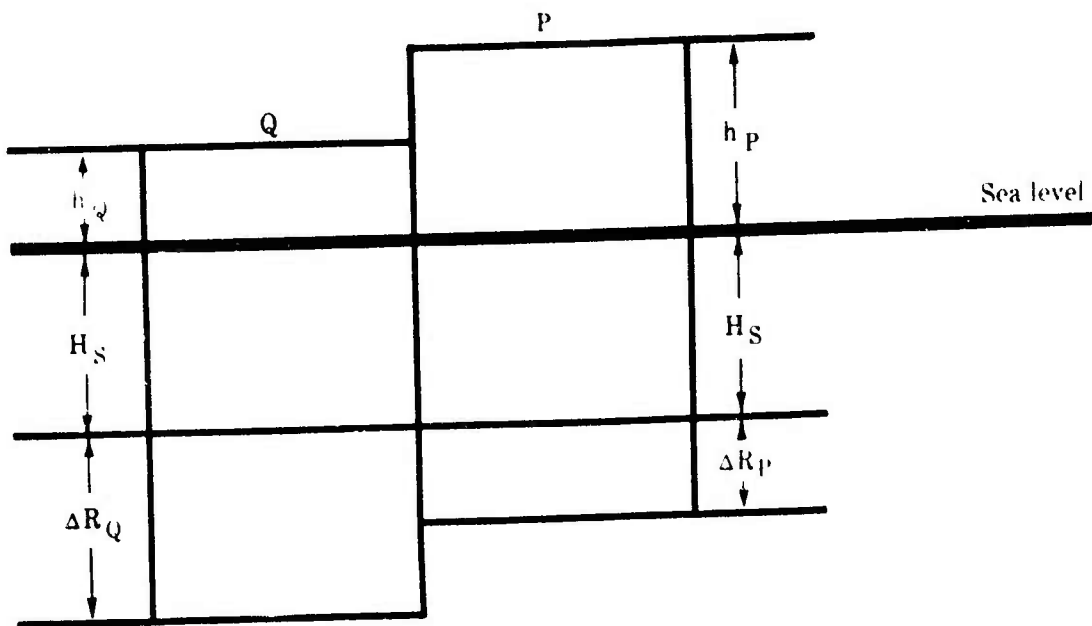
other values appropriate for the model into the general difference

equations (3.10-30) and (3.10-31) shows that

$$(\Delta g_F)_P - (\Delta g_F)_Q = (41.91)\,(2.67)\,(0.95 - 1.0) - [(41.91)\,(3.27 - 2.67)$$

$$(4.45 - 4.45) = -(6 - 0) = -6 \text{ mgal} \qquad (3.10\text{-}33)$$

$$(\Delta g_B)_P - (\Delta g_B)_Q = -[(41.91)\,(3.27 - 2.67)\,(4.45 - 4.45)] = 0$$

$$(3.10\text{-}34)$$

The free air anomaly result confirms that the relation

(3.8-9) reduces to (3.6-24) in that the second term vanishes, and

the Bouguer anomaly result confirms the relation (3.7-22) for

the case of an uncompensated topographic difference.

In straight forward fashion, the correction to be

applied for a prediction in terms of free air anomalies is given

directly by the above computation, in this case - 6 mgal—which

approximates the local correction actually required for some eroded

mountain areas. The correction to be applied for a prediction using

Bouguer anomalies is also - 6 mgal, not zero as is suggested by

the above computation. The reason for this is that the Bouguer

anomaly predicted for column P assuming compensation will be too

positive. With a constant degree of isostatic compensation,

equation (3.10-31) gives

$$(\Delta g_B)_P - (\Delta g_B)_Q = -2\pi k\,(3.27 - 2.67)\,(4.23 - 4.45) = +6 \text{ mgal}$$

where

$$\Delta R_P = \frac{2.67\,(0.95)}{3.27 - 2.67} = 4.23 \text{ km}$$

The actual difference, as computed by (3.10-34) is zero. Therefore, the correction to be applied is

$$(\delta \Delta g_B)_A - (\delta \Delta g_B)_C = 0 - 6 = -6 \text{ mgal}$$

where

$(\delta \Delta g_B)_A$ = actual difference in Bouguer anomaly

$(\delta \Delta g_B)_C$ = difference in Bouguer anomaly assuming a constant degree of compensation

Consequently, for prediction purposes, the correction computed by (3.10-30) is applicable to predictions made in terms of either the free air or the Bouguer anomaly.

For the case of ice load removal, the computation is somewhat more complex because the density of glacial ice (0.917 gm/cm^3) must replace the mean crustal density for the topographic segment of height $h_Q - h_P$. For this example, assume that $h_P = 0.7$ km and, as before, $h_Q = 1$ km then,

$$\Delta R = \frac{(0.7)(2.67) + (0.3)(0.917)}{3.27 - 2.67} = 3.57 \text{ km}$$

and

$$(\Delta g_F)_P - (\Delta g_F)_Q = (41.91)(0.917)(0.7 - 1.0)$$

$$- [(41.91)(3.27 - 2.67)(3.57 - 3.57)] = -12 \text{ mgal}$$

In fact, both highly eroded mountain areas and recently deglaceated regions are typified by anomalously negative gravity anomalies. In both cases, the over compensated crustal blocks should begin to rise in order to reattain a condition of isostatic equilibrium. The rate of uplift can often be correlated with the negative anomaly and a regional or local correction can be

developed from this relationship rather than by use of a crustal
model.

Similar models can be applied to compute gravitational
effects associated with other types of structures which, typically,
are isostatically unbalanced. The method fails in some special
situations such as areas of heavy sedimentation which, logically,
should be under compensated due to rapid accumulation of additional
surficial mass. By observation, however, such areas generally are
not characterized by a positive bias in gravity anomalies. A
possible explanation for this phenomenon is that the negative
gravitational effects of the low density surficial sediments tends
to counterbalance the positive gravitational effects of under
compensation.

3.10.5 Limitations of Airy Isostatic Theory

Airy isostatic theory assumes that isostatic compensation
is achieved totally by the crust floating in a denser plastic mantle
material. The Airy-Heiskanen model additionally assumes that
compensation is achieved entirely by variations in crustal thickness
(i.e., without variation in density). Recent interpretations of
seismic refraction and reflection data suggest that the Airy-
Heiskanen assumption is an oversimplification.

Maps of crustal thickness and seismic velocity recently
published by Pakiser and Zietz (Pakiser and Zietz, 1965), for
example, show that there is no appreciable crustal thickening
under most mountainous areas in the United States. Yet, the
Airy-Heiskanen model definitely requires that crustal thickening

take place under areas of high topography and vice versa. These
maps also show that the crust is abnormally thick in comparison
to topographic heights under the western Great Plains, and abnormally
thin in comparison to topographic elevations under the Basin and
Range province.

Consideration of density changes in the crust and
mantle as indicated by changes in seismic velocity, using the Airy-
Woollard isostatic model, satisfactorily explains much of the crustal
thickness variations which appear abnormal in terms of the
Airy-Heiskanen model (Woollard, 1966, 1968c, 1969b; Strange and
Woollard, 1964). However, even the Airy-Woollard model cannot
completely explain all observed crustal thickness relationships.
Evidently, isostatic compensation is not always totally achieved
by density contrasts at the crust-mantle boundary-in at least some
instances there must be additional density contrasts within the
mantle which account for part of the compensation. These have
yet to be modelled successfully.

Although Airy-type isostatic gravity analysis cannot
be applied too literally, they cannot be discarded either since
such analyses provide an understanding of certain types of gravity
anomaly occurrences which can be obtained in no other way.

3.11 Other Geophysical Considerations of Importance to Gravity
Prediction

Before attempting geophysical gravity prediction, the physical
scientist should be familar with the nature of lateral and vertical
variations in the crust and mantle of the earth, as deduced from

146

various types of geophysical measurements. The reader is referred
to the ample published literature to obtain this information.

In addition to the works authored or co-authored by
G. P. Woollard, the following are recommended: Jacobs et al., 1970;
Garland, 1971; Issacs et al., 1968; Jeffreys, 1970; and Stacey, 1969.

4. NORMAL GRAVITY ANOMALY PREDICTION METHOD (NOGAP)

4.1 Fundamental NOGAP Prediction Formula

The Normal Gravity Anomaly Prediction Method (NOGAP) can be used to predict mean gravity anomaly values for most continental $1° \times 1°$ areas whether or not any gravity measurements exist within those $1° \times 1°$ areas. For this reason, NOGAP is the geophysical gravity anomaly prediction method most frequently used, especially in regions which contain a minimum of gravity measurements.

Input data required for NOGAP predictions includes $1° \times 1°$ mean elevation values and geologic, tectonic, and geophysical maps and documents which provide information sufficient to enable analysis and interpretation of the structures and conditions which cause mean gravity anomaly variations. Some measured gravity data is helpful--but not required.

A $1° \times 1°$ mean Bouguer gravity anomaly is predicted by the NOGAP method as the sum of four terms, each of which is individually determined. The first two terms, basic predictor and regional correction, contain the regional component of the prediction. The two remaining terms, local geologic correction and local elevation correction, contain the local component of the prediction.

$$\overline{\Delta g}_B = BP + \overline{g}_R + \overline{g}_L + \overline{g}_E \qquad (4.1-1)$$

where

$\overline{\Delta g}_B$ = predicted $1° \times 1°$ mean Bouguer anomaly

BP = basic predictor

$\overline{g}_R$ = regional correction

$\overline{g}_L$ = local geologic correction

$\overline{g}_E$ = local elevation correction

The predicted $1° \times 1°$ mean free air anomaly is obtained from the predicted $1° \times 1°$ mean Bouguer anomaly by the use of equation (3.7-14)

$$\overline{\Delta g_F} = \overline{\Delta g_B} + 0.1119 \,\overline{h} \qquad (4.1-2)$$

where

$\overline{\Delta g_F}$ = predicted $1° \times 1°$ mean free air anomaly

$\overline{h}$ = $1° \times 1°$ mean elevation

4.2 Basic Predictor

4.2.1 Discussion

The existence of constant (linear) relationships between changes in the regional component of mean Bouguer gravity anomalies and changes in the corresponding mean elevations has been established conclusively by Woollard (1968b, 1969a) and Wilcox (1971). The simplicity, consistency, and almost universal occurrence of such relationships together with the fact that mean elevation data is the most widely available geophysical data on the continents makes this type of correlation an ideal foundation for the development of the fundamental prediction function called the basic predictor (BP).

The basic predictor used in NOGAP prediction is the equation of the linear regression between $1° \times 1°$ mean Bouguer anomaly values and the corresponding mean elevation values, essentially equation (3.5-8) or (3.7-27)

$$BP = \alpha_R + \beta_R \ \bar{h} \qquad\qquad (4.2\text{-}1)$$

where

   BP = basic predictor

α_R, β_R = regression constants

   $\bar{h}$ = mean elevation

The basic predictor equation (4.2-1) is derived in a region where the gravity anomaly field is known (control region) and applied to predict basic regional gravity anomaly values in an adjacent region (prediction region) which contains few or no gravity measurements. Both control and prediction regions should be contained within the same geologic/tectonic province.

The size of the geologic/tectonic province whose mean anomaly--mean elevation relationship can be defined by a single basic prediction function is variable. The province may be quite large (Europe, Rocky Mountains Cordillera, etc.) or rather small (Baltic Shield, Korean Peninsula, etc.). Also, different basic predictors sometimes are applicable to high, intermediate, and low mean elevations. The extent of applicability of each basic predictor must be established by careful observation of the relationships which exist within the control region.

In deriving and applying the basic prediction function, equation (4.2-1), the $1° \times 1°$ mean Bouguer anomaly values often are correlated with $1° \times 1°$ mean elevation values (ODM). Alternatively, a more consistent regression may be obtained by correlating $1° \times 1°$ mean Bouguer anomalies with one of two types of weighted $3° \times 3°$ mean elevation values (ME), Figure 4-1.

FIGURE 4-1

WEIGHTED 3° X 3° MEAN ELEVATIONS (ME)

Each square is a 1° x 1° area.

Numbers are weights to be assigned to each 1° x 1° mean elevation (ODM) when computing the ME.

The computed ME values are to be correlated with the 1° x 1° mean Bouguer anomaly value for the center 1° x 1° area.

ME_1

1	1	1
1	2	1
1	1	1

ME_2

1	2	1
2	4	2
1	2	1

The basic predictor can be interpreted geophysically as an indicator of the isostatic, crustal, and upper mantle density distribution conditions which characterize each geologic/tectonic province. The variable form of the basic predictor which is applicable to different provinces probably is caused by differing isostatic mechanisms and variations in crustal and upper mantle density distribution properties. A major strength of the NOGAP method is that such variations can be taken into account without having to construct precise models or make assumptions about the mechanisms involved.

4.2.2 Procedure

Step 1: Divide the total area to be worked into major geologic/tectonic provinces using published geologic/tectonic/ geophysical maps and documents.

Step 2: Compute and/or tabulate $1° \times 1°$ mean elevations (ODM) and weighted $3° \times 3°$ mean elevations (ME) for each geologic tectonic province. Predict and tabulate $1° \times 1°$ mean Bouguer anomalies $(\overline{\Delta g_B})$ for those regions of each geologic/tectonic province where measured gravity data is available (control regions).

Step 3: Determine local geologic corrections, $\overline{g}_L$, and local elevation corrections, $\overline{g}_E$, for all $1° \times 1°$ areas within the control region and insert these into the tabulations made in step 2.

Step 4: For each geologic/tectonic province, make plots of $(\overline{\Delta g_B} - \overline{g}_L)$ vs. ODM, $(\overline{\Delta g_B} - \overline{g}_L - \overline{g}_E)$ vs. ME_1, and $(\overline{\Delta g_B} - \overline{g}_L - \overline{g}_E)$ vs. ME_2. The value $(\overline{\Delta g_B} - \overline{g}_L)$ is the regional component of the $1° \times 1°$ mean Bouguer anomalies which corresponds to the ODM values; the value

$(\overline{\Delta g}_B - \overline{g}_L - \overline{g}_E)$ is the regional component of the $1° \times 1°$ mean Bouguer anomalies which corresponds to the ME values.

Step 5: Examine each plot. If a single regression line provides a good linear fit to the plotted points proceed to step 10. Otherwise, continue with step 6.

Step 6: Reconsider $\overline{g}_L$ determination. Revised correction values for some of the local structures in the control area may provide a better linear fit. In fact, this process is often helpful in refining local geologic corrections determined by the empirical or analytical methods in the prediction areas.

Step 7: Re-examine the geologic/tectonic province boundaries determined in step 1. Adjustment of these boundaries and/or definition of additional provinces frequently is the quickest way to create order out of chaos on the plots. Conversely, it may be possible to combine two or more provinces which have an identical mean anomaly--mean elevation relationship.

Step 8: Consider subdivision of provinces into high, intermediate, and/or low mean elevation regions. This procedure is most useful when the original plot shows linear segments joined by directional discontinuities.

Step 9: A slightly non-linear (curved line) relationship is one indicator of possible necessity to apply a regional correction, $\overline{g}_R$. An unacceptably large point scatter remaining after steps 6-8 have been completed is another indicator of a need for a $\overline{g}_R$. For basic predictor derivation in such cases, determine the regional correction, subtract it from $(\overline{\Delta g}_B - \overline{g}_L)$ and $(\overline{\Delta g}_B - \overline{g}_L - \overline{g}_E)$, and repeat steps 4-8 as necessary.

154

Step 10: Select the most consistent plot (smallest
point scatter) to represent each geologic/tectonic province.
Compute the final linear regression constants, α_R and β_R, and
associated error functions using a least squares solution
(Appendix D). The constants, α_R and β_R, are inserted into
equation (4.2-1) which is applied in the prediction region of
each province.

Options: Many who have considerable experience in
geophysical gravity prediction prefer to use a programmable
desk calculator (or high speed electronic computer in instances
where the amount of data is large) together with an analysis of
residuals to accomplish steps 4 through 9. However, use of the
plots as described is still desirable not only for bringing out
the rationale of the basic predictor derivation process but also
for recognizing gaps in information that need to be filled to
upgrade the constants in the equations derived when using this
approach.

Cautions: The procedure given above cannot be used
to obtain a basic predictor for those geologic/tectonic provinces
(1) where insufficient measured gravity data is available to
enable definition of a control region within that province or
(2) where there is insufficient variation in the mean elevation
values to enable determination of a correlation with variations
in mean gravity anomalies. The corrected average basic predictor
(Section 5.1) must be used in such cases.

4.3 Regional Correction

The basic predictor contains that portion of the regional component of mean Bouguer anomalies which is constant with respect to the mean elevation--mean anomaly correlation throughout a geologic/tectonic province. However, the basic predictor cannot control the gravitational effects of any long period changes in crustal structure, upper mantle structure, or isostatic characteristics within that geologic/tectonic province. Hence, a regional correction, $\bar{g}_{B}$, sometimes must be added to the basic predictor in order to describe the regional gravity anomaly field completely.

Unfortunately, there are as many techniques for determining regional corrections as there are geologic/tectonic provinces which require such corrections. Further, many geologic/tectonic provinces do not require any regional correction at all. Experience and judgement therefore, are indispensable elements of regional correction derivation.

Some indicators of situations requiring a regional correction are mentioned in Step 9 of the basic predictor derivation procedure. A regional correction which eliminates a curvature in the basic predictor relationship can be determined empirically with reference to the curve itself. In all other cases, geophysical evidence must be used to derive the regional correction.

The relationship most frequently used to establish a regional correction is a correlation between mean Bouguer anomalies and crustal thickness (depth of the Mohorovivic Discontinuity below sea level). Such correlations have been used to establish

regional corrections, for example, in the Baltic Shield, the
Caucasus, and portions of Siberia.

Other types of geophysical evidence which may be helpful in
deriving regional corrections include seismic velocity, density,
and possibly heat flow data.

4.4 Local Geologic Correction

4.4.1 Discussion

The local geologic correction, $\overline{g}_L$, accounts for variations
in the Bouguer gravity anomalies caused by uncompensated mass
distribution irregularities in local geologic structure.

Some local gravity anomaly variations are directly
related to near surface density contrasts. Consider, for example,
a basin-like depression in crystalline rocks of average density
which is filled with low density clastic sedimentary rocks. The
low density material occupying the basin contrasted with the
underlying higher density crystallines results in a localized
relative mass deficiency and, consequently, a localized gravity low.
The mechanisms involved here were explained during the discussion
of the geologic correction (Section 3.7.5).

The local correction, $\overline{g}_L$, for density contrast situations
can be determined either by empirical estimation or analytical
computation. Analytical computation involves construction of a
geological structure "model" using published geological data, and
application of formulas which enable computation of the local

gravitational effects of the "model" as a function of size, shape, depth, and density contrast.

Other local gravity anomaly variations, such as those caused by large grabens, are related to local variations in crustal thickness and density or to local isostatic effects. Local correction values for such structures can be determined either using isostatic models (as described in Section 3.10.4) or by empirical estimation.

Empirical estimation involves studies of the gravitational effects of different types of geological structures in areas where the gravity anomaly field is well known, identification of the local anomaly variation signatures of each structural type, and development of a local geologic correction table giving the average local gravitational effects of each structural feature. Local geologic correction values taken from the table are adjusted as necessary to account for unique structural variations in different prediction areas.

Local geologic effects determined by the computational methods are more precise--but not necessarily more accurate than those determined by empirical estimation. In fact, some types of local effects can be determined only by empirical estimation. Certain types of sedimentary basins, for example, exert a positive effect on the local gravity anomalies. In other cases, use of analytical computation in conjunction with empirical estimation produces the best results.

4.4.2 Analytical Computation

A local geologic correction, g_L, may be obtained for any surface point by the analytical computation method whenever two conditions are satisfied.

Condition A: The local gravitational effect is produced primarily by uncompensated density contrasts in near surface geological structure rather than by local crustal and isostatic abnormalities.

Condition B: The size, shape, depth, and density contrasts which define the local geological structures can be determined or estimated.

Examples of structural types which do and do not satisfy condition A are given in Table 4-1.

Published geological maps and documents sometimes provide detailed size, shape, and depth parameters for local geologic structures. More often, the most probable structural parameters must be developed from differing published interpretations.

Accurate rock density data, determined by laboratory measurements, is rarely available. Consequently, density values usually must be estimated using a knowledge of the rock types involved and average rock density tables such as Table 4-2. With sufficient measured gravity data, density profiling procedures (Nettleton, 1939, 1940) can give good results.

Quite frequently, known rock types of a particular local structure must be contrasted with the "basement" rocks. The value, 2.67 gm/cm^3, is commonly thought to be a good estimate of

TABLE 4-1

EXAMPLES OF STRUCTURES WHICH USUALLY

PRODUCE g_L BY DENSITY CONTRAST

Small to medium sized sediment filled depressions (basins)

Igneous intrusions

Igneous extrusions

Granites

Minor horsts and grabens

Some uplifts

EXAMPLES OF STRUCTURES WHICH USUALLY DO NOT

PRODUCE g_L BY DENSITY CONTRAST

Large geosynclinal type basins

Major horst and graben

Abnormal basins

Abnormal uplifts

Folded mountain ranges

Recently deglaceated areas

(Compiled from several G. P. Woollard documents)

TABLE 4-2

AVERAGE DENSITY

OF COMMON CRYSTALLINE ROCK TYPES

$(grams/centimeter^3)$

Meta sediments (slate, schist, quartzite, meta-sandstone, etc)	2.74
Acidic igneous (granite, granite gneiss, etc)	2.67
Intermediate igneous (quartz, granidiorite, granidiorite gneiss, diorite, tonalite, anorthosite, syenite, etc)	2.75
Basic igneous (diabase, gabbro, norite, etc)	2.99
Ultrabasic igneous (amphibolite, pyroxene, etc)	3.24
Extrusive igneous* Tertiary or younger Older than Tertiary	2.70 2.75
Average density for all basement rocks	2.74

*For basic to ultra basic extrusives, a greater density is likely.

(After Woollard, 1962; and Heiland, 1968)

average "basement" rock density. In fact, the figure 2.67 gm/cm^3
is the average density for granites as well as the average density
for all surface rocks including both the sedimentary and
crystalline types. Hence, 2.67 gm/cm^3 is not truly representative
of the "basement" unless the "basement" happens to be composed of
average granites.

Woollard (1962) has determined that 2.74 gm/cm^3 is
the best value to use for average "basement" density, and this
value is recommended for all gravity correlation work where more
specific data is lacking.

Average density contrast values can be obtained by
subtracting the average basement rock density value from the average
density value for specific rock types such as those given in
Table 4-2. The resulting density differences show that a negative
gravitational effect can be expected over acidic igneous rocks
and Tertiary extrusives, a positive effect can be expected over
basic and ultra basic igneous rocks, and that no local effect is
expected over meta-sediments, intermediate igneous rocks, and older
extrusives.

Determination of average density values appropriate for
sedimentary rocks is complicated by variations with age, depth of
burial, porosity, and other factors. The reader is referred to
Woollard (1962) and Strange and Woollard (1964a) for a detailed
discussion of sedimentary as well as crystalline rock density
determinations.

162

4.4.2.1 Sedimentary Basins

Use of analytical computation to obtain the local geologic correction for a sedimentary basin is best demonstrated by an example. Figure 4-2 shows a cross section of a small steep-walled sedimentary basin which is assumed to be roughly circular in plan view. Assume that published geological information used to construct the cross-sectional "model" gives the following parameters for the basin:

(1) The average density of the sedimentary rocks in the basin is $\sigma_S = 2.57$ gm/cm^3, which is a good average value for buried Cenezoic clastics.

(2) The basin is surrounded by basement rocks whose average density is estimated to be $\sigma_B = 2.74$ gm/cm^3.

(3) The surface extent (diameter) of the basin is x = 150 miles ≈ 240 km.

(4) The depth of the basin is 10,000 feet ≈ 3.0 km.

The volume occupied by the basin can be approximated by a vertical right circular cylinder, as shown by the dashed lines on Figure 4-2. The local gravity anomaly effect, g_L, of the relative mass deficiency within the sedimentary basin then can be computed using the simple gravitational attraction formulas for a vertical right circular cylinder. Figure 4-3 shows the formula and relations applicable for computing g_L at any point on the surface. Figure 4-4 shows an alternate formula which can be used to compute g_L at the surface point which lies on

the axis of the cylinder. Using the latter, and comparing the data given in Figure 4-2 to that required by Figure 4-4

$$\Delta\sigma = \sigma_S - \sigma_B = 2.57 - 2.74 = -0.17 \text{ gm/cm}^3$$

$$h = y = 3 \text{ km}$$

d = 0 (computation point is on the upper surface of the cylinder)

$$r = \frac{x}{2} = 120 \text{ km}$$

Using equation (4.4-3)

$$a = [(0 + 3)^2 + 120^2]^{\frac{1}{2}} = 120.04 \text{ km}$$

$$b = (0^2 + 120^2)^{\frac{1}{2}} = 120 \text{ km}$$

Finally, applying formula (4.4-2)

$$g_L = (41.91)(-0.17)(3 - 120.04 + 120) = -21 \text{ mgal}$$

The values of a and b computed above are very nearly equal. Hence, the term (h - a + b) in equation (4.4-2) is very nearly equal to h. Examination of Figure 4-4 shows that this always will be true when the lateral extent of the cylinder is much greater than its thickness. Thus, for $\sigma \gg h$, equation (4.4-2) reduces to

$$g_L = 41.91 \, \Delta\sigma \, h \qquad\qquad (4.4-5)$$

which may be recognized as the geologic correction equation (3.7-16).

In practice, equation (4.4-5) gives an excellent approximation of g_L at any point (not too close to the edge) on essentially horizontal structures (e.g., basins, flows, etc.) whose lateral extent is much greater than its thickness.

FIGURE 4-2

EXAMPLE OF SEDIMENTARY BASIN

FOR ANALYTICAL COMPUTATION

OF LOCAL GEOLOGIC EFFECT

σ_S = Density of sedimentary rocks = 2.55 gm/cm^3

σ_B = Density of basement rocks = 2.74 gm/cm^3

X = Extent (diameter) of sedimentary basin = 150 miles $\approx$ 240 km

y = Depth of sedimentary basin = 10,000 feet $\approx$ 3 km
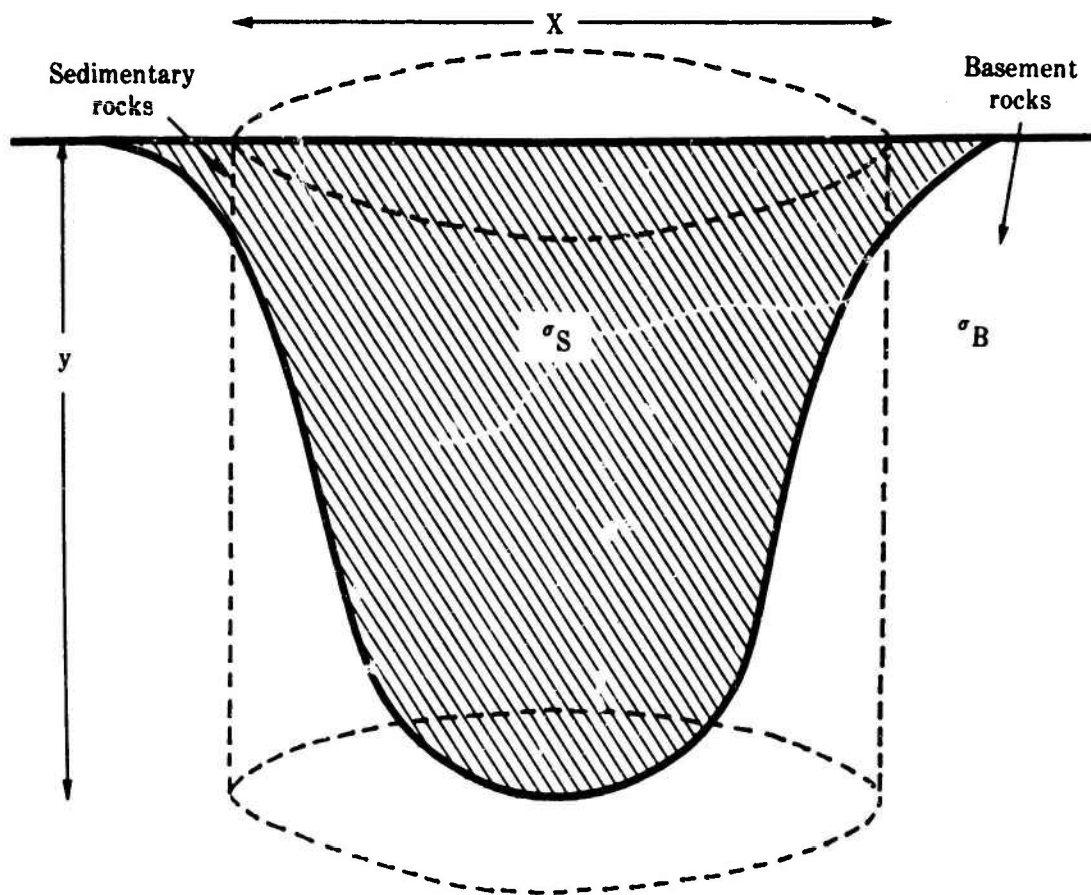
FIGURE 4-3

GRAVITATIONAL ATTRACTION

OF RIGHT CIRCULAR CYLINDER

$$g_L = 6.66 \; \Delta\sigma \; \omega \; h \qquad\qquad (4.4\text{-}1)$$

h in kilometers

ω is the solid angle subtended at the computation point by the
circular boundary of the horizontal plane through the mid point of the
cylinder.

$\Delta\sigma$ in gm/cm^3
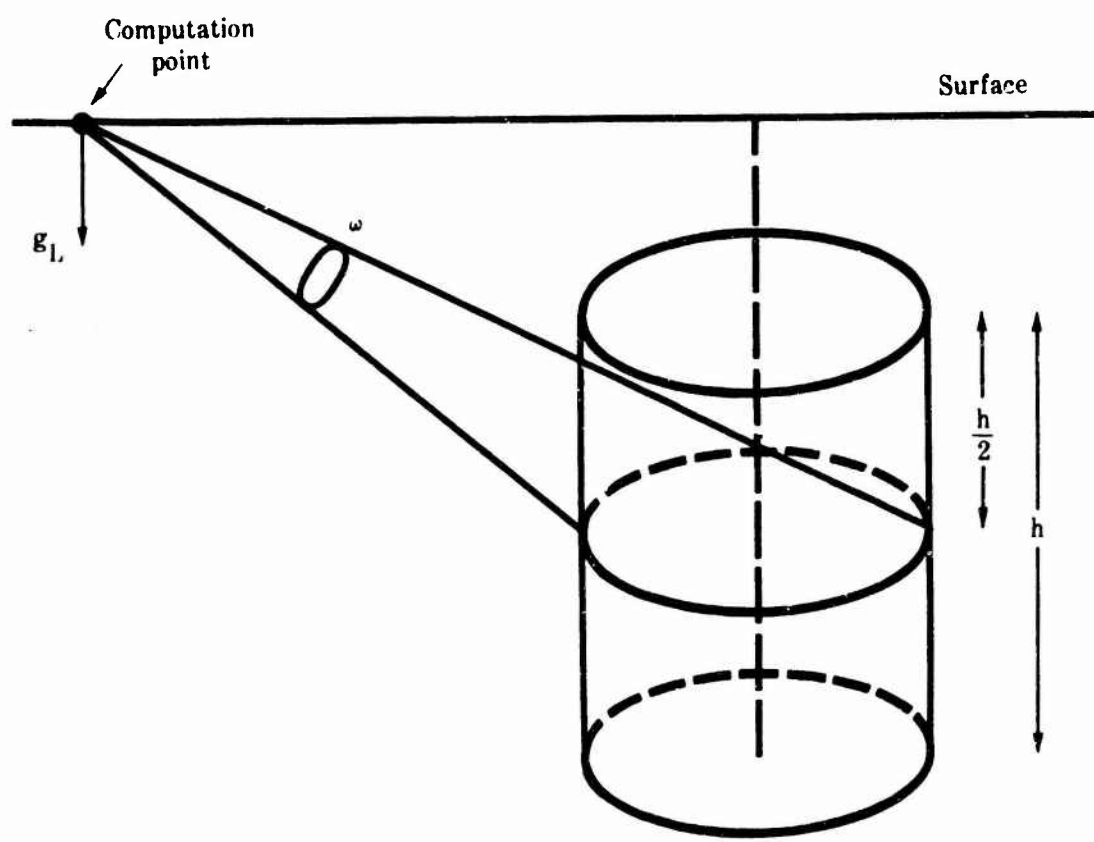
FIGURE 4-4

GRAVITATIONAL ATTRACTION

OF RIGHT CIRCULAR CYLINDER

AT A POINT ON THE AXIS OF THE CYLINDER

$$g_L = 41.91 \ \Delta\sigma \ (h - a + b) \qquad (4.4\text{-}2)$$

$$a = [(d + h)^2 + r^2]^{\frac{1}{2}} \qquad (4.4\text{-}3)$$

$$b = [d^2 + r^2]^{\frac{1}{2}} \qquad (4.4\text{-}4)$$

h, a, b, d, r in kilometers

$\Delta\sigma$ in gm/cm^3
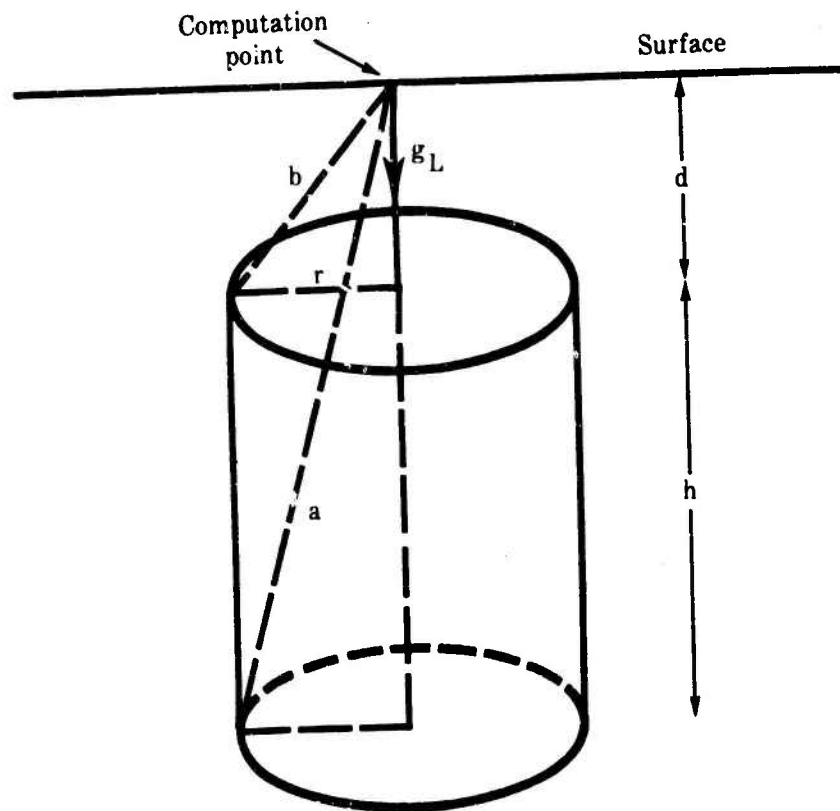
It may be convenient to use formula $(4.4-1)$ for certain types of structures where the condition for use of $(4.4-5)$ is not met. To use equation $(4.4-1)$ the solid angle, ω, must be evaluated. Charts published in Nettleton (1942) are recommended.

Values determined for g_L by these attraction formulas apply to the surface points for which they are computed. To obtain the mean local geological correction for a $1° \times 1°$ area, $\bar{g}_L$, compute g_L for several points which are evenly distributed throughout the $1° \times 1°$ area and average them.

A uniform average density was assumed for the rocks in the sedimentary basin of Figure $4-2$. Actually, sedimentary rock density usually increases as a function of depth of burial due to the effects of compaction. To account for this variation, the sedimentary basin can be stratified into density layers each of which can be approximated by a right circular cylinder (or other appropriate geometric figure). Then the increment of g_L generated by each layer can be calculated, and all such incremental g_L values summed to obtain the total effect. The slight increase in precision obtained in this manner, however, usually is not sufficient to justify the extra work involved for $1° \times 1°$ mean gravity anomaly prediction applications. The exception to this rule is the case of basins which are very irregular in plan view or cross section. Careful detailed modelling of such structures may give improved g_L values.

4.4.2.2 Buried Ridge or Uplifts

The local gravity anomaly effect, g_L, of buried ridges or anticlines can also be illustrated by examples. Figure 4-5 is a cross section of an elongated ridge or uplift in the basement rock beneath a cover of sedimentary rock. Assume that published geological information used to construct the "model" gives the following parameters:

Average density of sedimentary rock, σ_S = 2.57 gm/cm³

Average density of the basement rocks, σ_B = 2.74 gm/cm³

Height of ridge top above the average basement surface, h = 5000 feet ≈ 1.5 km

Depth of ridge top beneath the surface, d = 5000 feet ≈ 1.5 km

Average (normal) basement depth, y = 10,000 feet ≈ 3 km

The volume occupied by the ridge can be approximated by a horizontal right circular cylinder as shown by the dashed lines in Figure 4-5. The appropriate attraction formula is shown in Figure 4-6. Correlating the data given in Figure 4-5 to that required by Figure 4-6

$$\Delta\sigma = \sigma_B - \sigma_S = 2.74 - 2.57 = + 0.17 \text{ gm/cm}^3$$

$$r = \frac{h}{z} = 0.75 \text{ km}$$

$$z = d + r = 2.25 \text{ km}$$

For a computation point on the surface directly above the axis of the cylinder

$$x = 0$$

FIGURE 4-5

EXAMPLE OF A BURIED RIDGE

FOR ANALYTICAL COMPUTATION

OF LOCAL GEOLOGIC EFFECT

σ_S = Density of sedimentary rocks = 2.57 gm/cm^3

σ_B = Density of basement rocks = 2.74 gm/cm^3

h = Height of ridge = 5000 feet $\approx$ 1.5 km

y = Normal depth of basement = 10,000 feet $\approx$ 3 km

d = depth of ridge top = 5000 feet $\approx$ 1.5 km

Surface

Sedimentary rocks

σ_S

d

y

h

σ_B

Basement
rocks
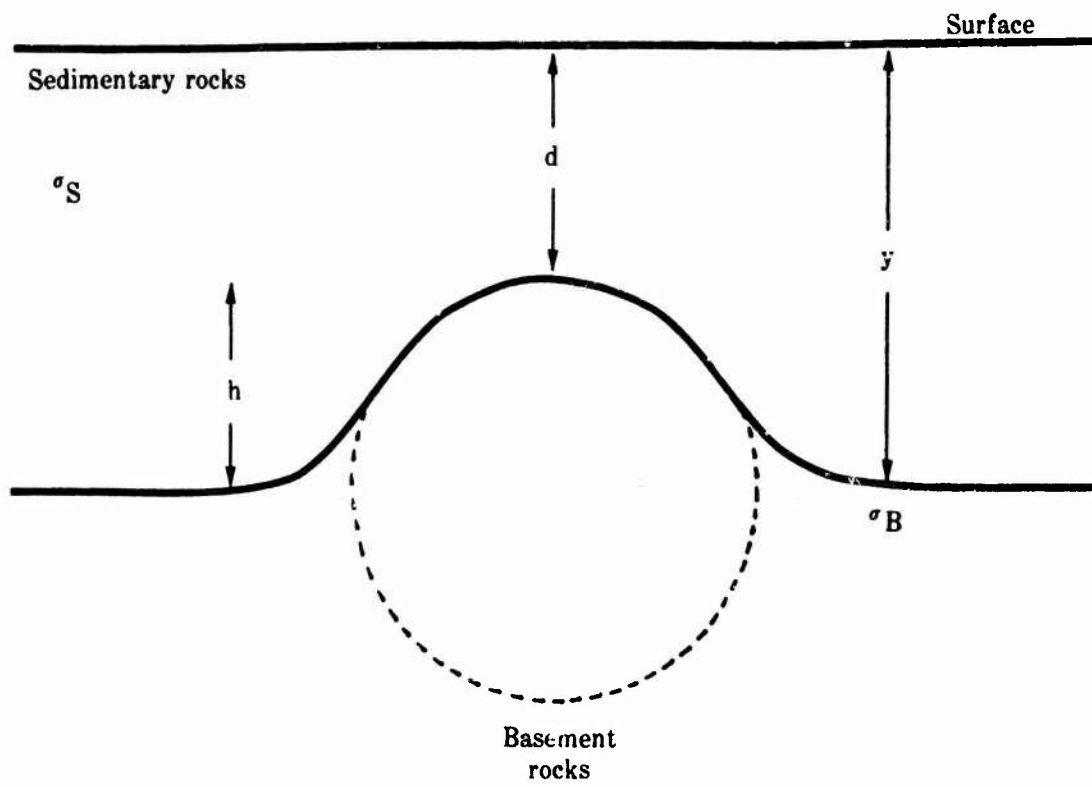
FIGURE 4-6

GRAVITATIONAL ATTRACTION

OF A HORIZONTAL CYLINDER

OF INFINITE EXTENT

$$g_L = 41.91 \frac{\Delta\sigma \ r^2 \ Z}{\ell^2} \qquad (4.4\text{-}6)$$

$$\ell^2 = X^2 + Z^2 \qquad (4.4\text{-}7)$$

d, r, X, Z in kilometers

$\Delta\sigma$ in gm/cm^3
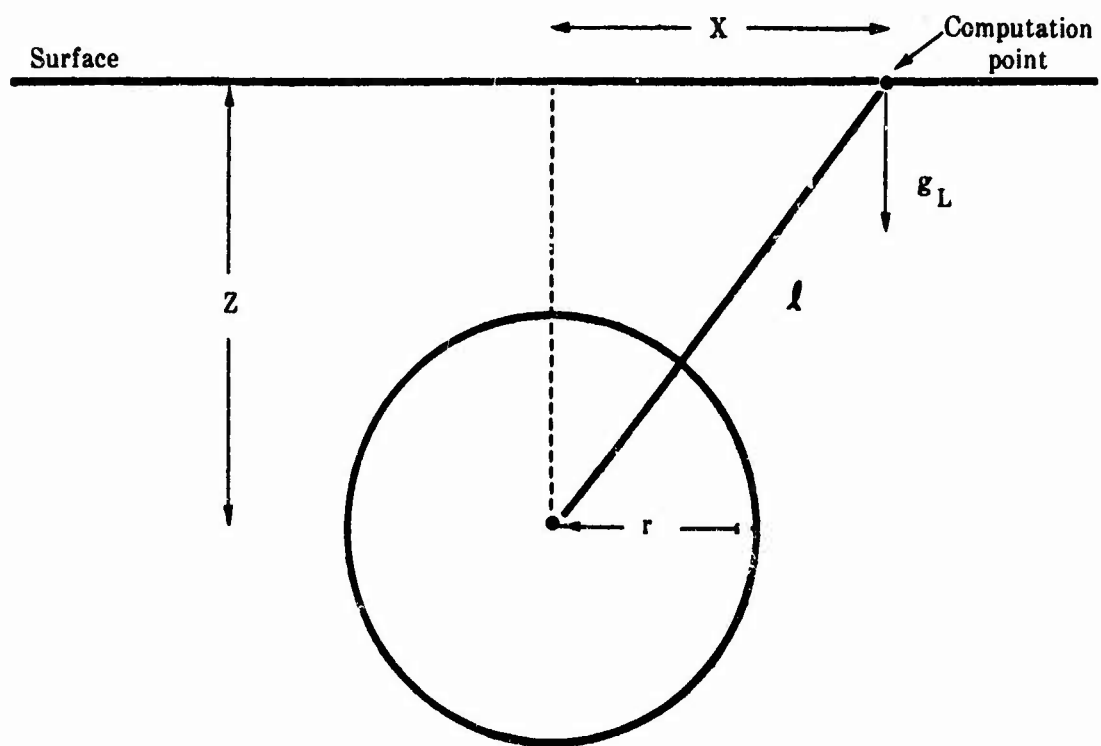
Applying equation (4.4-6)

$$g_L = \frac{(41.91)\ (0.17)\ (0.75)^2\ (2.25)}{0^2 + 2.25^2} = +\ 2\ \text{mgal}$$

Analysis of equation (4.4-6) shows that g_L decreases as the distance of the surface computation point from the ridge axis increases, and that buried ridges or uplifts must be very large and/or near the surface to generate an appreciable g_L.

If the buried ridge of Figure 4-5 happens to be located within the sedimentary basin of Figure 4-2, g_L at a surface point is computed as the combined effect of the two structures as illustrated by Figure 4-7.

4.4.2.3 Plutons and Other Local Structures

Analytical computation of g_L for plutons and other local structures is accomplished in a manner similar to that used in the examples given previously for basins and buried ridges. Approximate the structure by a regular geometric figure and compute g_L using the attraction formula appropriate for that figure. Geometric figures useful for approximation of various structures are listed in Table 4-3. Very irregular structures may have to be approximated by several contiguous figures. In the latter case, high speed computer computations are more efficient than hand calculations. See Beierle and Rothermel (1974) for a detailed listing of attraction formulas and a discussion of computation procedures.

In determining the $\bar{g}_L$ value for $1° \times 1°$ areas, smaller plutons can be ignored. Only fairly massive structures with appreciable density contrast contribute to $\bar{g}_L$. Table 4-4 lists types of igneous structures which do and do not affect the average $1° \times 1°$ $\bar{g}_L$ values.

4.4.2.4 Procedure

Step 1: Determine applicability of analytical computation method--see if both conditions A and B are satisfied.

Step 2: Construct the most probable "model" of the local structures using published geological data. Define size, shape, and depth parameters.

Step 3: Assign density values to local structures and the basement rock; compute density contrasts.

Step 4: Approximate structural "models" using regular geometric figures.

Step 5: Use the gravitational attraction formulas appropriate for each geometric figure to compute g_L values at surface points.(See Beierle and Rothermel, 1974).

Step 6: Average an even distribution of point g_L values within each $1° \times 1°$ area to obtain the mean $\bar{g}_L$ needed for gravity prediction.

Step 7: Compare computed $\bar{g}_L$ with value determined by empirical estimation and adjust as necessary.

Options: In some attraction formulas, use of an average depth for the $1° \times 1°$ area will give a $1° \times 1°$ mean $\bar{g}_L$ directly. In such cases, reduce the computed g_L in proportion to

FIGURE 4-7

EXAMPLE OF BURIED RIDGE

WITHIN A SEDIMENTARY BASIN

Dimensions of each structure are identical to those of structures
shown in Figures 4-2 and 4-5.

$$g_L \text{ for basin} \qquad - 21 \text{ mgal}$$

$$g_L \text{ for buried ridge} \quad \underline{+ \ 2 \text{ mgal}}$$

Total g_L at computation point   − 19 mgal
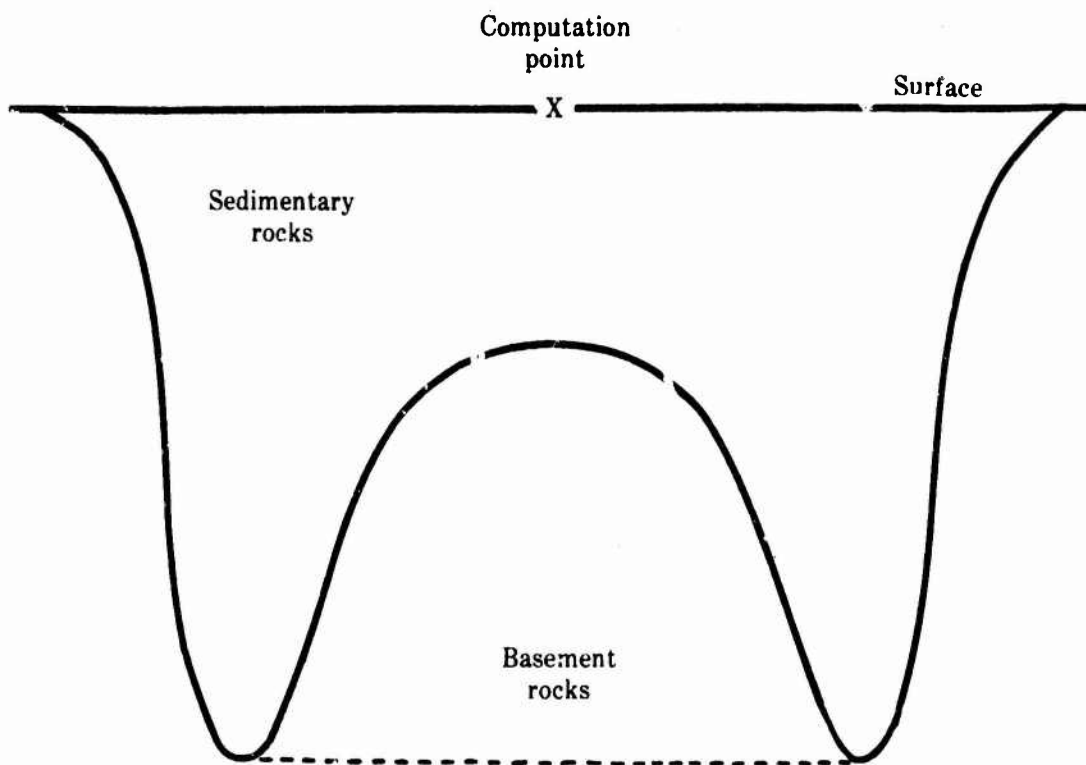
TABLE 4-3

EXAMPLES OF REGULAR GEOMETRIC FIGURES

WHICH CAN BE USED TO APPROXIMATE

LOCAL GEOLOGIC STRUCTURES

STRUCTURE	GEOMETRIC FIGURE
Lopolith, Batholith	Sphere, Hemisphere, Inverted Cone
Laccolith	Hemisphere, Sheet
Caldera	Vertical Rt. Circular Cylinder
Linear Uplift, Buried Ridge	Horizontal Rt. Circular Cylinder
Basin	Rectangular Prism, Vertical Rt. Circular Cylinder, Inverted Cone
Vertical Displacement	Rectangular Prism, Offset
Irregular Features	Group of Prisms

TABLE 4-4

IGNEOUS STRUCTURES WITH/WITHOUT 1° X 1° GRAVITY EFFECTS

Structures Affecting 1° x 1° Mean $\bar{g}_L$	Structures Not Affecting 1° x 1° Mean $\bar{g}_L$
Batholiths	Sills
Laccoliths	Dikes
Large Lopoliths	Shallow Seated Small Plutons
Large Deep Seated Plutons	Thin Flows
Thick Extensive Flows	Small Calderas
Large Calderas	

NOTE: Density contrast must be significant

the percentage of the 1° x 1° area covered by the local structure.
Computations may be done most efficiently using programmable desk
calculators for cases involving a relatively small amount of data.
Otherwise, use of high speed computers is recommended.

Cautions: The analytical computation procedure
can be deceptively simple. Actually, a great deal of skill and
experience is needed to construct a satisfactory "model" and to
evaluate the goodness of the computed g_L values. The situation
where the anomalous mass distribution of near surface geologic
features is partially compensated isostatically is particularly
difficult to handle. In the latter case, the computed g_L values
must be reduced in proportion to degree of compensation which is
estimated to exist.

4.4.3 Empirical Estimation

The heart of the empirical estimation method is Table 4-5,
and Table 4-6 which give the average 1° x 1° local gravity anomaly
effects which are generated by a number of geological structure
types. The table contains values originally proposed by Strange
and Woollard (1964b) and Woollard and Strange (1966) which have been
modified as necessary based upon several years of geophysical
gravity anomaly prediction experience.

4.4.3.1 Discussion of Local Correction Tables

Although the corrections given in Tables 4-5
and 4-6 are derived primarily from empirical evidence, they also
have a sound theoretical foundation.

Note, for example, that the correction for
basins containing relatively old clastic sediments is smaller than
that for basins containing relatively young clastic sediments. The
reason for this is that the older sediments are usually denser than
the younger ones because of (1) greater compaction due to greater
depth of burial, (2) the longer time of being subjected to the pressure
of overlying strata, and/or (3) having been more deeply buried in
the past than at present. The greater density of the older sediments
produces a smaller density contrast with the surrounding crystallines
and, hence, a smaller local geologic correction.

No correction is ever made for basins containing
carbonate sediments since these rock types have average densities
very nearly equal to 2.74 gm/cm^3--so that there is very little, if
any, density contrast with the surrounding basement rock.

In similar manner, the other corrections given
in the Tables can be shown to be compatible with the expected
density contrast and/or local isostatic imbalance situations which
characterize each structural type.

Specific types of areas where no consistent
local correction can be made include Paleozoic sedimentary basins in
stable shield areas, such as the Illinois Basin, very large
geosynclinal basins where isostatic effects counterbalance effects
of sediments, such as the Gulf Coastal area, folded and thrust
faulted mountains such as the Montana Rockies, flood basalt, such
as the Columbia Basalt Plateau region, and stable plains areas such
as the central U. S. (Kansas, Nebraska, the Dakotas, etc.).

TABLE 4-5

TABLE OF LOCAL GEOLOGIC CORRECTIONS
(Part 1)

Corrections given in milligals

1. Granites, Intrusives, Volcanism

    a. Large granitic batholith (e.g., Idaho Batholith)   -50

    b. Other granitic bodies   -20

    c. Ultrabasic intrusives   +20

    d. Tertiary extrusions   -10

    e. Trapped basic and ultrabasic extrusives (e.g., Snake River Downwarp, Mid Continent High)   +40

2. Sediment Filled Depressions (Basins)

    a. Most small to medium sized basins

      (1) Containing 10,000* feet or more of Cenozoic or Cretacious clastic sediments   -20*

      (2) Containing 20,000* feet or more of early Mesozoic or Palezoic sediments   -20*

      (3) Containing carbonate sediments

    b. Large geosynclinal basins

      (1) Containing 20,000* feet or more of Cenozoic clastic sediments   -10*

      (2) Containing pre-Cenozoic clastic sediments

      (3) Containing carbonate sediments

    c. Abnormal basins--due to crustal subsidence, etc.

      (1) Superimposed on shield areas   +20**

      (2) Intermountain (e.g., Hungarian Basin)   +20**

*Reduce correction in proportion to lesser sediment thickness

**Use average of corrections determined from 2a and 2c

TABLE 4-6

TABLE OF LOCAL GEOLOGIC CORRECTIONS
(Part 2)

Corrections given in milligals

3. <u>Fault Bounded Downwarps</u>

    a. Major graben

        (1) Intermountain   -40

        (2) Not in mountains   -50

    b. Minor graben   -20

4. <u>Uplifts</u>

    a. Horsts (fault bounded uplifts)

        (1) Major, intermountain   +30

        (2) Major, not in mountains   +40

        (3) Minor   +20

    b. Abnormal uplifts--due to crustal dilation, etc.

        (1) Superimposed on shield   -30

        (2) Plateaus of eustatic uplift   -15

    c. Other uplifts (not fault bounded)   0 to +20

5. <u>Local Isostatic Imbalance</u>

    a. Folded mountain ranges

        (1) Mesozoic or younger   -10

        (2) Palezoic or older   0

    b. Areas of recent deglaceation

        (1) Major Pleistocene glaciers   -15

        (2) Minor glaciers   0

        (3) Glaciers older than Pleistocene   0

4.4.3.2 Use of Local Correction Tables

Tables 4-5 and 4-6 give the average 1° x 1° local geologic correction $\overline{g}_L$ for structures which occupy all or most of the 1° x 1° area. Corrections given must be reduced proportionally for structures which occupy only a portion of the 1° x 1° area.

When two or more structures requiring a correction occupy the same 1° x 1° area, the applicable $\overline{g}_L$ is computed as the weighted average of the correction for each structure. The weights depend upon the portion of the 1° x 1° area covered by each structure.

For example, suppose 75% of the 1° x 1° area incorporates 10,000 feet of Conezoic clastic sediments in a basin which is about 2° x 2° in extent, and that the other 25% of the same 1° x 1° area incorporates a small horst. The correction for the basin is 0.75 (-20) = - 15 mgal. The correction for the horst is 0.25 (+20) = + 5 mgal. The final correction for the 1° x 1° area is (-15 + 5) = - 10 mgal.

Gravity measurements, where available, should be used to refine the average values given in the table for application to specific structures. Lacking gravity measurements, refinement of the corrections must be based upon experience and geologic intuition.

4.5 Local Elevation Correction

4.5.1 Discussion

A local elevation correction, $\overline{g}_E$, is required whenever 3° x 3° mean elevations (ME) and simple 1° x 1° mean Bouguer anomalies

are used in the basic predictor formulation. The $\bar{g}_E$ accounts for the local gravity anomaly effects of the differences between the $3° \times 3°$ mean elevations and the actual mean elevations of the $1° \times 1°$ areas for which mean anomalies are being predicted.

No local elevation correction is needed when $1° \times 1°$ mean elevations (ODM) are used in the basic predictor formulation.

In view of the local Bouguer anomaly relation (3.7-22)

$$(\Delta g_B)_P = (\Delta g_B)_Q$$

it may seem surprising that a local elevation correction is required to account for the difference between the $1° \times 1°$ and $3° \times 3°$ mean elevation level. However, equation (3.7-22) applies to terrain corrected Bouguer anomalies whereas non-terrain corrected Bouguer anomalies are generally used in NOGAP prediction. The equivalent of (3.7-22) for non-terrain corrected Bouguer anomalies is obtained by inserting equations (3.7-10) and (3.7-12) into equation (3.6-24) which gives the relation

$$(\Delta g_B)_P - (\Delta g_B')_Q = - TC_P + TC_Q \qquad (4.5-1)$$

If P is interpreted as the $1° \times 1°$ mean value and Q as the $3° \times 3°$ mean value, then the local correction, $\bar{g}_E$, necessary to convert a mean Bouguer anomaly predicted with a $3° \times 3°$ mean elevation to a value compatible with the $1° \times 1°$ mean elevation is

$$\bar{g}_E = - TC_P + TC_Q \qquad (4.5-2)$$

where

TC_P = average terrain correction for $1° \times 1°$ mean anomalies

TC_Q = average terrain correction value for $3° \times 3°$ mean anomalies

Values determined by Voss (1972b) for TC_P and TC_Q are

$$TC_P = 0.021 \text{ mgal/meter}$$

$$TC_Q = 0.008 \text{ mgal/meter}$$

Hence,

$$\bar{g}_E = -0.013 \, \delta h \qquad\qquad (4.5\text{-}3)$$

where

$$\delta h = h_P - h_Q = ODM - ME$$

Extensive testing has proven that equation (4.5-3) works well in most areas.

4.5.2 Procedure

Use equation (4.5-3) to determine the local correction whenever the basic predictor is formulated in terms of $3° \times 3°$ mean elevations (ME) and simple $1° \times 1°$ mean Bouguer anomalies.

Omit the local elevation correction whenever the basic predictor is formulated in terms of $1° \times 1°$ mean elevations (ODM).

4.6 Evaluation of NOGAP Predictions

4.6.1 Evaluation Formulas

Using fundamental principles of error theory it can be shown that the standard errors of NOGAP prediction are given by

$$E_B = (e_{B\,P}^2 + e_R^2 + e_L^2 + e_E^2)^{\frac{1}{2}} \qquad (4.6\text{-}1)$$

$$E_F = (E^2_{\,B} + 0.01 \, e^2_{\,H})^{\frac{1}{2}} \qquad (4.6\text{-}2)$$

where all E and e values are standard errors in milligals except for

e_H which is a standard error in meters. Specifically,

E_B = error of $1° \times 1°$ mean Bouguer anomaly predicted by equation (4.1-1)

E_F = error of $1° \times 1°$ mean free air anomaly predicted by equation (4.1-2)

e_{BP} = error of basic predictor

e_R = error of regional correction

e_L = error of local geologic correction

e_E = error of local elevation correction

e_H = error of $1° \times 1°$ mean elevation (ODM)

The error of basic predictor, e_{BP}, is given by

$$e_{BP} = [(\overline{h}\, e_\beta)^2 + (\beta_R\, e_{\overline{h}})^2]^{\frac{1}{2}} \qquad (4.6-3)$$

where

$\overline{h}$ = mean elevation used in basic predictor, equation (4.2-1)

e_β = error in β_R constant of basic predictor equation found using the error propagation formula (D-11) given in Appendix D

β_R = regression slope constant used in basic predictor equation

$e_{\overline{h}}$ = error of mean elevation value used in basic predictor equation

It usually can be assumed in continental areas that the measured gravity data used to derive the basic predictor is error-free. In the rare situations where this is not the case, add the term $e_{\Delta g}^2$ under the radical in equation (4.6-3), where $e_{\Delta g}$ is the error of the measured gravity data.

The errors, e_R and e_L, are estimates of the accuracy of the corrections, $\overline{g}_R$ and $\overline{g}_L$, respectively. Where no values for $\overline{g}_R$ and $\overline{g}_L$ can be determined, then e_R and e_L represent estimates of the

errors incurred by not accounting for local and regional gravity anomaly variations in the prediction.

In estimating values for e_R and e_L, it should be noted that the point scatter in the basic predictor derivation plots is caused primarily by the combined effects of e_R and e_L and, therefore, can be used to determine a first approximation of the average effects of e_R and e_L in the prediction area.

The error in local elevation correction is given by

$$e_E = 0.01 \ (e_H{}^2 + e^2{}_{ME})^{\frac{1}{2}} \qquad (4.6\text{-}4)$$

The error term, e_E, is omitted when the correction $\overline{g_E}$ is not used in the NOGAP prediction.

4.6.2 Proven Reliability of NOGAP Prediction

It is very difficult to establish precise reliability data for NOGAP prediction because the method generally is used in regions which contain very little if any measured gravity data for comparison with the predicted values. However, the overall reliability of the method can be proven by citing three lines of evidence.

Several years ago a number of NOGAP geophysical predictions were made in regions of Eurasia and North America where there was, at the time, very limited amounts of measured gravity data. Some time after the predictions were completed, measured data which covered these prediction areas quite well was acquired by the DOD Gravity Library. Using the measured gravity data, $1° \times 1°$ mean anomalies were computed by conventional methods

and then compared to the 1° x 1° mean values predicted by the NOGAP method. The standard deviation between "measured" and geophysically predicted 1° x 1° mean anomalies are shown in Table 4-7.

Additionally, a test project was conducted in the European area. NOGAP geophysical predictions were made using a very small, poorly distributed sampling of the measured gravity data which exists in the region. The predicted 1° x 1° mean values were compared with "measured" values computed using all measured data. The results are shown in Table 4-8.

Finally, Strange and Woollard (1964b) made geophysical predictions in the United States using a NOGAP-type method. The standard error of these predictions was ± 13 mgal.

It is apparent from the preceding that NOGAP predictions have an accuracy range of 5 to 20 mgal. Most modern predictions fall into a 9 to 15 mgal accuracy range. These figures are not bad considering the minimum input of measured gravity data for most NOGAP predictions. With adequate amounts of measured gravity data, of course, NOGAP accuracies of 1-2 mgal can be attained easily.

TABLE 4-7

STANDARD ERRORS OF GEOPHYSICALLY

PREDICTED 1° X 1° MEAN ANOMALIES

AREA	NUMBER OF 1° X 1° AREAS	RANGE OF PREDICTED VALUES $\overline{\Delta g}_F$ (mgal)	STANDARD ERROR (mgal)
NORTH AMERICA	294	+52 to -61	± 15
EURASIA	159	+128 to - 100	± 9

TABLE 4-8

RELIABILITY OF NOGAP PREDICTIONS

IN WESTERN EUROPE

TYPE AREA	ERROR RANGE (mgal)
Small Basins	~10
Large Basins	~15
Basement exposures	5-10
Geosynclinal mountains	10-20
Graben and Plateaus	5-10
Coastal lowlands	~10

5. MODIFICATIONS AND VARIATIONS - NOGAP PREDICTION

5.1 Corrected Average Basic Predictor

Whenever possible, the NOGAP basic predictor is derived by regression analysis in a control region for application in the prediction region of the same geologic/tectonic province. This approach fails whenever the amount or distribution of measured gravity data within a geologic/tectonic province is insufficient to enable definition of a control region for that province. In such cases, a corrected average basic predictor is needed to enable $1° \times 1°$ mean anomaly prediction by the NOGAP method.

The (uncorrected) average basic predictor function recommended for most applications is

$$BPA = - 0.0894 \ ME_1 \qquad (5.1-1)$$

where

BPA = average basic predictor

ME_1 = weighted $3° \times 3°$ mean elevation, as defined by Figure 4-1,
in meters

Equation (5.1-1) is determined as the mean of the empirically derived equation (5.1-11) and the theoretically derived equation (5.1-12). Other average basic predictor functions having more limited application can be derived by empirical means.

Two special corrections must be added to the average basic predictor to obtain a basic predictor value which is suitable for use in the fundamental NOGAP prediction formula (4.1-1). Thus,

$$BP = BPA + \bar{g}_{IC} + \bar{g}_{DC} \qquad (5.1-2)$$

where

BP = basic predictor for use in (4.1-1)

BPA = average basic predictor from (5.1-1)

$\bar{g}_{IC}$ = isostatic-crustal correction

$\bar{g}_{DC}$ = gravitational effect of distant compensation

The value given by equation (5.1-2) is the corrected average basic predictor.

5.1.1 Empirically Derived Average Basic Predictors

It has been established that variations in the Bouguer gravity anomaly are tantamount to changes in the amount of compensation present, equation (3.8-11). Using Airy isostatic hypothesis, these changes in compensation and, hence, Bouguer anomaly can be interpreted in terms of variations in crustal thickness, equation (3.10-31). Airy isostatic theory also demands variations in crustal thickness to accompany variations in topographic elevation, equation (3.10-16). Seismic evidence and gravitational analysis (Woollard, 1959, 1966, 1968c, 1969b; Strange and Woollard, 1964; Demnitskaya, 1959) show that, on an average worldwide basis, the relations observed between elevation, crustal thickness, and Bouguer anomaly are quite close to those predicted by Airy isostatic theory. In addition, many departures from une Airy theory predictions can be ascribed to variations in the density of the crust and mantle and to some regional isostatic imbalance. These average worldwide relationships provide an excellent foundation for development of average basic predictor functions.

Demnitskaya (1959) has compiled worldwide maps of crustal thickness and compared these data with worldwide Bouguer anomaly and elevation data. Using least squares solution, she determined that the following expressions represent the average relationship between crustal thickness and elevation or Bouguer anomaly.

$$H = 35 \ (1 - \tanh 0.0037 \ \Delta g_B) \qquad (5.1-3)$$

$$H = 33 \ \tanh (0.38 \ h - 0.18) + 38 \qquad (5.1-4)$$

where

H = crustal thickness in kilometers

Δg_B = Bouguer gravity anomaly in milligals

h = elevation in kilometers

Equating the two above expressions and solving for the Bouguer anomaly gives

$$\Delta g_B = - 270.27 \ \tanh^{-1} \ [0.94286 \ \tanh \ (0.38 \ h - 0.18) + 0.00857] \quad (5.1-5)$$

To use equation (5.1-5) as an average basic predictor, replace Δg_B with BPA and h with the appropriate mean elevation in kilometers.

When used as an average basic predictor, equation (5.1-5) gives favorable results in the Eurasian area but fails in North America (Durbin, 1962). This result suggests, logically, that Demnitskaya's measured data was heavily concentrated in the Eurasian area--giving heavier weight to this area in the least squares solution.

Woollard (1959) performed a similar worldwide analysis of crustal thickness, elevation, and Bouguer anomaly data from which the following equations were derived by Durbin (1961).

$$\Delta g_B = 0.115 \ (H + 94.1)^2 - 444.4 \qquad (5.1\text{-}6)$$

$$H = (-1605.358 \ h + 12392.620)^{\frac{1}{2}} - 143.322 \qquad (5.1\text{-}7)$$

which, when the second is substituted into the first gives, after some simplification

$$\Delta g_B = h \ (2.643 \ h - 103) \qquad (5.1\text{-}8)$$

Equation (5.1-8), which can be converted into an average basic predictor function in a manner similar to (5.1-5), gives good results in North America but fails in Eurasia (Durbin, 1962).

A linear equation with quite general application can be derived from relations published by Woollard (1962) based upon more extensive data than was used in 1959.

$$H = 33.4 - 0.085 \ \Delta g_B \qquad (5.1\text{-}9)$$

$$H = 33.2 + 7.5 \ h \qquad (5.1\text{-}10)$$

Equating the two above equations and solving for Δg_B gives

$$\Delta g_B = -88.2 \ h \qquad (5.1\text{-}11)$$

where h is in kilometers and a small constant term has been dropped. Converting to an average basic predictor gives

$$BPA = -0.0882 \ \bar{h} \qquad (5.1\text{-}12)$$

where $\bar{h}$ is an appropriate mean elevation value in meters.

Being worldwide average relations equations (5.1-5), (5.1-8), and (5.1-12) must represent the elevation-Bouguer anomaly correlation for the worldwide average isostatic condition. On a worldwide basis, isostatic compensation is complete.

5.1.2 A Theoretically Derived Average Basic Predictor

To derive an average basic predictor theoretically,
assume that complete isostatic equilibrium exists and compute the
Bouguer anomaly which corresponds to this condition as a function of
mean elevation. An isostatic model can be set up for this purpose
using Airy-Heiskanen isostatic theory, Figure 5-1. A radius of 166 km
is chosen for the model since this radius will enclose approximately
a $3°$ x $3°$ area--the smallest area likely to be in complete isostatic
equilibrium (Woollard, 1962). (Hence, the h term in equation (5.1-11)
must also be a $3°$ x $3°$ mean elevation).

Approximate the compensating root of the Airy-Heiskanen
isostatic model by a vertical right circular cylinder, Figure 5-2,
and compute the gravitational attraction of the compensation using
formula (4.4-2), (4.4-3), and (4.4-4), Figure 4-4. The result is
the Bouguer anomaly corresponding to a condition of isostatic
equilibrium for a $3°$ x $3°$ mean elevation of 1 km.

$$a = [(30 + 4.45)^2 + 166^2]^{\frac{1}{2}} = 169.537 \text{ km}$$

$$b = (30^2 + 166^2)^{\frac{1}{2}} = 168.689 \text{ km}$$

$$\Delta\sigma = 2.67 - 3.27 = -0.6 \text{ gm/cm}^3$$

$$\Delta g_{B_{n=1}} = (41.91)(-0.6)(4.45 - 169.537 + 168.689) = -90.6 \text{ mgal/km}$$

Generalizing this result for any elevation gives the
average basic predictor

$$\text{BPA} = -0.0906 \, \bar{h} \qquad\qquad (5.1-13)$$

where $\bar{h} = 3°$ x $3°$ mean elevation in meters, essentially ME_1
(Figure 4-1).

5.1.3 The Need for Corrections to Average Basic Predictors

The regional component of the Bouguer anomaly, controlled by the basic predictor, is generated by both local and distant distributions of the compensating masses as well as by density anomalies in the crust and upper mantle. Yet the theoretical derivation of the average basic predictor assumes that isostatic compensation is complete (that is, there are no uncompensated regional density anomalies) and takes into account only that compensation which is within a 166 kilometer radius. Also, an assumption that compensation is achieved by the Airy-Heiskanen mechanism was made in the derivation.

The empirically derived average basic predictors are also tied to the Airy isostatic model and represent a condition of complete isostatic equilibrium. Also, the random effects of distant compensation must be averaged out. The close correspondence between the empirical equation (5.1-12) and the theoretical equation (5.1-13) is further evidence that the empirical and theoretical models, in fact, must have very similar properties.

Although the average basic predictor certainly is quite accurate as an expression representing worldwide average conditions, it is logical that some corrections are necessary to convert the average basic predictor to a form which is suitable for use in the NOGAP prediction formula. This is true because, in general, the geophysical properties of any given prediction area will not correspond exactly to the worldwide average properties.

A good understanding of how well the average basic predictor will approximate the actual mean Bouguer anomaly--mean elevation relationship within a given region can be obtained from

FIGURE 5-1

AIRY-HEISKANEN ISOSTATIC MODEL

FOR AVERAGE BASIC PREDICTOR DERIVATION

$\sigma_S = 2.67$ gm/cm^3

$\sigma_m = 3.27$ gm/cm^3

$H_S = 30$ km

$F/R = 1/4.45$

Let: $r = 166$ km

        $h = 1$ km

Then: $R = 4.45$ km
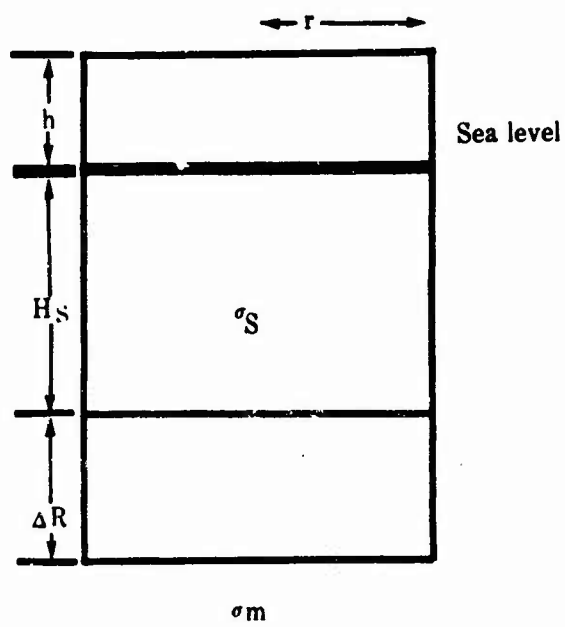
FIGURE 5-2

MODELLING OF COMPENSATION

USING VERTICAL RIGHT CIRCULAR CYLINDER

AND AIRY-HEISKANEN ISOSTASY

H_S = 30 km

ΔR = 4.45 km

r = 166 km
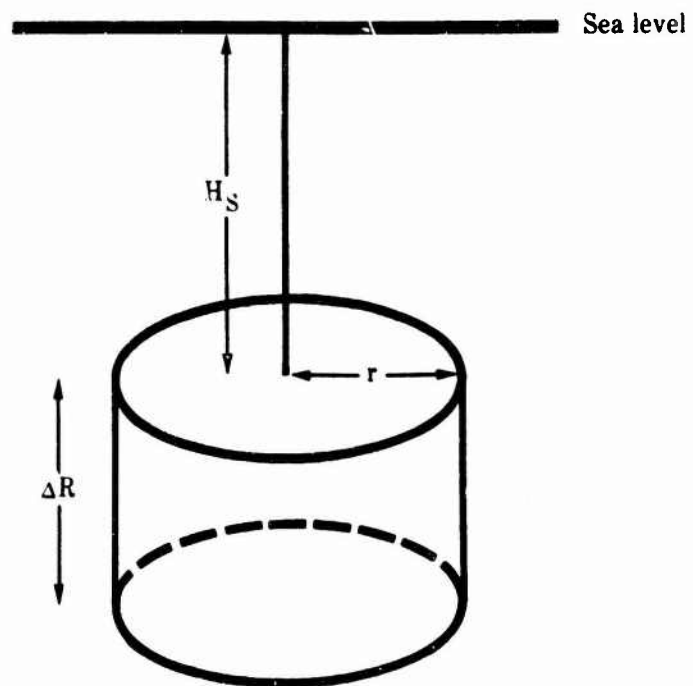
FIGURE 5-3

AVERAGE BASIC PREDICTOR

SUPERIMPOSED ON OBSERVED RELATIONS

OF 3° X 3° MEAN ELEVATIONS AND BOUGUER ANOMALIES

Basic figure from Woollard (1969b)

OBSERVED RELATIONS OF 3°×3° MEAN ELEVATIONS AND BOUGUER ANOMALIES
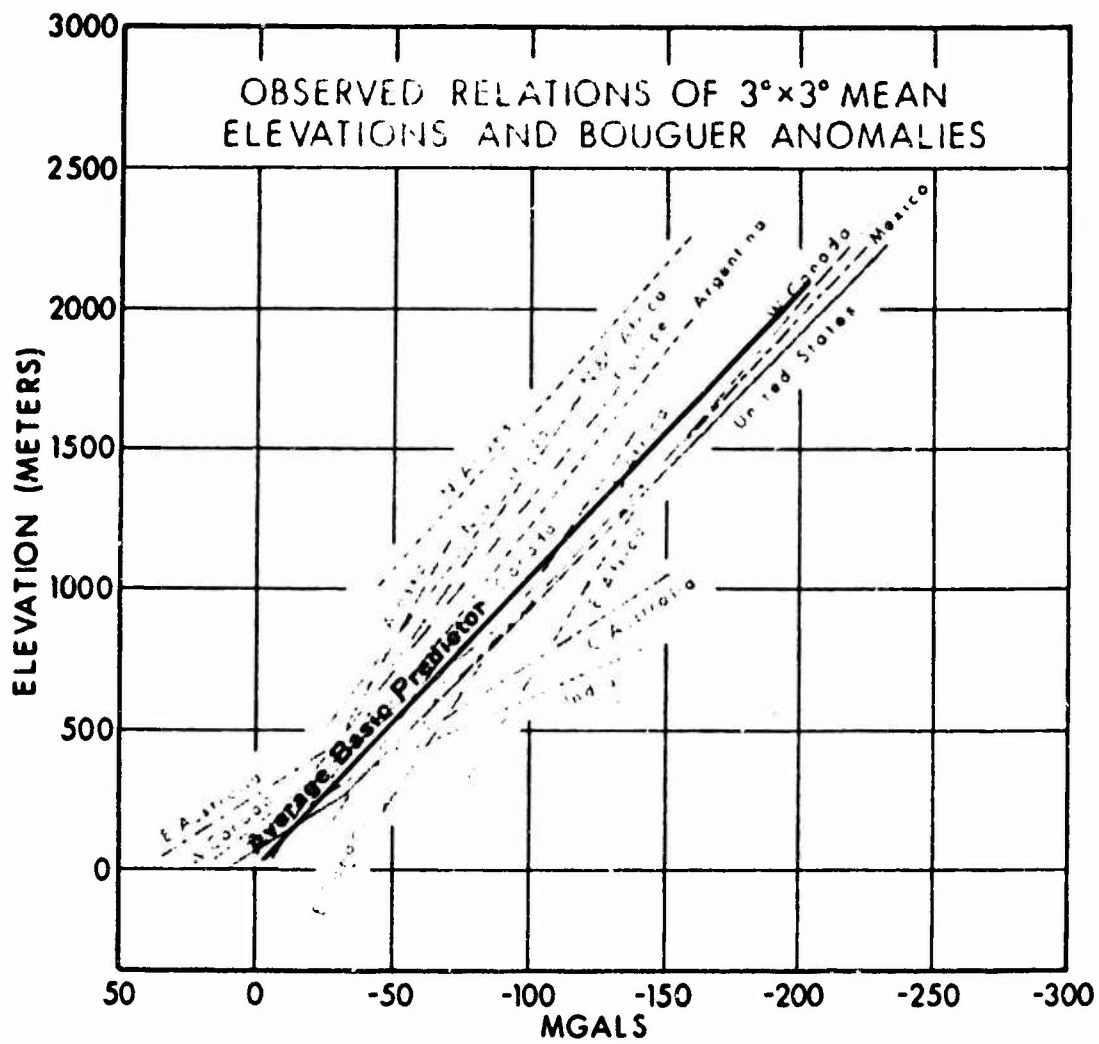
Figure 5-3. This figure was obtained by superimposing the line
generated by equation (5.1-1) onto Figure 1 of Woollard (1969b),
which shows observed relations of 3° x 3° mean elevations and Bouguer
anomalies for 18 continental regions throughout the world. The
comparison shows that (1) use of a basic predictor specifically
determined for application within a given region is always
preferable and (2) some corrections are essential if the average
basic predictor is to give satisfactory results for many regions.

5.1.4 Distant Compensation Correction

The distant compensation correction accounts for the
gravitational effects of the compensating masses which lie outside
of the 166 kilometer radius included in the theoretical derivation
of the average basic predictor. This correction can be obtained
easily from maps by Karki et al. (1961). These maps are designed
to provide a value for use in the isostatic correction, g_I, where
the effect of compensation is positive. For Bouguer anomaly
prediction, however, the effect of compensation is negative.
Therefore,

$$\bar{g}_{DC} = - g_{DTC} \qquad (5.1\text{-}14)$$

where

$\bar{g}_{DC}$ = Bouguer gravity effect of distant compensation for use in
equation (5.1-2)

g_{DTC} = Isostatic gravity effect of distant topography and its
compensation read from maps by Karki et al. (1961).

5.1.5 Isostatic-Crustal Correction

The isostatic-crustal correction accounts for (1) regional departures from isostatic balance, (2) the existence of crustal and upper mantle density distributions other than those predicted by Airy isostatic models, and (3) very long period (global) variations in the gravity anomaly field caused by deep seated mass perturbations.

As was true in the case of the regional correction, there are nearly as many approaches for developing isostatic-crustal corrections as there are geologic/tectonic provinces which require such corrections. The evidence and methods which can be used tend to follow a limited number of patterns some of which are discussed in the following paragraphs. Extended discussions of other types of regionality factors which must be considered in developing isostatic-crustal corrections are included in Woollard (1968b, 1969a).

Evidence for regional departures from isostatic balance includes rapid uplift or subsidence of the crust, recent glaciation or deglaciation, rapid erosion, etc. Regions suspected of being out of isostatic balance should be compared with other regions having similar characteristics and ample measured gravity data. An isostatic-crustal correction can be derived for the latter and applied to the former.

Strange and Woollard (1964a) have derived an isostatic-crustal correction for two types of regions where crustal and upper mantle density distributions differ from those predicted by the Airy isostatic model. These are (1) regions where both mean crustal seismic velocity (and, hence, density) and upper mantle seismic

velocity (density) are abnormally high and the crust is thicker

than predicted by Airy theory (example: Northern Great Plains), and

(2) regions where both mean crustal and upper mantle velocity are

abnormally low and the crust is thinner than predicted by Airy

theory (example: Southern Basin and Range province). These regions

must not be long and narrow. Using empirical relations between

crustal thickness and regional gravity anomalies, Strange and Woollard

have developed an isostatic-crustal correction determination

procedure for such regions. The procedure is this:

Step 1: Determine actual crustal thickness from
published interpretations of seismic velocity data.

Step 2: Determine the crustal thickness predicted by
Airy theory from Figure II-9 of Strange and Woollard (1964a).

Step 3: Enter actual minus predicted crustal thickness
into Figure II-11 of Strange and Woollard (1964a) and read the
isostatic-crustal correction.

A good approximation of the very long period (global)

variations in the gravity anomaly field can be obtained as the

difference between the global gravity field value computed from the

low degree spherical harmonics (derived by satellite perturbation

analysis) and the value given by the theoretical gravity formula

(Strange and Woollard, 1964a).

Any measured gravity data which exists in the prediction

region can be used as a rough check of the regional component of

the Bouguer gravity prediction given by the corrected average basic

predictor. Of course, local effects must be removed from the measured
data before it is compared to the value given by the corrected
average basic predictor.

Careful deductive reasoning combined with considerable
skill and judgement is necessary to enable development of accurate
values for the isostatic-crustal correction for prediction areas
which contain no measured gravity data.

5.1.6 Evaluation of the Corrected Average Basic Predictor

The standard error of the corrected average basic
predictor computed by equations (5.1-2) and (5.1-1) is given by

$$e_{BF} = [(0.09\ e_{\bar{h}})^2 + e^2{}_{IC}]^{\frac{1}{2}} \qquad (5.1-15)$$

where

e_{BP} = error of corrected average basic predictor in milligals

$e_{\bar{h}}$ = error of the mean elevation value used in the average basic
   predictor equation (5.1-1) in meters.

e_{IC} = error of the isostatic-crustal correction in milligals

The value obtained by (5.1-15) is to be used in equation
(4.6-2) for NOGAP prediction evaluation.

Since the average basic predictor is quite accurate as
an expression representing the worldwide average relationship
between mean Bouguer anomalies and mean elevations, there is no term
in (5.1-15) involving the slope constant error, e_β. Likewise, the
distant compensation correction is "correct" by definition, and,
hence not an error factor in (5.1-15).

The error, e_{IC}, is an estimate of the accuracy of the correction, $\bar{g}_{IC}$. Where no value for $\bar{g}_{IC}$ can be determined, then e_{IC} represents the error incurred by not accounting for actual regional isostatic and crustal conditions.

Results of a test project in Europe provide some guidance for the expected reliability of NOGAP predictions made using the corrected average basic predictor. Details are given in Table 5-1.

5.2 Basic Predict_ _ Multiple Regression

Comparatively little research has been completed to determine the nature of the multiple (combined) relationships between Bouguer gravity, mean elevation, and other geophysical parameters. Nonetheless, it should be possible to define a basic predictor of the form

$$BPM = a + bx + cy + dz + \ldots \qquad (5.2\text{-}1)$$

where

BPM = multiple basic predictor

a, b, c, d, . . . = multiple regression constants

x, y, z, . . . = geophysical variables such as mean elevation, crustal thickness, depth to crystalline basement, etc.

Based upon results of research conducted to date, multiple basic predictors such as (5.2-1) appear to apply to regions which are comparitively localized in extent. Also, the multiple basic predictors incorporate part or all the local and regional correction terms as well. A study by Vincent and Strange (1970) indicates that the multiple regression prediction can give excellent results.

TABLE 5-1

RELIABILITY OF NOGAP PREDICTIONS

USING CORRECTED AVERAGE BASIC PREDICTORS

IN WESTERN EUROPE

TYPE AREA	ERROR RANGE (mgal)
Small Basins	~10
Large Basins	15-25
Basement Exposures	5-20
Geosynclinal Mountains	15-25
Grabens and Plateaus	10-15
Coastal Lowlands	~10

5.3 <u>Normal Gravity Anomaly Prediction-Free Air Version</u> (GAPFREE)

Basic predictor functions are generally determined in terms
of mean Bouguer gravity anomaly--mean elevation relationships
because of the strong, well-defined correlation which usually
exists between these two parameters. However, a basic predictor
function also can be derived in terms of mean free air anomaly--mean
elevation relationships. The major difficulty with the latter
approach is that the free air linear basic predictor relation is
frequently very nearly parallel to the elevation axis which results
in an ill-defined basic predictor equation, for example, equation
(3.6-33).

Gravity anomaly prediction using a free air basic prediction
(GAPFREE) is similar in form to NOGAP prediction, and theoretically
at least should give identical results whenever the free air basic
predictor is well defined. The fundamental prediction equation
is

$$\overline{\Delta g_F} = BPF + \overline{g}_R + \overline{g}_L + \overline{g}_{EF} \qquad (5.3-1)$$

where

$\overline{\Delta g_F}$ = predicted $1° \times 1°$ mean free air anomaly

BPF = free air basic predictor

$\overline{g}_R$ = regional correction

$\overline{g}_L$ = local correction

$\overline{g}_{EF}$ = local free air elevation correction

The predicted $1° \times 1°$ mean Bouguer anomaly is obtained from
the predicted $1° \times 1°$ mean free air anomaly by use of equation
(3.7-14)

$$\overline{\Delta g_B} = \overline{\Delta g_F} - 0.1119 \, \overline{h} \qquad (5.3-2)$$

where

$\overline{\Delta g}_B$ = predicted 1° x 1° mean Bouguer anomaly

$\overline{h}$ = 1° x 1° mean elevation

The free air basic predictor used for GAPFREE prediction is the equation of the linear regression between 1° x 1° mean free air anomaly values and the corresponding mean elevation values.

$$BPF = \alpha + \beta\overline{h} \qquad (5.3-3)$$

where

BPF = free air basic predictor

α, β = regression constants

$\overline{h}$ = mean elevation

The procedure for free air basic predictor derivation are similar to those outlined for the standard NOGAP basic predictor, and either 1° x 1° or 3° x 3° mean elevations may be used.

The regional and local geologic corrections are obtained in the same manner as for standard NOGAP prediction.

The local free air elevation correction, used only when 3° x 3° mean elevations are involved in the free air basic predictor, is obtained from equation (3.6-25)

$$(\Delta g_F)_P = (\Delta g_F)_Q + 0.1119 \, \delta h - TC_P + TC_Q \qquad (5.3-4)$$

where P is interpreted as the 1° x 1° mean value and Q as the 3° x 3° mean value. Thus,

$$g_{EF} = 0.1119 \, \delta h - TC_P + TC_Q \qquad (5.3-5)$$

The value of $(-TC_P + TC_Q)$ is given by (4.5-3) to be $-0.013 \, \delta h$. Therefore,

$$g_{EF} = 0.099 \ \delta h$$

where

$$\delta h = h_P - h_Q = ODM - ME$$

Evaluation of GAPFREE prediction is similar to evaluation of NOGAP prediction.

6. GRAVITY DENSIFICATION AND EXTENSION METHOD (GRADE)

6.1 Discussion

In regions where a limited amount of measured gravity data is available, conventional averaging methods often do not yield accurate $1° \times 1°$ mean anomalies. When geologic structure is considered in the prediction process, however, the resulting $1° \times 1°$ mean can be quite accurate (Scheibe, 1965). The Gravity Densification and Extension (GRADE) method is the gravity correlation prediction procedure most often used to incorporate structural considerations into $1° \times 1°$ mean gravity anomaly predictions in continental regions of limited measured gravity data availability.

The GRADE method uses gravity correlations to densify and extend the known gravity field by interpolation. The mean anomalies are predicted using both the measured and interpolated data.

Input data required for GRADE prediction is the same as for NOGAP prediction plus an average of from two to ten gravity measurements per $1° \times 1°$ area within the prediction region.

In GRADE prediction, the locations of all available gravity measurements are plotted on a map base of suitable scale. Then the Bouguer gravity anomaly values for all plotted points are graphically compared with the corresponding values of various types of numerical geophysical or geological data which are known continuously throughout the prediction region. All correlations are noted and the equations which express the interrelationships between correlated data are developed. These equations are used to interpolate Bouguer anomaly values for an even distribution of points within each $1° \times 1°$ area.

All measured and interpolated Bouguer anomaly values are annotated on the plot, and the combined field is contoured using geologic/tectonic structure maps as additional control. The final mean $1° \times 1°$ mean anomaly values are read from the completed contour charts.

The applicability of correlations found is usually limited to a single geologic/tectonic province and, occasionally, to individual geologic formations. For this reason, Bouguer anomaly interpolations are extended only into regions which are structurally homogeneous with the region in which the correlations being used were determined. This property is actually a strength of the method because each gravitationally significant local structural variation is taken into account.

In addition, the measured gravity data used in the method automatically controls much of the regional component of the gravity anomaly field. Hence, GRADE predictions are well controlled both locally and regionally.

Some examples of the types of data which can be used to establish correlations for GRADE interpolation are given in Table 6-1.

6.2 Procedure

Step 1: Obtain plots showing the locations of all gravity measurements available within the prediction region. A scale of 1:1,000,000 is generally used for $1° \times 1°$ prediction. Annotate Bouguer anomaly values at measurement sites.

Step 2: Obtain all numerical geological and geophysical data available in the prediction region. Sources of such data are listed in Table 6-1. If necessary, construct contour maps of each type of

TABLE 6-1

SOME EXAMPLES OF NUMERICAL GEOLOGIC AND GEOPHYSICAL

DATA WHICH CAN BE USED TO ESTABLISH

CORRELATIONS FOR GRADE INTERPOLATION

DATA	SOURCES
Crustal Thickness	Crustal Maps, Profiles (seismic, gravimetric)
Depth to Mohorovicic Discontinuity	Crustal Maps, Profiles (seismic, gravimetric)
Depth to Intra-Crustal Discontinuities	Crustal Maps (seismic, gravimetric)
Thickness of Sedimentary Rocks	Tectonic Maps
Depth to Basement	Tectonic Maps
Seismic Wave Velocity	Seismic Data
Crustal or Near Surface Density Variations	Seismic Data, Density Maps, Crustal Profiles
Elevation	Topographic Maps

218

data to obtain a representation showing how the data varies in value throughout the prediction region. Annotate (or tabulate) values for each type of data, read from the contour maps, at the gravity measurement sites on the plots made in Step 1.

Step 3: Subdivide the prediction region into geologic/tectonic provinces using published geologic and tectonic maps and documents.

Step 4: For each geologic/tectonic province, make plots (graphs) of Bouguer anomaly values against the values of the various types of numerical geological and geophysical data at the gravity measurement sites.

Step 5: Examine each plot. If a single regression line provides a good linear fit to the plotted points proceed to Step 8. Otherwise continue with Step 6.

Step 6: Re-examine the geologic/tectonic province boundaries determined in Step 3. Adjustment of these boundaries and/or definition of additional provinces may help achieve good linear relationships. Conversely, it may be possible to combine two or more provinces which have the same relationships.

Step 7: Consider subdivision of plots into high, intermediate, and low elevation regions, especially when the original plot shows linear segments joined by directional discontinuities.

Step 8: Select the most consistent plot (smallest point scatter) to represent each geologic/tectonic province. Compute linear regression coefficients using a least squares solution (Appendix D).

Step 9: Use the correlation formulas determined in Step 8 to interpolate Bouguer gravity anomaly values at an even distribution of points within the prediction region. Where the Bouguer anomaly gradient

is small, a total of 5 to 10 measured and interpolated values per 1° x 1° area should be sufficient. With a larger gradient, 20 or more points per 1° x 1° area may be required. Annotate the additional Bouguer anomaly values on the plots made in Step 1.

Step 10: Contour the densified and extended Bouguer gravity anomaly field on the final annotated plots. Use local variations in geological structure as additional control in constructing the contours.

Step 11: Read the final 1° x 1° mean Bouguer anomaly values from the completed contour plots.

Step 12: Compute the final 1° x 1° mean free air anomaly using equation (4.1-2).

Options: Experienced people generally prefer to use programmable desk calculators or high speed computers to accomplish Steps 4 through 9. Using the plots as described, however, is an aid both in understanding the processes involved and in defining where the data could have alternate interpretations.

6.3 Crustal Parameter Variations

A stronger correlation sometimes exists between the numerical geophysical data and the two geophysical parameters, mean crustal density and crustal root increment, than between the geophysical data and the Bouguer gravity anomaly data. Consequently, it is sometimes advantageous to use these two crustal parameters in lieu of the Bouguer gravity anomaly in GRADE prediction.

Expressions for the two crustal parameters are obtained using Airy-Woollard isostatic theory. The basic relationships are given by equations (3.10-20) and (3.10-31) which may be written in the form

$$\Delta R = \frac{\sigma_C h + (\sigma_C - \sigma_S) H_S}{\sigma_m - \sigma_C} \qquad (6.3-1)$$

$$\Delta g_B = -2\pi k (\sigma_m - \sigma_C) \Delta R \qquad (6.3-2)$$

where all symbols are defined in section 3.10.

Solve (6.3-2) for ΔR, equate to (6.3-1) and solve the resulting expression for σ_C to obtain

$$\sigma_C = \frac{2\pi k \sigma_S H_S - \Delta g_B}{2\pi k (H_S + h)} \qquad (6.3-3)$$

Equations (6.3-1) and (6.3-3) are used to obtain values for the two crustal parameters, σ_C and ΔR, at each gravity measurement site. These parameters are plotted individually against the numerical geophysical data, and the best correlations are used to interpolate additional σ_C and ΔR values at an even distribution of points within the prediction region. Then equation (6.3-2) is used to convert the interpolated crustal parameters to interpolated Bouguer anomaly values which are then contoured, as usual.

6.4 Mountain Modification

The standard GRADE method sometimes gives inadequate results in rugged mountainous areas where the available measured gravity data is not distributed well enough to represent rapid structural and topographic changes. The mountain modification of the GRADE method often enables more reliable predictions to be made in such areas.

Pairs of measurement sites are selected such that the lines connecting the pairs cross the structural trends at nearly right angles. The Bouguer anomalies or crustal parameters are plotted against the numerical geophysical data at the end points (measurement sites) of each line. Then a linear interpolation is used to obtain Bouguer anomaly or parameter values at equal intervals along each line. The measured and interpolated values are contoured and the means read in the usual manner.

6.5 Evaluation of GRADE Prediction

6.5.1 Evaluation Formulas

Considering the fundamental principles of error theory, the standard error of GRADE prediction is given by

$$E_B = \frac{e_I}{(m + \frac{n}{2})^{\frac{1}{2}}} \qquad (6.5-1)$$

$$E_F = (E^2_B + 0.01 \, e^2_H)^{\frac{1}{2}} \qquad (6.5-2)$$

where E and e values are standard errors in milligals except e_H which is a standard error in meters. Specifically,

E_B = error of 1° x 1° mean Bouguer anomaly predicted by GRADE procedures

E_F = error of 1° x 1° mean free air anomaly predicted by equation (4.1-2)

e_I = error of interpolated Bouguer anomalies

e_H = error of 1° x 1° mean elevation (ODM)

m = number of measured gravity values in the 1° x 1° area

n = number of interpolated gravity values in the 1° x 1° area

The error of the interpolated Bouguer anomalies is given by

$$e_I = [(Pe_\beta)^2 + (\beta e_p)^2]^{\frac{1}{2}} \qquad (6.5\text{-}3)$$

where

P = average value of the numerical geophysical data in the correlation used for the 1° x 1° area

e_p = error of the numerical geophysical data used

β = slope constant of the linear correlation equation used for interpolation

e_β = error of the slope constant given by the error propagation formula (Appendix D)

When crustal parameters are used, compute an error for each parameter using equation (6.5-3)—this gives $e_{\Delta R}$ for the root increment and e_C for mean crustal density. Then

$$e_I = 40 \left[\{(\sigma_M - \sigma_C) \, e_R\}^2 + (\Delta R \, e_C)^2 \right] \qquad (6.5\text{-}4)$$

where ΔR and σ_C are average values for the 1° x 1° area.

For the mountain modification, use $m + n/4$ in the denominator of (6.5-1).

6.5.2 Test Reliability of GRADE Predictions

A test project to evaluate GRADE prediction reliability has been conducted in the European area. Values predicted using the GRADE method and variable amounts of measured data were compared with "measured" values computed using all measured gravity data. The results are shown in Table 6-2.

TABLE 6-2

RELIABILITY OF <u>GRADE</u> PREDICTIONS

IN WESTERN EUROPE

1. Normal Areas

Average Number Measurements per 1° x 1°	Error Range (mgal)			Standard Error (mgal)
	0-4	5-9	10-14	
2	70%	20%	10%	± 7
5	75%	25%	—	± 5
10	100%	—	—	+ 2

2. Rugged Areas--Mountain Modification

Average Number Measurements per 1° x 1°	Error Range (mgal)				Standard Error (mgal)
	0-4	5-9	10-14	> 15	
3	35%	15%	25%	25%	+ 15

7. EXTENDED GRAVITY ANOMALY PREDICTION METHOD (EXGAP)

7.1 Discussion

The Extended Gravity Anomaly Prediction Method (EXGAP) was derived originally as an extension of the NOGAP method. The original version, as described in Wilcox et al. (1972) and Wilcox (1968) was somewhat awkward in its expression and recommended usage. The method is presented here in a revised and more adequate form.

The EXGAP method is useful for $1° \times 1°$ areas which contain only one or two gravity measurements and for which a valid NOGAP basic predictor equation has been determined. It is based on the assumption that the regional inverse linear relationship between point Bouguer anomalies and elevations within the $1° \times 1°$ area is parallel to the regional mean Bouguer anomaly--mean elevation relationship expressed by the basic predictor. In general, this assumption is sufficiently valid for $1° \times 1°$ anomaly predictions.

The relations involved are shown graphically in Figure 7-1. From this figure, it is evident that

$$\overline{\Delta g_B} = (\Delta g_B - g_L) - \beta (h - \overline{h}) \tag{7.1-1}$$

where

$\overline{\Delta g_B} = 1° \times 1°$ mean Bouguer anomaly

$\overline{h} = 1° \times 1°$ mean elevation

$\Delta g_L = $ Bouguer anomaly computed at the measurement site

$h = $ elevation of the measurement site

$g_L = $ local geologic correction at the measurement site

$\beta = $ slope constant of the NOGAP basic predictor

Equation (7.1-1) is the EXGAP prediction formula. All parameters required by this formula are "known" except for the local geologic correction, g_L, which must be determined by the analytical computation method described in Section 4.4.2. (Empirical estimation cannot be used for a g_L value which applies to a particular measurement site). Hence, application of the EXGAP method is limited to areas where local geological effects can be computed by the analytical method.

Results are always improved when more than one gravity measurement is available within the $1° \times 1°$ area for which a prediction is desired. In such cases, apply equation (7.1-1) independently for each measurement and take an average.

The predicted free air anomaly is obtained using equation (4.1-2).

7.2 Evaluation of EXGAP Prediction

The standard error of EXGAP prediction is given by

$$E_B = [e^2_{\Delta g} + e^2_L + \{(h - \bar{h})\, e_\beta\}^2 + (\beta\, e_h)^2 + (\beta\, e_{\bar{h}})^2]^{\frac{1}{2}} \quad (7.2-1)$$

$$E_F = [E_B^2 + 0.01\, e_h^2]^{\frac{1}{2}} \quad (7.2-2)$$

where all E and e values are standard errors. Specifically,

E_B = error of $1° \times 1°$ mean Bouguer anomaly (mgal) predicted by equation (7.1-1)

E_F = error of $1° \times 1°$ mean free air anomaly (mgal) predicted by equation (4.1-2)

$e_{\Delta g}$ = error of Bouguer anomaly (mgal) at the measurement site

e_L = estimated error of local geologic correction (mgal)

h = elevation at the measurement site (meters)

$\bar{h}$ = error of mean elevation used in the NOGAP basic predictor (meters)

FIGURE 7-1

EXGAP RELATIONS
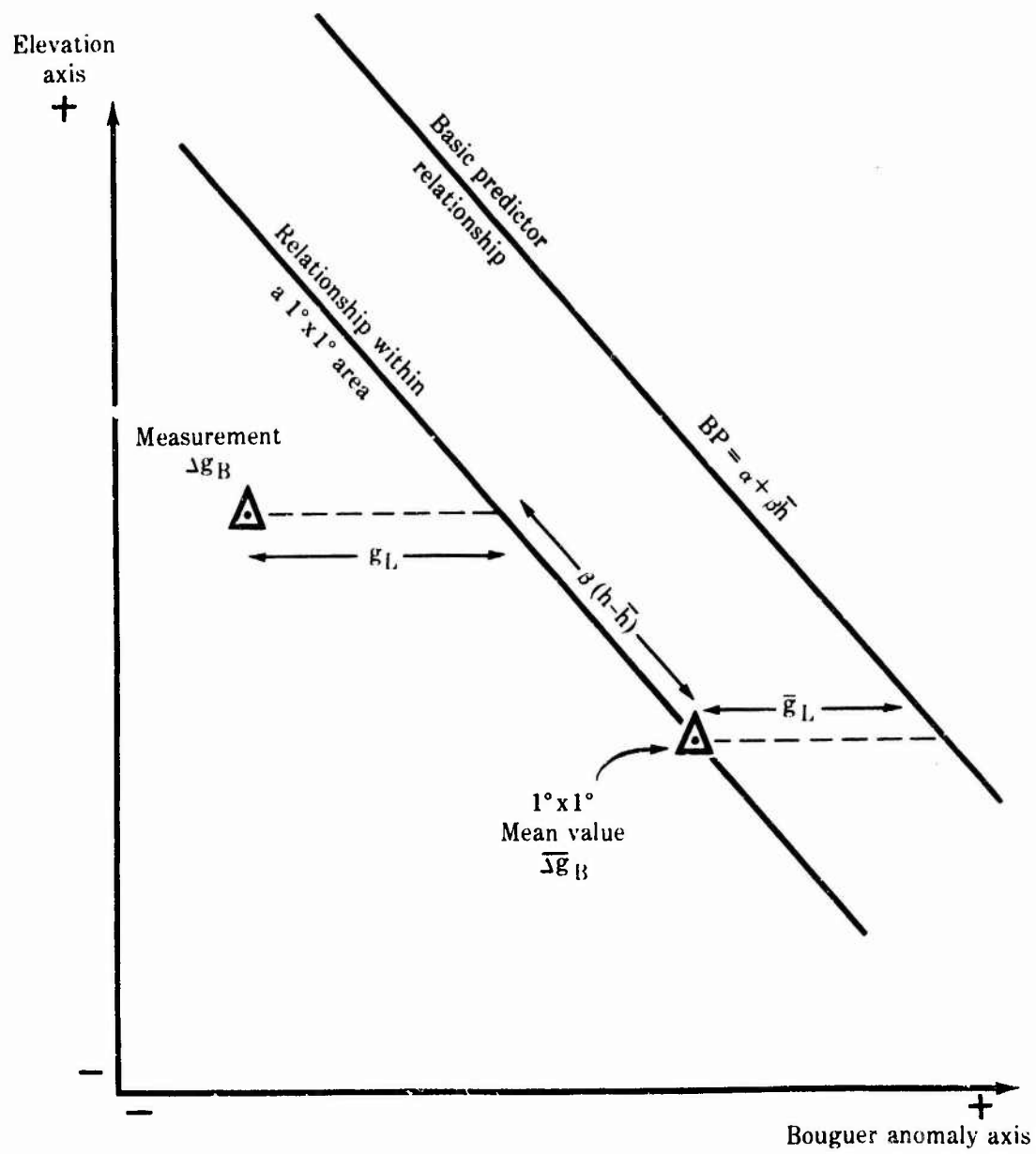
e_β = error of the slope constant of the NOGAP basic predictor

e_h = error of the elevation at measurement site (meters)

$e_{\bar{h}}$ = error of mean elevation (meters)

β = NOGAP slope constant

When two or more computations are averaged, the error is given by

$$E_B = \left[\frac{E_{B_1}^2 + E_{B_2}^2 + \ldots}{n} \right]^{\frac{1}{2}} \qquad (7.2-3)$$

where

n = number of measurements used

8. UNREDUCED GRAVITY ANOMALY PREDICTION METHOD (UNGAP)

8.1 Discussion and Method

The Unreduced Gravity Anomaly Prediction (UNGAP) method relies
on correlations between the unreduced surface anomaly defined by
equation (3.9-1)

$$\Delta g_S = g_0 - \gamma \qquad (8.1-1)$$

and elevation data within major geologic/tectonic provinces.

The unreduced surface anomaly is almost always more strongly
correlated (larger coefficient of correlation) with elevation than
either the free air or the Bouguer anomaly (Rothermel, 1973). This
is true in both a local and a regional sense. Also, only a relatively
small amount of measured data is required to establish usable
correlations. The distribution of this measured data within
$1^\circ \times 1^\circ$ areas is not important for UNGAP prediction. These properties
constitute the major strengths of the UNGAP method.

The major difficulty of the method is that valid basic predictor
relationships frequently must be deciphered from a complicated suite
of local relationships. Nevertheless, the UNGAP method has proven
to be very useful in some situations where a NOGAP basic predictor
cannot be determined--either due to an ill defined relationship
between regional elevations and Bouguer anomalies or due to insufficient
amounts and/or distributions of measured gravity data to enable
definition of a control region.

The normal local relationship between unreduced surface anomaly
and elevation is given by equation (3.9-7).

$$(\Delta g_S)_P = (\Delta g_S)_Q - 0.3086 \, \delta h + 2 \, \pi \, k \, \sigma \, \delta h - TC_P + TC_Q \quad (8.1\text{-}2)$$

which, when $(\Delta g_S)_Q$ is taken to be at sea level and elevation dependent terms are combined, can be written in the general form

$$\Delta g_S = \zeta + \theta h \quad\quad\quad (8.1\text{-}3)$$

Equation (8.1-3) can be viewed as the form of the UNGAP basic predictor.

The UNGAP basic predictor is derived in the following manner. A plot is made of unreduced surface anomalies against elevation for gravity measurement sites within major geologic/tectonic provinces. These plots almost always show the existence of strong linear relationships between these two variables which can be expressed in terms of equation (8.1-3). Generally, there will be a unique value of the constants, ζ and θ, for each $1° \times 1°$ area. With locally homogeneous structure, ζ and θ will vary slowly and uniformly from one $1° \times 1°$ area to the next--or they may not vary at all. More rapid changes in ζ and θ may take place across breaks in local structure and across major province boundaries. However, all of these variations are merely superimposed on the dominant term, 0.3086 h, in (8.1-2) so that the UNGAP relationship (8.1-3) is always well behaved.

Subtraction of analytically computed or estimated local geologic effects from the unreduced anomaly values before construction of the plot sometimes yields one or more very well defined relationships. In such cases, the slope and intercept constant of each relationship are determined by a least squares fit (Appendix L).

In other cases, the plot will show a more complex suite of local relationships which must be merged graphically into a single average local relationship. Then the slope and intercept constants determined graphically for the average relationships are used to define the UNGAP basic predictors.

Insertion of the $1° \times 1°$ mean elevation, $\overline{h}$, into

$$\overline{\Delta g_S} = \zeta + \theta \overline{h} \qquad (8.1\text{-}4)$$

where ζ and θ have been determined as above gives a basic prediction of the corresponding $1° \times 1°$ mean unreduced surface anomaly, $\overline{\Delta g_S}$. Local geologic corrections, determined analytically or empirically, should be added to the basic prediction where possible. However, caution must be used when the basic predictor was determined by the merging process which rather arbitrarily forces "corrections" into individual $1° \times 1°$ relationships in order to obtain an average curve. Careful observation of the manner in which θ and ζ vary from one $1° \times 1°$ to the next on the plots may help in the development of empirical local adjustments to the basic prediction when the latter was determined by merging.

The $1° \times 1°$ mean free air and Bouguer anomalies are computed by

$$\overline{\Delta g_F} = \overline{\Delta g_S} + 0.3086\,\overline{h} \qquad (8.1\text{-}5)$$

$$\overline{\Delta g_B} = \overline{\Delta g_F} - 0.1119\,\overline{h} \qquad (8.1\text{-}6)$$

where

$\overline{\Delta g_F} = 1° \times 1°$ mean free air anomaly

$\overline{\Delta g_B} = 1° \times 1°$ mean Bouguer anomaly

$\overline{h} = 1° \times 1°$ mean elevation in meters

$\overline{\Delta g}_S$ = 1° x 1° mean unreduced surface anomaly

8.2 Evaluation of UNGAP Prediction

The standard error of UNGAP predictions is given by

$$E_S = (e_{BP}^2 + e_L^2)^{\frac{1}{2}} \qquad (8.2\text{-}1)$$

$$E_F = (E_S^2 + 0.1\ e_{\overline{h}}^2)^{\frac{1}{2}} \qquad (8.2\text{-}2)$$

$$E_B = (E_F^2 + 0.01\ e_{\overline{h}}^2)^{\frac{1}{2}} \qquad (8.2\text{-}3)$$

where all E and e values are standard errors. Specifically,

E_F = error of predicted 1° x 1° mean free air anomaly, mgal

E_B = error of predicted 1° x 1° mean Bouguer anomaly, mgal

E_S = error of predicted 1° x 1° mean unreduced surface anomaly, mgal

$e_{\overline{h}}$ = error of 1° x 1° mean elevation, meters

e_L = estimated error of local geologic corrections, mgal

e_{BP} = error of the basic predictor, mgal

The error of the basic predictor is given by

$$e_{BP} = [(\theta\ e_h)^2 + (h\ e_\theta)^2]^{\frac{1}{2}} \qquad (8.2\text{-}4)$$

or,

$$e_{BP} = [(\theta\ e_h)^2 + e_M^2]^{\frac{1}{2}} \qquad (8.2\text{-}5)$$

where

θ = slope constant in (8.1-4)

e_θ = error in constant of the basic predictor found using the error propagation formula (D-11) in Appendix D.

e_M = estimated error of merging determined from the plot "scatter"

Equation (8.2-4) is used when the basic predictor is determined by a least squares solution. Equation (8.2-5) is used when the basic predictor is determined by merging.

9. GEOLOGIC ATTRACTION INTERPOLATION METHOD (GAIN)

9.1 Discussion and Method

The Geologic Attraction Interpolation (GAIN) Method can be
used to predict 1° x 1° mean gravity anomalies in regions where the
local gravitational variations are caused entirely by near surface
density contrasts. A few gravity measurements must be available to
control the regional gravity variations. Methods of the GAIN type
have yielded excellent results in Wyoming (Strange and Woollard,
1964a) and in the south-central United States (Durbin, 1961a).

Methods of the GAIN type are used most frequently in regions
where sedimentary rocks overlie a cyrstalline basement and it is
this type of application which is discussed in the following
paragraphs.

In the GAIN method, several geologic cross sections are
constructed and then converted into density variation cross sections
using a density--depth relationship appropriate for the area being
worked. Data describing the density sections is entered into a two
dimensional attraction computer program and the gravitational effects
of density contrasts in the local geologic structures are computed
at intervals along the sections. The computed effects are used to
interpolate gravity anomaly values at points between gravity measurement
sites. The field of measured and interpolated values is contoured
with respect to local geologic structure and the final 1° x 1° mean
Bouguer anomalies are read from the completed contoured charts.

The geologic cross sections are constructed across the centers
and perp:ndicular to the longest dimension of the geologic structures
in the region. Each profile must pass through at least two gravity
measurement sites which, preferably, are located on basement rock
outcrops. Enough profiles should be constructed so that every
$1^\circ \times 1^\circ$ area contains a portion of one of the profiles.

The geologic cross section itself is compiled from the best
available geologic and tectonic maps and related textual data
using standard methods.

In converting the geologic cross sections to density sections,
density values for the crystalline basement and overlying sediments
can be obtained from well log data, or in the absence of such data,
by application of Chapter III of Woollard (1962). All sedimentary
rocks equal in density to the crystalline rocks are treated as
basement rocks. Density values determined for the sedimentary rocks
can be averaged and used to construct a sediment to basement density
contrast vs. depth curve. Density increase with depth tends to be
exponential for clastic sediments (see Figure IV-3, Strange and Woollard,
1964a). Recent near surface unconsolidated deposits may have a nearly
constant density--not varying with depth.

The density contrast vs. depth curve is applied to convert the
geologic cross section to a density contrast cross section. The
density section typically consists of near parallel layers which
cut across the geologic formation boundaries.

Data from the density cross sections are entered into a two dimensional attraction computer program and the gravitational effects of the density section are computed. These local effects are superimposed on the regional field as defined by the gravity measurement. A computed profile of local gravitational effects is shown superimposed on a "fixed" regional field defined by measured data in Figure 9-1.

As shown by Figure 9-1, the location of each gravity measurement has been plotted along the profile of local effects. The value of the local effect at each measurement site is subtracted from the Bouguer anomaly value at that site to yield the regional component at that site. The regional component is plotted on another graph whose ordinate is the regional component of the Bouguer anomaly and whose abscissa is along the profile (Figure 9-2). The plotted points are interconnected with straight lines which define the regional trend. Then the interpolated Bouguer anomaly for any point between the observation sites is the sum of the regional trend (from Figure 9-2) and the local gravitational effect (from Figure 9-1) at that point.

Interpolated Bouguer anomalies are plotted at frequent intervals along each profile on a map base of suitable scale. For $1° \times 1°$ prediction, a 1:1,000,000 scale is satisfactory. The plotted points are contoured with respect to local geologic structure and topography, and the final $1° \times 1°$ mean Bouguer anomalies are read from the completed contoured map. The final $1° \times 1°$ mean free air anomaly is computed by equation (4.1-2).

Additional details of GAIN application are given in Section IV of Strange and Woollard (1964a).

9.2 Evaluation of GAIN Prediction

The standard error of GAIN prediction is given by

$$E_B = (e^2_{\Delta g} + e^2_L)^{\frac{1}{2}} \qquad (9.2-1)$$

$$E_F = (E_B^2 + 0.01 \, e^2_{\overline{h}})^{\frac{1}{2}} \qquad (9.2-2)$$

where all E and e values are standard errors. Specifically,

E_B = error of $1° \times 1°$ mean Bouguer anomaly (mgal) predicted by GAIN procedures

E_F = error of $1° \times 1°$ mean free air anomaly predicted by equation (4.1-2)

$e_{\Delta g}$ = error of Bouguer anomaly (mgal) at the measurement sites

e_L = estimated error of computed local geologic effects (mgal)

$e_{\overline{h}}$ = error of $1° \times 1°$ mean elevation (meters)

238

FIGURE 9-1

COMPUTED GRAVITY EFFECTS PROFILE

(See Figure 9-2 for numerical interpolation data)
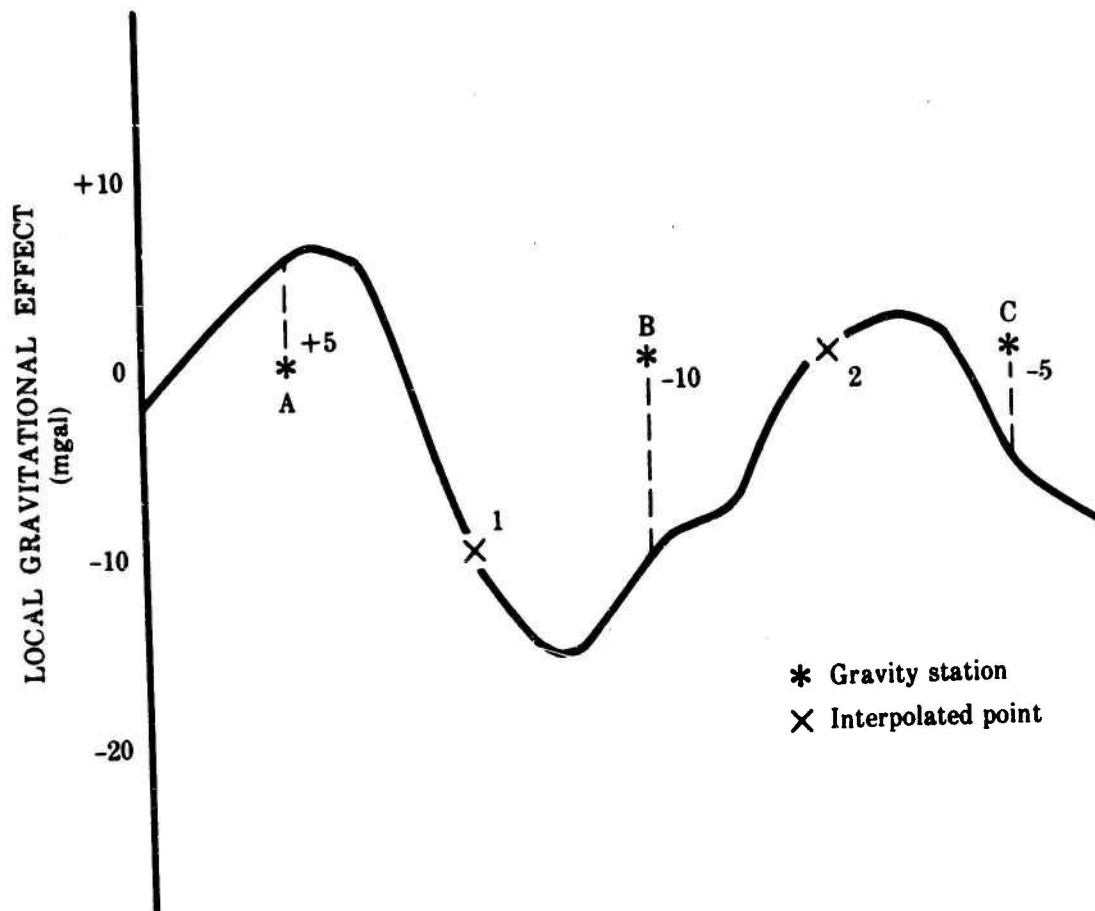
FIGURE 9-2

REGIONAL TREND PROFILE

MEASURED DATA	OBSERVED Δg_B	PLOTTED Δg_B
Gravity Station A	− 170 mgal	− 170 − (+5) = − 175 mgal
Gravity Station B	− 185 mgal	− 185 − (−10) = − 175 mgal
Gravity Station C	− 160 mgal	− 160 − (−5) = − 155 mgal

INTERPOLATED DATA	REGIONAL Δg_B	LOCAL EFFECT	TOTAL Δg_B
Point 1	− 175 mgal	− 10 mgal	− 185 mgal
Point 2	− 165 mgal	0 mgal	− 165 mgal
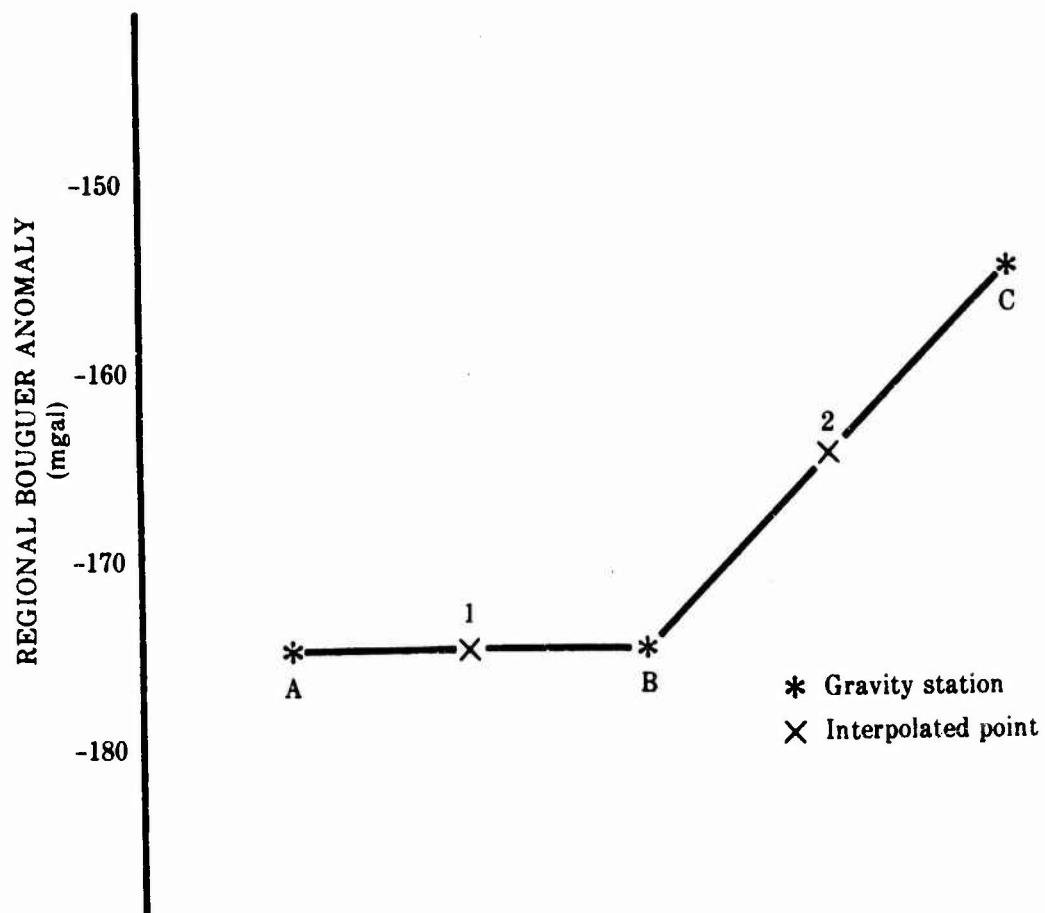
10. CONCLUDING COMMENTS ABOUT GEOPHYSICAL PREDICTION METHODS

A number of geophysical gravity anomaly prediction methods have been described and discussed in some detail. Of these, NOGAP, EXGAP, UNGAP, and GAPFREE are applied to extend $1° \times 1°$ mean gravity anomaly coverage into regions which contain very limited, if any, measured gravity data. The two interpolation methods, GRADE and GAIN, are applied to densify existing fields of measured gravity data for the purpose of $1° \times 1°$ mean gravity anomaly prediction. All these methods give values which are superior to those which can be obtained by use of the measured data alone with conventional averaging techniques.

Since no two geologic and tectonic settings are exactly identical, it is safe to say that none of the geophysical methods ever has been applied twice in exactly the same manner. In fact, many variations to each method are possible and the scientist doing the prediction always must be alert for new ways to adapt the standard methods so that they "fit" different regions. Therefore, the procedure discussed must be regarded as a general guide rather than a cookbook list of recipes.

Experience, insight, and judgment factors are very important in geophysical gravity prediction. The best way to learn it is to do it!

APPENDIX A.

DERIVATION OF FORMULA
FOR BOUGUER PLATE CORRECTION

Author's note: The following mathematical development for the
Bouguer plate correction is based on that given in Heiskanen and
Moritz (1967) and does not represent original work by the writer.

The other appendixes do represent original work by the writer.

1. <u>Definition of Symbols Used</u> (Figure A-1)

   a =   height of point, P, above origin

   h =   height of cylinder above origin

   r =   radius of cylinder

   dV =   volume element within cylinder

   x, y, z =   rectangular coordinates

   a, s, z =   cylindrical coordinates

   t_1 =   slant distance from point, P, to top edge of cylinder

   t_2 =   slant distance from point, P, to bottom edge of cylinder

   ℓ =   distance from point, P, to volume element, dV

   σ =   density of material contained within the cylinder

   U_P =   gravitational potential at P

   k =   gravitational constant

   g_P =   gravitational force at P

   g_c =   gravitational force on axis at upper surface of the cylinder

   g_b =   gravitational force of the Bouguer plate at a point on
           its upper surface

FIGURE A-1

FIGURES FOR DERIVATION OF

BOUGUER PLATE CORRECTION
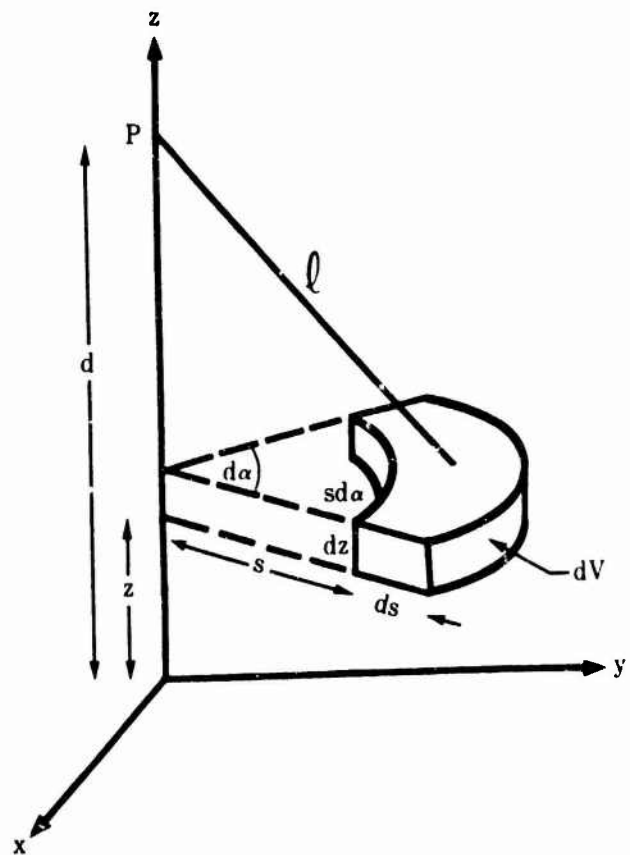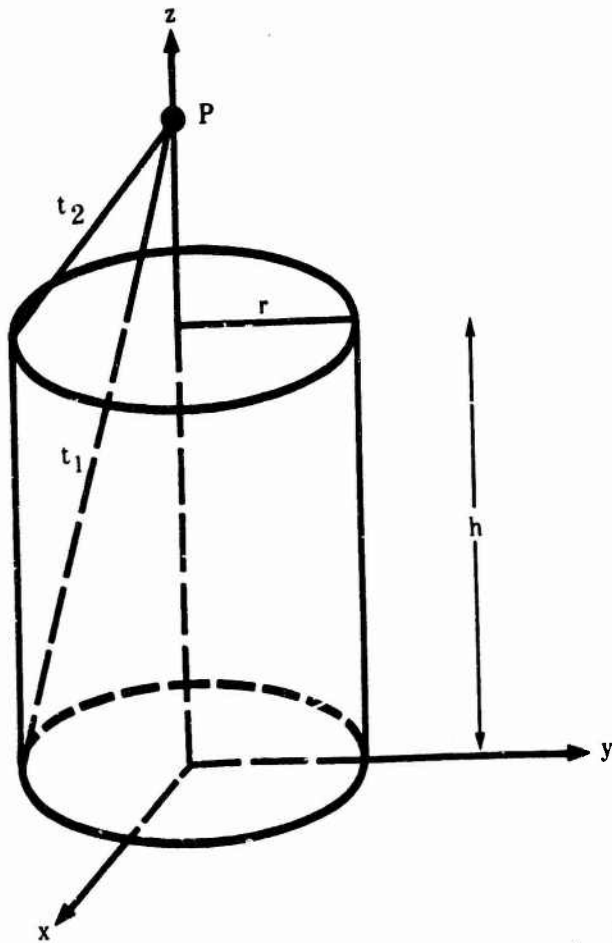
2. <u>Vertical Attraction of a Homogeneous Right Circular Cylinder</u>

<u>at an External Point Situated on the Axis of the Cylinder</u>

The potential of any solid body at an external point is given by

$$U_P = k \iiint \frac{\sigma}{\ell} \, dV \tag{A-1}$$

If the point is located on the axis of a right circular cylinder then, from Figure A-1

$$\ell = (s^2 + \{d - z\}^2)^{\frac{1}{2}} \tag{A-2}$$

$$dV = dx \, dy \, dz = s \, ds \, d\alpha \, dz \tag{A-3}$$

Also, from Figure A-1, it is evident that the integration limits are, for the cylinder,

$$0 \text{ to } 2\pi \text{ for } \alpha$$
$$0 \text{ to } r \text{ for } s \tag{A-4}$$
$$0 \text{ to } h \text{ for } z$$

Thus, with the density being constant, equation (A-1) may be written

$$U_P = k \, \sigma \int_{z=0}^{h} \int_{s=0}^{r} \int_{\alpha=0}^{2\pi} \frac{s \, ds \, d\alpha \, dz}{(s^2 + \{d - z\}^2)^{\frac{1}{2}}} \tag{A-5}$$

Integration of (A-5) with respect to α gives

$$U_P = k \, \sigma \int_{z=0}^{h} \int_{s=0}^{r} \frac{s \, ds \, dz}{(s^2 + \{d - z\}^2)^{\frac{1}{2}}} \cdot \alpha \Big|_{0}^{2\pi}$$

and evaluation between the limits 0 and 2π leaves

$$U_P = 2 \, \pi \, k \, \sigma \int_{z=0}^{h} \int_{s=0}^{r} \frac{s \, ds \, dz}{(s^2 + \{d - z\}^2)^{\frac{1}{2}}} \tag{A-6}$$

In order to integrate (A-6) with respect to s, note that

$$\frac{d}{dx} (x^2 + a^2)^{\frac{1}{2}} = \frac{x \, dx}{(x^2 + a^2)^{\frac{1}{2}}}$$

Therefore (A-6) integrated with respect to s gives

$$U_P = 2 \pi k \sigma \int_{z=0}^{h} (s^2 + \{d - z\}^2)^{\frac{1}{2}} \, dz \, \Big|_0^r$$

and evaluation between the limits 0 and r leaves

$$U_P = 2 \pi k \sigma \int_{z=0}^{h} \lceil z - d + (\{d - z\}^2 + r^2)^{\frac{1}{2}} \rceil \, dz \qquad (A-7)$$

In (A-7), note that

$$(\{d - z\}^2 + r^2)^{\frac{1}{2}} = (\{d^2 + r^2\} - 2dz + z^2)^{\frac{1}{2}}$$

which is of the form

$$(ax^2 + bx + c)^{\frac{1}{2}}$$

where

$a = 1$

$b = -2d$

$c = (r^2 + d^2)^{\frac{1}{2}}$

$x = z$

Integral tables give the form

$$\int (ax^2 + bx + c)^{\frac{1}{2}} \, dx = \frac{2ax + b}{4a} (ax^2 + bx + c)^{\frac{1}{2}}$$

$$+ \frac{4ac - b^2}{8a \sqrt{a}} \ln [2ax + b + 2 (a \{ax^2 + bx + c\})^{\frac{1}{2}}]$$

In consideration of the above and after some simplification

$$\int (\{d - z\}^2 + r^2)^{\frac{1}{2}} = -\frac{1}{2} (d - z) (r^2 + \{d - z\}^2)^{\frac{1}{2}}$$

$$\hspace{6cm} \text{(A-8)}$$

$$-\frac{1}{2} r^2 \ln [d - z + (\{d - z\}^2 + r^2)^{\frac{1}{2}}] + \frac{1}{2} r^2 \ln 2$$

The constant term, $\frac{1}{2} r^2 \ln 2$, in (A-8) will vanish during

evaluation of the definite integral and, hence, may be dropped.

Now, note that

$$\frac{d}{dz} [\frac{1}{2} (d - z)^2] = (z - d) dz \hspace{2cm} \text{(A-9)}$$

Considering the results (A-8) and (A-9), integration of (A-7)

with respect to z gives

$$U_p = 2 \pi k \sigma [\frac{1}{2} (d - z)^2 - \frac{1}{2} (d - z) (r^2 + \{d - z\}^2)^{\frac{1}{2}}$$

$$-\frac{1}{2} r^2 \ln (d - z + \{(d - z)^2 + r^2\}^{\frac{1}{2}}] \quad \Big|_0^h$$

and evaluation between the limits 0 and h leaves the final expression

for potential generated by the cylinder at P.

$$U_p = \pi k \sigma \{(d - h)^2 - d^2 - (d - h) (r^2 + \{d - h\}^2)^{\frac{1}{2}}$$

$$+ d (r^2 + d^2)^{\frac{1}{2}} - r^2 \ln [d - h + (\{d - h\}^2 + r^2)^{\frac{1}{2}}] \hspace{1cm} \text{(A-10)}$$

$$+ r^2 \ln [d + (d^2 + r^2)^{\frac{1}{2}}]\}$$

The vertical gravitational attraction of the cylinder at P is

the negative derivative of the potential at P with respect to the

vertical axis of the cylinder

$$g_p = -\frac{\partial U_p}{\partial d} \hspace{2cm} \text{(A-11)}$$

Operating on (A-10) according to (A-11) gives, after considerable simplification

$$g_P = 2 \pi k \sigma [h + (r^2 + (d - h)^2)^{\frac{1}{2}} - (r^2 + d^2)^{\frac{1}{2}}] \qquad \text{(A-12)}$$

which may also be written (Figure 4-4)

$$g_P = 2 \pi k \sigma [h - t_1 + t_2] \qquad \text{(A-13)}$$

Now let the point, P, descend to the upper surface of the cylinder. At this point, $d = h$, and (A-12) becomes

$$g_S = 2 \pi k \sigma [h + r - (r^2 + h^2)^{\frac{1}{2}}] \qquad \text{(A-14)}$$

3. <u>Attraction of the Bouguer Plate at a Point Situated on Its Upper Surface</u>

The Bouguer Plate is a right circular cylinder of infinite radius and height, h. To obtain the gravitational attraction of the Bouguer plate at a point on its upper surface, take the limit of (A-14) as r approaches infinity

$$g_B = 2 \pi k \sigma h + 2 \pi k \sigma \lim_{r \to \infty} [r - (r^2 + h^2)^{\frac{1}{2}}] \qquad \text{(A-15)}$$

According to L'Hospital's Rule

$$\lim_{x \to \infty} f(x) = \lim_{x \to \infty} \frac{d}{dx} f(x)$$

when

$$\lim_{x \to \infty} f(x) \to \infty$$

Applying L'Hospital's Rule to the second term of (A-15)

$$\lim_{r \to \infty} [r - (r^2 + h^2)^{\frac{1}{2}}] = \lim_{r \to \infty} \frac{\partial}{\partial r} [r - (r^2 + h^2)^{\frac{1}{2}}]$$

250

$$= \lim_{r \to \infty} \left[1 - \frac{r}{(r^2 + h^2)^{\frac{1}{2}}} \right]$$

$$= \lim_{r \to \infty} \left[1 - \frac{1}{(1 - h^2/r^2)^{\frac{1}{2}}} \right]$$

$$= 0$$

Therefore, (A-15) reduces to the form

$$g_B = 2 \pi k \sigma h \qquad\qquad (A\text{-}16)$$

which is the Bouguer Plate correction.

APPENDIX B.

AN ERROR COVARIANCE FUNCTION FOR $1° \times 1°$ MEAN
ANOMALY VALUES PREDICTED BY THE NOGAP METHOD

Error covariance functions are frequently of use in error propagation studies to determine the accuracy of various geodetic quantities computed using the $1° \times 1°$ mean anomalies. Heiskanen and Moritz (1967) give some appropriate error covariance formulas for gravity prediction where ample observed gravity data is available. The following derivation is intended to develop an error covariance formula which can be applied in the case when little or no observed data exists, and when $1° \times 1°$ mean anomaly prediction is done using a NOGAP-type procedure.

The basic NOGAP prediction formula, used to predict $1° \times 1°$ mean anomalies within a <u>prediction area</u> containing little or no observed gravity data, may be written in the form,

$$\Delta \bar{g}_{PT} = BP_P + RC_P + LC_P \qquad (B-1)$$

where

$\Delta \bar{g}_{PT}$ = predicted mean anomaly for the $1° \times 1°$ area designated
       "area P"

BP_P = basic predictor for area P

RC_P = regional correction(s) for area P

LC_P = local correction(s) for area P

Local corrections, LC, are determined individually for each $1° \times 1°$ prediction and are based upon an analysis of local geological/ geophysical mass anomalies which exist within each $1° \times 1°$ area. The regional corrections, RC, are functions which vary slowly from one $1° \times 1°$ area to the next and express small changes in the regional gravity anomaly field provided by the basic predictor.

The basic predictor, BP, is a prediction of the stable regional part of the gravity anomaly field. It is given by

$$BP_P = \alpha + \beta\overline{h}_P \qquad (B-2)$$

where

$\overline{h}_P$ is a mean elevation value corresponding to area P

α, β are constants

Insertion of (B-2) into (B-1) gives an expanded version of the basic NOGAP prediction formula

$$\widetilde{\Delta g}_{PP} = \alpha + \beta\overline{h}_P + RC + LC \qquad (B-3)$$

The constants α and β are the intercept and slope constants, respectively, of a linear regression between $\widetilde{\Delta g}_{PR}$ and $\overline{h}_P$ for $1° \times 1°$ blocks within a control area where sufficient observed gravity data is available to obtain accurate mean anomaly values using conventional data averaging methods. Both the control area and prediction area must be contained within the same overall regional structure such that the α and β constants determined in the control area are also applicable in the prediction area. For this reason, the error relationships of the basic predictor are identical in the control and prediction areas. The equation appropriate for linear

regression in the <u>control area</u> is

$$\tilde{\Delta g}_{PO} - RC_P - LC_P = \alpha + \beta \bar{h}_P \tag{B-4}$$

where

$\tilde{\Delta g}_{PO}$ = mean anomaly predicted for area P from observed data

Regional and local corrections are subtracted from $\tilde{\Delta g}_{PO}$ in order to obtain a uniform regional gravity anomaly value, $\tilde{\Delta g}_{PR}$, which can be expressed in the linear form of the basic predictor. With the definition,

$$\Delta g_{PR} = \tilde{\Delta g}_{PO} - RC_P - LC_P \tag{B-5}$$

equation (B-4) for the control area becomes

$$\tilde{\Delta g}_{PR} = \alpha + \beta \bar{h}_P \tag{B-6}$$

The procedures used and errors involved in predicting the local and regional corrections are identical in both the control and prediction areas. Consequently, the error relationships of LC and RC together with those of the regional gravity field, are adequately expressed in the single value, $\tilde{\Delta g}_{PR}$.

The intercept value, α, is the gravity anomaly value corresponding to zero mean elevation. Moving α to the left side of equation (B-6) has the effect of translating the mean elevation-mean anomaly coordinate axes such that the regression line relating the gravity and elevation parameters is constrained to pass through the point (0, 0). The translation has no effect whatsoever on the slope constant, β, or the error relationships. Accordingly, (B-6) becomes

$$(\tilde{\Delta g}_{PR} - \alpha) = \beta \bar{h}_P \tag{B-7}$$

Now define $\overline{h}_m$ to be the mean value of all $\overline{h}_P$ within the control area, and

$$\overline{\Delta h} = \overline{h}_P - \overline{h}_m \tag{B-8}$$

where

$$\overline{h}_m = M\{\overline{h}_P\} \tag{B-9}$$

Then, (B-9) becomes

$$(\tilde{\tilde{\Delta g}}_{PR} - \alpha) = \beta\overline{\overline{\Delta h}}_P + \beta\overline{h}_m$$

or

$$(\tilde{\tilde{\Delta g}}_{PR} - \alpha - \beta\overline{h}_m) = \beta\overline{\overline{\Delta h}}_P$$

Since both α and $\beta\overline{h}_m$ represent gravity values, let

$$\tilde{\tilde{\Delta g}}_P = (\tilde{\tilde{\Delta g}}_{PR} - \alpha - \beta\overline{h}_m) \tag{B-10}$$

to obtain

$$\tilde{\tilde{\Delta g}}_P = \beta\overline{\overline{\Delta h}}_P \tag{B-11}$$

which is merely the control area prediction equation (B-4) written in a simpler form which is most useful for error analysis. Both $\tilde{\tilde{\Delta g}}_P$ and $\overline{\Delta h}$ are variables which are centered about zero by the operations (B-10) and (B-8) respectively, as is required by the following statistical computations.

Thus, $\tilde{\tilde{\Delta g}}_P$ is a form of the mean gravity anomaly predicted for the $1° \times 1°$ area designated as area P by the NOGAP gravity correlation prediction procedures. It includes all error factors due to basic predictor, regional corrections, and local corrections, and represents error conditions in both the control and prediction areas.

If the correct value of the mean gravity anomaly for area P (corresponding in form to the predicted value $\tilde{\overline{\Delta g}}_P$) is $\overline{\Delta g}_P$, then the true error of prediction, E_P, is given by

$$E_P = \overline{\Delta g}_P - \tilde{\overline{\Delta g}}_P \qquad (B-12)$$

Insertion of (B-11) into (B-12) gives

$$E_P = \overline{\Delta g}_P - \beta \overline{\Delta h}_P \qquad (B-13)$$

Squaring (B-13) yields

$$E_P{}^2 = (\overline{\Delta g}_P - \beta \overline{\Delta h}_P)(\overline{\Delta g}_P - \beta \overline{\Delta h}_P)$$

or

$$E_P{}^2 = \overline{\Delta g}_P{}^2 - 2\beta \overline{\Delta g}_P \, \overline{\Delta h}_P + \beta^2 \overline{\Delta h}_P{}^2 \qquad (B-14)$$

Now, form the average of (B-14) over the control area. In so doing, adapt the statistical definitions of Heiskanen and Moritz (1967) as follows

$$M\{E^2\} = m^2{}_P$$

$$M\{\overline{\Delta g}_P{}^2\} = \overline{C}_0$$

$$M\{\overline{\Delta g}_P \, \overline{\Delta h}_P\} = \overline{B}_0 \qquad (B-15)$$

$$M\{\overline{\Delta h}_P{}^2\} = \overline{A}_0$$

where

$M\{E^2\}$ = the average value of E^2

m = the standard error of prediction

$\overline{C}_S$ = the auto-covariance (average product) of mean gravity anomalies which are a constant distance, S, apart

$\overline{B}_S$ = the cross-covariance of mean gravity anomaly and mean elevation values which are a constant distance, S, apart

$\overline{A}_S$ = the auto-covariance of mean elevation values which are a
constant distance, S, apart

For S=0, as is the case in (B-15), the values $\overline{C}_0$, $\overline{B}_0$, and $\overline{A}_0$
represent the variances.

In consideration of the definitions (B-15), averaging (B-14)
yields

$$M \{E^2\} = M \{\overline{\Delta g_P}^2\} - 2\beta \ M \{\overline{\Delta g_P \ \Delta h_P}\} + \beta^2 \ M \{\overline{\Delta h_P}^2\}$$

or

$$m^2 = \overline{C}_0 - 2\beta \ \overline{B}_0 + \beta^2 \ \overline{A}_0 \qquad\qquad (B-16)$$

The value of β for most accurate prediction is found by
minimizing the standard prediction error expressed by (B-16) as a
function of β. Accordingly

$$\frac{\partial m^2}{\partial \beta} = - 2 \ \overline{B}_0 + 2\beta \ \overline{A}_0 = 0$$

or

$$\beta = \frac{\overline{B}_0}{\overline{A}_0} \qquad\qquad (B-17)$$

It can be shown that the value of β obtained by (B-17) is
identical to that obtained by linear regression analysis of equation
(B-4).

To obtain the correlation of prediction errors for two
different $1^\circ \ x \ 1^\circ$ areas, it is necessary to form the error covariance
σ_{PQ}, which by definition is

$$\sigma_{PQ} = M \{E_P \ E_Q\} \qquad\qquad (B-18)$$

Inserting (B-13) into (B-18) gives

$$\sigma_{PQ} = M \{E_P E_Q\} = M \{(\overline{\Delta g}_P - \beta \overline{\Delta h}_P)(\overline{\Delta g}_Q - \beta \overline{\Delta h}_Q)\}$$

or

$$\sigma_{PQ} = M \{\overline{\Delta g}_P \overline{\Delta g}_Q\} - \beta M \{\overline{\Delta g}_P \overline{\Delta h}_Q\} - \beta M \{\overline{\Delta g}_Q \overline{\Delta h}_P\} + \beta^2 M \{\overline{\Delta h}_P \overline{\Delta h}_Q\}$$

$$(B-19)$$

Performing the indicated averaging gives the error covariance

$$\sigma_{PQ} = \overline{C}_{PQ} - 2\beta \overline{B}_{PQ} + \beta^2 \overline{A}_{PQ} \qquad (B-20)$$

where

$\overline{C}_{PQ}$ = auto-covariance of mean gravity anomalies which are a

constant distance, S=PQ, apart

$\overline{B}_{PQ}$ and $\overline{A}_{PQ}$ are similarly defined

To form the error covariance function, compute σ_{PQ} as a function
of S=PQ.

The error covariance function, as derived, is applicable over
both control and prediction areas for $1° \times 1°$ mean anomalies
predicted by the NOGAP prediction procedure.

APPENDIX C.

GENERALITY OF EQUATIONS (3.6-24) AND (3.6-25)

IN EVALUATING THE EFFECT OF LOCAL TOPOGRAPHY ON GRAVITY

Equations (3.6-24) and (3.6-25), which express the effect of local topographic variations on the free air gravity anomaly, were derived with reference to a very simple topographic model (Figure 3-2). It will be demonstrated in this Appendix that these equations, in fact, have general application to all topographic settings. It will also be shown that equation (3.6-23) is a more general form of the well known reduction of Poincare and Prey (see Heiskanen and Moritz, 1967, page 163).

Figure C-1 is a general topographic model where the points P and Q, between which the difference in gravitational attraction of the topography is to be determined, are both located on a slope. The locally uncompensated feature is considered to be the topographic mass above the elevation h_R and below the elevation h_S. The gravitational attraction of the mass within this feature must be removed from observed gravity at P and Q to correct the equality (3.6-18) for the case that the feature is wholly uncompensated.

Reading from Figure C-1, it is evident that

$$(g_T)_P = (g_1)_P - (g_2)_P - (g_4)_P \qquad (C-1)$$

$$(g_T)_Q = (g_1)_Q + (g_2)_Q - (g_4)_Q \qquad (C-2)$$

where

$(g_T)_P$ = gravitational attraction at P of the locally uncompensated mass within the hill

$(g_T)_Q$ = gravitational attraction at Q of the locally uncompensated

mass within the hill

$(g_1)_P$ = gravitational attraction at P of the mass within the

region labeled A on Figure C-1

$(g_1)_Q$ = gravitational attraction at Q of the mass within the

region labeled B on Figure C-2

$(g_2)_P$, $(g_2)_Q$, $(g_4)_P$, $(g_4)_Q$ are similarly defined

The signs of $(g_2)_P$ and $(g_4)_P$ are negative since removal of mass in the hill beneath P will reduce the value of gravity measured at P. The sign of $(g_1)_P$ is positive because the removal of mass in the hill which is situated above P will increase the value of gravity measured at P. Similar comments apply to explain the signs of the terms relating to the point Q.

Using (C-1) and (C-2) to correct (3.6-18) for the case of no compensation gives the relation

$$(\Delta g_S)_P + (g_1)_P - (g_2)_P - (g_4)_P$$

$$= (\Delta g_S)_Q + (g_1)_Q + (g_2)_Q - (g_4)_Q - 0.3086 \, \delta h \qquad (C-3)$$

Equation (C-3) which is valid for the general model (Figure C-1) corresponds to equation (3.6-19) which is valid for the simple topographic model (Figure 3-2). Converting (C-3) to the free air anomaly by (3.6-14) and the definition, $\Delta g_S = g_0 - \gamma$

$$(\Delta g_F)_P + (g_1)_P - (g_2)_P - (g_4)_P$$

$$= (\Delta g_F)_Q + (g_1)_Q + (g_2)_Q - (g_4)_Q \qquad (C-4)$$

FIGURE C-1

TOPOGRAPHIC VARIATION

GENERAL MODEL 1
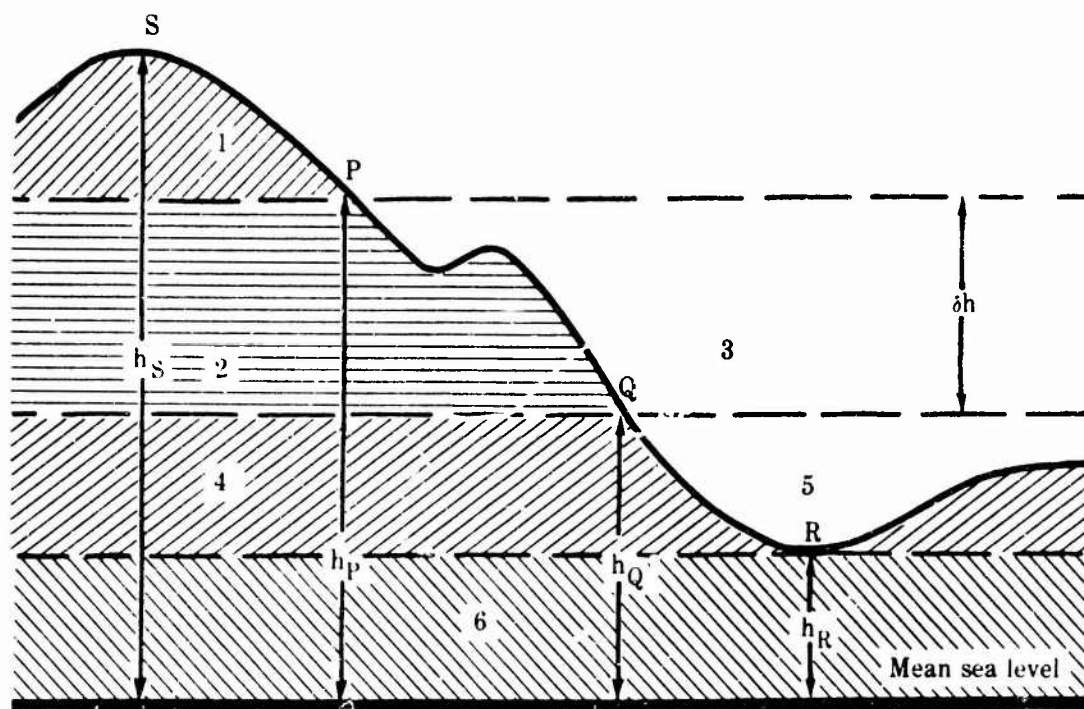
It remains to be shown that the general relations (3.6-24) and (3.6-25) are identical to (C-4). Equation (3.6-24) is

$$(\Delta g_F)_P = (\Delta g_F)_Q + 2 \pi k \sigma \delta h - TC_P + TC_Q \qquad (C-5)$$

Insertion of the value, $\sigma = 2.67 \text{ gm/cm}^3$, and the value of the gravitational constant gives equation (3.6-25).

$$(\Delta g_F)_P = (\Delta g_F)_Q + 0.1119 \delta h - TC_P + TC_Q \qquad (C-6)$$

Since $\delta h = h_P - h_Q$, equation (C-5) may be written

$$(\Delta g_F)_P - 2 \pi k \sigma h_P + TC_P = (\Delta g_F)_Q - 2 \pi k \sigma h_Q + TC_Q \qquad (C-7)$$

which may be recognized as one form of the equation (3.7-22). The terms, $2 \pi k \sigma h$, are just the simple Bouguer correction, g_B, so that (C-7) may be written

$$(\Delta g_F)_P - (g_B)_P + TC_P = (\Delta g_F)_Q - (g_B)_Q + TC_Q \qquad (C-8)$$

From Figure C-1 and the definitions of the Bouguer and terrain corrections, it is evident that

$$
\begin{aligned}
(g_B)_P &= (g_2)_P + (g_3)_P + (g_4)_P + (g_5)_P + (g_6)_P \\
TC_P &= (g_1)_P + (g_3)_P + (g_5)_P \\
(g_B)_Q &= (g_4)_Q + (g_5)_Q + (g_6)_Q \\
TC_Q &= (g_1)_Q + (g_2)_Q + (g_5)_Q
\end{aligned}
\qquad (C-9)
$$

Insertion of equations (C-9) into (C-8) gives, after some simplification,

$$
\begin{aligned}
(\Delta g_F)_P &+ (g_1)_P - (g_2)_P - (g_4)_P - (g_6)_P \\
&= (\Delta g_F)_Q + (g_1)_Q + (g_2)_Q - (g_4)_Q - (g_6)_Q
\end{aligned}
\qquad (C-10)
$$

Since layer 6 is an infinite plane layer with respect to both points P and Q, then

$$(g_6)_P = 2 \pi k \sigma h_R = (g_6)_Q$$

and (C-10) reduces to

$$(\Delta g_F)_P + (g_1)_P - (g_2)_P - (g_4)_P$$

$$= (\Delta g_F)_Q + (g_1)_Q + (g_2)_Q - (g_4)_Q \tag{C-11}$$

which is identical to the previously derived equation (C-4). Hence, the general applicability of (3.6-24) and (3.6-25) is proven.

It is a simple matter to extend the relations derived for general model 1 (Figure C-1) to the situation known by general model 2 (Figure C-2). Model 1 represents the general case for gentle to moderate topography, whereas model 2 represents the general case for rugged topography.

Model 2 is complicated by the existence of a second uncompensated local feature which exerts a gravitational attraction at the points P and Q. For the case of Figure C-2, it is evident that

$$(g_1)_P = (g_1)_P + (g_7)_P - (g_2)_P - (g_4)_P - (g_3)_P - (g_9)_P \tag{C-12}$$

$$(g_1)_Q = (g_1)_Q + (g_2)_Q + (g_7)_Q + (g_8)_Q - (g_4)_Q - (g_9)_Q \tag{C-13}$$

Using (C-12) and (C-13) to correct (3.6-18) for the case of no compensation gives the relation

$$(\Delta g_C)_P + (g_1)_P + (g_7)_P - (g_2)_P - (g_4)_P - (g_8)_P - (g_9)_P \tag{C-14}$$

$$= (\Delta g_C)_Q + (g_1)_Q + (g_2)_Q + (g_7)_Q + (g_8)_Q - (g_4)_Q - (g_9)_Q - 0.3086 \, h$$

FIGURE C-2

TOPOGRAPHIC VARIATION

GENERAL MODEL 2
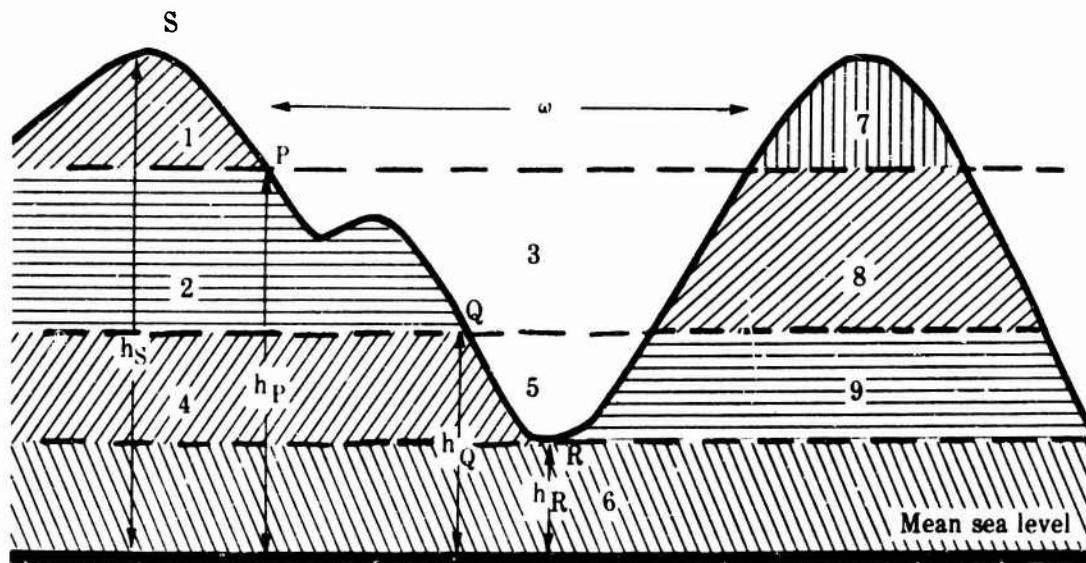
Proof that (3.6-24) reduces to (C-14) for the case of Figure C-2 is left as an exercise for the reader. The generalization of the Figure C-2 model to the case of many adjacent locally uncompensated features is obvious.

The two limiting situations of the Figure C-2 model are of interest. One limiting case is approached as the width, ω, of the valley becomes large. In this case, the attraction of the second hill becomes negligible, i.e.,

$$\text{As } \omega \to \text{ large}$$

$$(g_7)_i \to 0$$

$$(g_8)_i \to 0 \qquad\qquad (C-15)$$

$$(g_9)_i \to 0$$

where $i = P$ or Q

Insertion of the limits (C-15) into the relation (C-14) yields the relation (C-3) which applies to the model of Figure C-1.

The other limiting case of Figure C-2 is when the width, ω, of the valley becomes small. Then

$$\text{As } \omega \to 0$$

$$(g_1)_i + (g_7)_i \to 2\,\pi\,k\,\sigma\,(h_S - h_P)$$

$$(g_2)_i + (g_8)_i \to 2\,\pi\,k\,\sigma\,(h_S - h_P) \qquad (C-16)$$

$$(g_4)_i + (g_9)_i \to 2\,\pi\,k\,\sigma\,(h_S - h_P)$$

where $i = P$ or Q. Insertion of the limiting relations (C-16) into (C-14) gives

$$(\Delta g_S)_P + 2 \pi k \sigma (h_S - h_P) - 2 \pi k \sigma (h_P - h_Q) - 2 \pi k \sigma (h_Q - h_R)$$

$$= (\Delta g_S)_Q + 2 \pi k \sigma (h_S - h_P) + 2 \pi k \sigma (h_P - h_Q) - 2 \pi k \sigma (h_Q - h_R)$$

$$- 0.3086 \, \delta h$$

which, since $\delta h = h_P - h_Q$, reduces to

$$(\Delta g_S)_Q = (\Delta g_S)_P - 4 \pi k \sigma \, \delta h + 0.3086 \, \delta h \qquad (C-17)$$

With $\sigma = 2.67$ gm/cm^3 and the usual value for k, the above becomes

$$(\Delta g_S)_Q = (\Delta g_S)_P + 0.0848 \, \delta h \qquad (C-18)$$

Equations (C-17) and (C-18) may be recognized as the reduction
of Poincare and Prey which is used to obtain the value of gravity
at a point (Q) within the earth at a distance δh below a surface
point (P).

APPENDIX D.

LEAST SQUARES SOLUTION

AND ERROR FUNCTIONS

FOR NOGAP BASIC PREDICTORS

1. Linear Regression

The linear basic predictor used for the NOGAP method is given
by equation (4.2-1)

$$BP = \alpha_R + \beta_R \ \overline{h} \tag{D-1}$$

where

BP = basic predictor, a regional Bouguer gravity anomaly value

α_R = the (Bouguer anomaly axis) intercept constant

β_R = the slope constant

$\overline{h}$ = the mean elevation form used for the basic predictor
relationship

Replacing the predicted value BP by the measured value Δg_B and
dropping subscripts gives error equations of the form

$$V_i = \alpha + \beta \ \overline{h}_i - \Delta g_i \tag{D-2}$$

A least squares solution using the error equations (D-2) and a
Gaussian reduction of the normal equations gives the following
results

$$\beta = \frac{\Sigma \ (G_i \ H_i)}{\Sigma \ H^2_i} \tag{D-3}$$

$$\alpha = \frac{\Sigma \ (\Delta g_i)}{n} - \frac{\Sigma \ \overline{h}_i}{n} \ \beta \tag{D-4}$$

$$\mu = \left[\frac{\Sigma \, G_i{}^2 - \beta \, \Sigma \, (G_i \, H_i)}{n - 2} \right]^{\frac{1}{2}} \tag{D-5}$$

$$R = \frac{\Sigma \, (G_i \, H_i)}{(\Sigma \, G^2{}_i \, \Sigma \, H^2{}_i)} \tag{D-6}$$

$$[\beta\beta] = \frac{1}{\Sigma \, H^2{}_i} \tag{D-7}$$

$$[\alpha\beta] = - \frac{\Sigma \, \overline{h}_i}{n} \, [\beta\beta] \tag{D-8}$$

$$[\alpha\alpha] = \frac{1}{n} - \frac{\Sigma \, \overline{h}_i}{n} \, [\alpha\beta] \tag{D-9}$$

$$e_\alpha = \mu \, \sqrt{[\alpha\alpha]} \tag{D-10}$$

$$e_\beta = \mu \, \sqrt{[\beta\beta]} \tag{D-11}$$

$$e_{(\alpha + \beta h)} = \mu \, \sqrt{[\alpha\alpha] + 2h \, [\alpha\beta] + h^2 \, [\beta\beta]} \tag{D-12}$$

$$G_i = \Delta g_i - \frac{\Sigma \, \Delta g_i}{n} \tag{D-13}$$

$$H_i = \overline{h}_i - \frac{\Sigma \, \overline{h}_i}{n} \tag{D-14}$$

In the above,

n = number of "measurements"

R = correlation coefficient

$[\alpha\alpha]$, $[\alpha\beta]$, $[\beta\beta]$ = weight and correlation numbers

e_α = error of intercept concept

e_β = error of slope constant

μ = standard error of weight unit

G_i, d_i are center gravity coordinates

2. Multiple Regression

The basic predictor form using a multiple correlation is

$$BP = a + bx + cy + dz \qquad (D\text{-}15)$$

Replacing the predicted value BP by the measured value Δg gives error equations of the form

$$V_i = a + bx_i + cy_i + dz_i - \Delta g_i \qquad (D\text{-}16)$$

A least squares solution using the error equations (D-16) and a Gaussian reduction of normal equations give the following results where brackets indicate summation:

$$d = \frac{d\ell.\ 3}{dd.\ 3} \qquad (D\text{-}17)$$

$$c = \frac{c\ell.\ 2}{cc.\ 2} - \frac{cd.\ 2}{cc.\ 2}\ d \qquad (D\text{-}18)$$

$$b = \frac{b\ell.\ 1}{bb.\ 1} - \frac{bd.\ 1}{bb.\ 1}\ d - \frac{bc.\ 1}{bb.\ 1}\ c \qquad (D\text{-}19)$$

$$a = \frac{[\Delta g]}{n} - \frac{[z]}{n}\ d - \frac{[y]}{n}\ c - \frac{[x]}{n}\ b \qquad (D\text{-}20)$$

$$\mu = \left[\frac{ee.\ 4}{n-4}\right]^{\frac{1}{2}} \qquad (D\text{-}21)$$

$$e_a = \mu \sqrt{(\alpha\alpha)} \qquad\qquad (D\text{-}22)$$

$$e_b = \mu \sqrt{(\beta\beta)} \qquad\qquad (D\text{-}23)$$

$$e_c = \mu \sqrt{(\gamma\gamma)} \qquad\qquad (D\text{-}24)$$

$$e_d = \mu \sqrt{(\Delta\Delta)} \qquad\qquad (D\text{-}25)$$

$$e_{\Delta g} = a + bx + cy + dz = [(\alpha\alpha) + x^2 (\beta\beta) + y^2 (\gamma\gamma) + z^2 (\Delta\Delta) + 2x (\alpha\beta)$$
$$+ 2y (\alpha\gamma) + 2z (\alpha\Delta) + 2xy (\beta\gamma) + 2xz (\beta\Delta) + 2yz (\Delta\Delta)]^{\frac{1}{2}} \qquad (D\text{-}26)$$

$$(\alpha\Delta) = -\frac{dm.\ 3}{dd.\ 3} \qquad\qquad (D\text{-}27)$$

$$(\alpha\gamma) = -\frac{cm.\ 2}{cc.\ 2} - \frac{cd.\ 2}{cc.\ 2} (\alpha\Delta) \qquad\qquad (D\text{-}28)$$

$$(\alpha\beta) = -\frac{bm.\ 1}{bb.\ 1} - \frac{bd.\ 1}{bb.\ 1} (\alpha\Delta) - \frac{bc.\ 1}{bb.\ 1} (\alpha\gamma) \qquad (D\text{-}29)$$

$$(\alpha\alpha) = \frac{1}{n} - \frac{[z]}{n} (\alpha\Delta) - \frac{[y]}{n} (\alpha\gamma) - \frac{[x]}{n} (\alpha\beta) \qquad (D\text{-}30)$$

$$(\beta\Delta) = -\frac{dn.\ 3}{dd.\ 3} \qquad\qquad (D\text{-}31)$$

$$(\beta\gamma) = -\frac{ch.\ 2}{cc.\ 2} - \frac{cd.\ 2}{cc.\ 2} (\beta\Delta) \qquad\qquad (D\text{-}32)$$

$$(\beta\beta) = \frac{1}{bb.\ 1} - \frac{bd.\ 1}{bb.\ 1} (\beta\Delta) - \frac{bc.\ 1}{bb.\ 1} (\beta\gamma) \qquad (D\text{-}33)$$

$$(\gamma\Delta) = -\frac{dp.\ 3}{dd.\ 3} \tag{D-34}$$

$$(\gamma\gamma) = \frac{1}{cc.\ 2} - \frac{cd.\ 2}{cc.\ 2}\ (\gamma\Delta) \tag{D-35}$$

$$(\Delta\Delta) = \frac{1}{dd.\ 3} \tag{D-36}$$

$$bb.\ 1 = [x^2] - \frac{[x]\ [x]}{n} \tag{D-37}$$

$$bc.\ 1 = [xy] - \frac{[x]\ [y]}{n} \tag{D-38}$$

$$bd.\ 1 = [xz] - \frac{[x]\ [z]}{n} \tag{D-39}$$

$$be.\ 1 = -[x\Delta g] + \frac{[x]\ [\Delta g]}{n} \tag{D-40}$$

$$cc.\ 2 = [y^2] - \frac{[y]\ [y]}{n} - \frac{(bc.\ 1)\ (bc.\ 1)}{bb.\ 1} \tag{D-41}$$

$$cd.\ 2 = [yz] - \frac{[y]\ [z]}{n} - \frac{(bc.\ 1)\ (bd.\ 1)}{bb.\ 1} \tag{D-42}$$

$$ce.\ 2 = -[y\Delta g] + \frac{[y]\ [\Delta g]}{n} - \frac{(bc.\ 1)\ (b\ell.\ 1)}{bb.\ 1} \tag{D-43}$$

$$dd.\ 3 = [z^2] - \frac{[z]\ [z]}{n} - \frac{(bd.\ 1)\ (bd.\ 1)}{bb.\ 1} - \frac{(cd.\ 2)\ cd.\ 2)}{cc.\ 2} \tag{D-44}$$

$$d\ell.\ 3 = -[z\angle g] + \frac{[z]\ [\Delta g]}{n} - \frac{(bd.\ 1)\ (b\ell.\ 1)}{bb.\ 1} - \frac{(cd.\ 2)\ (c\ell.\ 2)}{cc.\ 2} \tag{D-45}$$

$$\ell\ell.\ 4 = [\Delta g^2] - \frac{[\Delta g]\ [\Delta g]}{n} - \frac{(b\ell.\ 1)\ (be.\ 1)}{bb.\ 1}$$

$$\tag{D-46}$$

$$- \frac{(c\ell.\ 2)\ (c\ell.\ 2)}{cc.\ 2} - \frac{(d\ell.\ 3)\ (d\ell.\ 3)}{dd.\ 3}$$

$$\text{bm. 1} = \frac{[x]}{n} \tag{D-47}$$

$$\text{cm. 2} = \frac{[y]}{n} - \frac{(\text{bc. 1}) \, (\text{bm. 1})}{\text{bb. 1}} \tag{D-48}$$

$$\text{dm. 3} = \frac{[z]}{n} - \frac{(\text{bd. 1}) \, (\text{bm. 1})}{\text{bb. 1}} - \frac{(\text{cd. 2}) \, (\text{cm. 2})}{\text{cc. 2}} \tag{D-49}$$

$$\text{cn. 2} = \frac{\text{bc. 1}}{\text{bb. 1}} \tag{D-50}$$

$$\text{dn. 3} = \frac{\text{bd. 1}}{\text{bb. 1}} - \frac{(\text{cd. 2}) \, (\text{cn. 2})}{\text{cc. 2}} \tag{D-51}$$

$$\text{dp. 3} = \frac{\text{cd. 2}}{\text{cc. 2}} \tag{D-52}$$

APPENDIX E.

DIGEST OF CONVENTIONAL METHODS

A summary of conventional methods used to predict 1° x 1° mean gravity anomalies is included for the convenience of the reader. Additional details may be found in Defense Mapping Agency Aerospace Center (1973).

1. Observed Gravity Averages

The averaging method is the simplest method for determining 1° x 1° mean Bouguer gravity anomalies and can be relied upon to provide accurate mean values when a large number of gravity observation stations are evenly distributed throughout the 1° x 1° area. Two computational schemes are in common usage. The 1° x 1° mean Bouguer anomalies can be computed as the arithmetic mean of the observed Bouguer anomaly values at all observation stations within the 1° x 1° area. Alternatively, averages may be computed individually for each $10'$ x $10'$ component of the 1° x 1° area, then the $10'$ x $10'$ components are averaged to obtain the final 1° x 1° mean values. The latter procedure automatically compensates for minor irregularities in gravity observation station distribution within the 1° x 1° area.

2. Gravity Anomaly Map Contouring

The contouring method is usually a most reliable method for determining 1° x 1° mean Bouguer gravity anomalies and provides accurate values even when the gravity observation stations are

unevenly distributed within the 1° x 1° area. The location of
each gravity observation station is plotted on a map sheet of
suitable scale. The corresponding Bouguer anomaly value is annotated.
Iso-anomaly contours are interpolated from the anomaly values and
drawn on the map. Plotting and contouring may be done visually and
by hand, or mechanically using computer contouring programs and
automatic plotting equipment. The 1° x 1° mean Bouguer anomaly value
may be determined with a sufficient degree of accuracy from the
completed contour map as the average of the interpolated values for
the four corner points, the four mid points on each side and the
center point taken twice (Woollard, 1969a).

3. Statistical Prediction

The statistical methods which can be used to compute 1° x 1°
mean gravity anomalies provide values of somewhat greater reliability
than the contouring method in some cases, less in others. The
degree of reliability depends on the amount and distribution of
observed gravity data coverage and how well the numerical process
involved can simulate the actual geophysical and geological
structures which produce the gravity anomaly variations.

The statistical prediction program for mean gravity anomalies
is based on the formulation developed by Moritz and later modified
for practical application by Rapp. A set of gravity anomaly
covariance coefficients is required as input data. These coefficients
are derived from observed gravity anomaly values within a relatively
large area such as a 5° x 5° region and statistically represent the

average rate of change with respect to distance with the gravity anomaly field within that region. The derived coefficient set is used to predict mean gravity anomalies for small size surface elements within the larger region. In normal practice, mean gravity anomalies are computed for each 5' x 5' component of a 1° x 1° area. The 5' x 5' values are then averaged to obtain 1° x 1° mean gravity anomalies.

To obtain optimum results when using the statistical approach in mean gravity anomaly predictions, care must be exercised to insure insofar as possible that the gravity anomaly covariance coefficients used for the prediction are derived from a region having the same gravity field characteristics as the area in which the mean anomaly predictions are being made.

REFERENCES

1. Agocs, W. B., "Least Squares Residual Anomaly Determination," Geophysics, Vol. 16, No. 4, pp 686-696, 1951.

2. Anderle, R. S., Determination of the Earth's Geoid by Satellite Observations, U. S. Naval Weapons Lab Tech Report No. 2027, 1966.

3. Andreyev, B. A., and I. G. Klushkin, "Geological Interpretation of Gravity Anomalies," Nedra, Leningrad, 1965.

4. Ballew, R. W., D. M. Scheibe, and E. J. Wetzker, "Reduction of Gravity Observations: Theory and Discussion," Technical Memorandum No. TM-10, USAF Aeronautical Chart and Information Center, 1961.

5. Beers, L. O., "The Earth's Gravity Field from a Combination of Satellite and Terrestrial Gravity Data," Hawaii Institute of Geophysics Technical Report 71-18, 1971.

6. Beierle, Charles W. and W. J. Rothermel, "Gravitational Modeling," Defense Mapping Agency Aerospace Center (DMAAC) Reference Publication No. 74-002, 1974.

7. Bomford, G., Geodesy. Oxford University Press, Third Edition, 1971.

8. Breville, Gerald L., Charles W. Beierle, Joseph R. Sanders, James T. Voss, and Luman E. Wilcox, "A Bouguer Gravity Anomaly Map of South America," paper presented to the 43rd Annual International Meeting of the Society of Exploration Geophysicists, DMAAC Technical Paper 73-2, 1973.

9. Daugherty, K. I., "Prediction of Gravity in Oceanic Areas from Depth and Geologic Age," Hawaii Institute of Geophysics, University of Hawaii, 1974.

10. Defense Mapping Agency Aerospace Center, "Computational Methods for Determining 1° x 1° Mean Gravity Anomalies and Their Accuracy," DMAAC Reference Publication 73-0001, 1973.

11. Demnitskaya, R. M., "Method of Research of the Geological Structure of the Crystalline Mantle of the Earth," Soviet Ceology, No. 1, 1959.

12. Dobrin, M. B., Introduction to Geophysical Prospecting, McGraw Hill Book Co., New York, 1960.

13. Durbin, W. P., Jr., "Investigation of the Determination of Gravity Anomalies from Geologic Structures and Formations," paper presented to the 21st Annual Meeting of ACSM, 1961a.

14. Durbin, W. P., Jr., "Correlation of Gravity and Geologic Data," paper presented at 10th Pacific Science Congress, Honolulu, Hawaii, 1961b.

15. Durbin, W. P., Jr., "Some Correlations of Gravity and Geology," Proceedings of the Symposium on Geodesy in the Space Age, Inst. Geodesy Photogrammetry, Cartography, Publ, 15, Ohio State University, Columbus, 1961c.

16. Durbin, W. P., Jr., "Geophysical Correlations," Gravity and Crustal Studies, Progress Report, USAF Aeronautical Chart and Information Center, 1962.

17. Durbin, W. P., Jr., "Geophysical Correlations," in Gravity Anomalies: Unsurveyed Areas, A.G.U. Geophysical Monograph Series No. 9, pp 85-88, 1966.

18. Durbin, W. P., Jr., L. E. Wilcox, and J. T. Voss, "A Geophysical Geoid of Eurasia," EOS 53: 4, p 343, 1972 (Abstract).

19. Garland, G. D., The Earth's Shape and Gravity, Pergammon Press, 1965.

20. Garland, G. D., Introduction to Geophysics, W. B. Saunders Company, Philadelphia, Pa., 1971.

21. Golizdra, G., Ya., "On Isostatic Equilibrium of the Earth's Crust on the Ukranian Shield," Izvestia, Physics of the Solid Earth, No. 10, 1972, pp 44-55.

22. Guier, W. H. and R. R. Newton, "The Earth's Gravity Field as Deduced from the Doppler Tracking of Five Satellites," Journal of Geophysical Research, Vol. 70, pp 4613-4626, 1965.

23. Hayford, John F., "The Figure of the Earth and Isostasy from Measurements in the United States," USC&GS Special Publication No. 82, 1909.

24. Hayford, John F., and William Bowie, "The Effect of Topography and Isostatic Compensation Upon the Intensity of Gravity," USC&GS Special Publication No. 10, 1912.

25. Heiland, D. A , Geophysical Exploration, Hafner Publishing Co., New York, 1968.

26. Heinricks, J. G., "Mean Anomalous Gravity Accuracy," (Abstract) Transactions A.G.U., 44 (4), 859, 1963.

27. Heiskanen, W. A., and Helmut Moritz, Physical Geodesy, W. H. Freeman and Co., San Francisco, 1967.

28.   Heiskanen, W. A., and F. A. Vening Meinesz, <u>The Earth and Its Gravity Field</u>, McGraw-Hill Book Co., Inc., New York, 1958.

29.   Isaacs, B., J. Oliver, and L. R. Sykes, "Seismology and the New Global Tectonics," <u>Journal of Geophysical Research</u>, Vol. 73, No. 18, pp 5855-5899, 1968.

30.   Jacobs, J. A., R. D. Russel, and J. T. Wilson, <u>Physics and Geology</u>, McGraw-Hill Book Company, New York, 1970.

31.   Jeffreys, Sir Harold, <u>The Earth</u>, Cambridge University Press, Fifth Edition, 1970.

32.   Karki, P., L. Kivioja, and W. A. Heiskanen, "Topographic Isostatic Reduction Maps for the World for the Hayford Zones 18-1, Airy Heiskanen System, T=30 km," Publications of the Isostatic Institute of the International Association of Geodesy, No. 35, 1961.

33.   Kaula, W. M., A Review of Geodetic Parameters, NASA, TN D-1947, 1963.

34.   Kaula, W. M., "Global Harmonic and Statistical Analysis of Gravimetry," in <u>Gravity Anomalies: Unsurveyed Areas</u>, AGU Monograph Series No. 9, pp 58-67, 1966a.

35.   Kaula, W. M., "Orbital Perturbations from Terrestrial Gravity Data," UCLA, 1966b.

36.   Kaula, W. M., "Test and Combination of Satellite Determinations of the Gravity Field with Gravimetry," <u>Journal of Geophysical Research</u>, Vol. 71, pp 5303-5314, 1966c.

37.   Kaula, W. M., "Geophysical Implications of Satellite Determinations of the Earth's Gravitational Field," <u>Space Science Reviews</u>, Vol. 7, pp 769-794, 1967.

38.   Kaula, W. M., "A Tectonic Classification of the Main Features of the Earth's Gravitational Field," <u>Journal of Geophysical Research</u>, 74:20, pp 4807-4826, 1969.

39.   Kaula, W. M., "Earth's Gravity Field: Relation to Global Tectonics," <u>Science</u> 169, pp 982-985, 1970a.

40.   Kaula, W. M., <u>Global Gravity and Tectonics</u>, Publication No. 835, Institute of Geophysics and Planetary Physics, UCLA, 1970b.

41.   Khan, M. A., "Figures of the Earth and Mean Anomalies Defined by Satellite Orbital Perturbations," in <u>The Earth's Crust and Upper Mantle</u>, AGU Monograph Series No. 13, pp 293-304, 1969.

42. Khan, M. A., "Some Geophysical Implications of the Satellite Determined Geogravity Field," Geophysical Journal Royal Ast Soc, 23, pp 15-43, 1971.

43. Khan, M. A., "Nature of Satellite Determined Gravity Anomalies in the Use of Artificial Satellites," AGU Monograph Series No. 15, pp 99-106, 1972.

44. Khan, M. A., and G. P. Woollard, "A Review of Perturbation Theory as Applied to the Determination of Geopotential," Hawaii Institute of Geophysics Technical Report 68-1, 1968.

45. Khan, M. A., G. P. Woollard, and K. I. Daugherty, Statistical Analysis of the Relation of Marine Gravity Anomalies to Bathymetry, HIG-71-20, AF Contract F23601-C-0100, Hawaii Institute of Geophysics, University of Hawaii, 1971.

46. Koch, K. R., "Geophysical Interpretation of Density Anomalies of the Earth Computed From Satellite Observations and Gravity Measurements," Zeitschrift Fur Geophysik 38, pp 75-84, 1972.

47. Kohnlein, W., "The Geometric Structure of the Earth's Gravitational Field in Geodetic Parameters for a 1966 Smithsonian Institution Standard Earth," Vol. 3, SAO Special Report 200, pp 21-102, 1966.

48. Lebart, L., "Mise au point concesnant les methodes d'extrapolations statistiques des donnees gravimetriques," (Discussions of the methods of statistical extrapolations of gravimetric data), Bulletin d'Information No. 29, Bureau Gravimetrique International, July 1973, p I-21-I-32.

49. Moberly, R., and M. A. Khan, "Interpretation of the Sources of the Satellite Determined Gravity Field," Nature 223, pp 263-267, 1969.

50. Nettleton, L. L., "Determination of Density for Reduction of Gravimeter Observations," Geophysics, Vol. 4, pp 176-183, 1939.

51. Nettleton, L. L., Geophysical Prospecting for Oil, McGraw-Hill Book Co., Inc., New York, 1940.

52. Nettleton, L. L., "Gravity and Magnetic Calculation," Geophysics, Vol. 7, No. 3, pp 293-310, 1942.

53. Nettleton, L. L., "Regionals, Residuals, and Structures," Geophysics, Vol. 19, No. 1, pp 1-22, 1954.

54. Pakiser, L. C., and Isidore Zietz, "Transcontinental Crustal and Upper Mantle Structure," Review of Geophysics, Vol. 3, No. 4, pp 505-520, 1965.

55. Rapp, Richard H., "The Extension of the Gravity Net to the Unsurveyed Areas of the Earth: Statistical Methods," in Gravity Anomalies: Unsurveyed Areas, AGU Monograph Series No. 9, pp 49-52, 1966.

56. Rothermel, W. J., "Gravimetric-Crustal Density Method," unpublished manuscript, 1964.

57. Rothermel, W. J., Personal Communications to the author, 1973.

58. Rothermel, W. J., G. J. Seelman, and I. T. Tumey, "Geo-Gravity Report No. 2, USSR, Ferghana Valley," USAF Aeronautical Chart and Information Center Report, 1963.

59. Scheibe, Donald M., "Density and Distribution of Observations in Determining Mean Gravity Anomalies," USAF Aeronautical Chart and Information Center, 1965.

60. Simpson, Stephen M., Jr., "Least Squares Polynomial Fitting to Gravitational Data and Density Plotting by Digital Computers," Geophysics, Vol. 19, No. 2, pp 255-269, 1954.

61. Slettene, R. L., L. E. Wilcox, R. S. Blouse, and J. R. Sanders, "A Bouguer Gravity Anomaly Map of Africa," paper presented to the 54th Annual Meeting of the American Geophysical Union, DMAAC Technical Paper 73-3, 1973.

62. Stacey, Frank D., Physics of the Earth, John Wiley and Sons, New York, 1969.

63. Strange, W. E., "A Gravity Field for the Northern Hemisphere Based on Observed and Geophysically Predicted Anomalies," paper presented at the International Symposium on Earth Gravity Models and Related Problems, 1972.

64. Strange, W. E., and G. P. Woollard, "The Use of Geologic and Geophysical Parameters in the Evaluation, Interpolation, and Prediction of Gravity," HIG-64-17, AF23(601)-3879, Hawaii Institute of Geophysics, University of Hawaii, 1964a.

65. Strange, W. E., and G. P. Woollard, "The Prediction of Gravity in the United States Utilizing Geologic and Geophysical Parameters," HIG-64-18, AF23(601)-3879, Hawaii Institute of Geophysics, University of Hawaii, 1964b.

66. Uotila, U. A., "Harmonic Analysis of Worldwide Gravity Material," Publications of the Isostatic Institute of International Association of Geodesy, Vol. 39, 1962.

67. USAF Aeronautical Chart and Information Center (ACIC), "Bouguer Gravity Anomaly Map of Asia," Scale 1:9,000,000, 1971a.

282

68. USAF Aeronautical Chart and Information Center, "1° x 1° Mean Free Air Gravity Anomalies," ACIC Reference Publication No. 29, 1971b.

69. Vincent, Samir F., and William E. Strange, "Gravity Correlation Studies for Determination of the Gravity Field of the Earth," Computer Sciences Corporation, USAETL Contract No. DAAK 02-69-C-0139, 1970.

70. Voss, James T., "Empirically Determined Terrain Corrections," paper presented to Fall Annual Meeting, American Geophysical Union, 1972a.

71. Voss, James T., Personal Communications to the author, 1972b.

72. Wilcox, L. E., "The Prediction of 5° x 5° Mean Anomalies in Gravimetrically Deficient Areas," USAF Aeronautical Chart and Information Center, DOD Gravity Services Branch, 1966.

73. Wilcox, L. E., "Geological and Geophysical Methods for Interpolation of Gravity Anomalies," prepared for presentation to the XVI General Assembly of the IUGG, 1967.

74. Wilcox, L. E., "Summary of Gravity Correlation Methods for Prediction of 1° x 1° Mean Free-Air Anomalies," USAF Aeronautical Chart and Information Center, DOD Gravity Services Branch, 1968.

75. Wilcox, L. E., "An Investigation of Areal Gravity Elevation Relations Using Covariance and Empirical Techniques," Hawaii Institute of Geophysics Report HIG-71-10, 1971.

76. Wilcox, L. E., W. J. Rothermel, and J. T. Voss, "The Bouguer Gravity Anomaly Map of Asia," Defense Mapping Agency Aerospace Center, 1972.

77. Woollard, G. P., "Gravity Anomalies and Geologic Structure," Transactions of the AGU, Part I, pp 96-106, 1937.

78. Woollard, G. P., "The Effect of Geologic Corrections on Gravity Anomalies," Transactions of the AGU, Part I, pp 85-90, 1938.

79. Woollard, G. P., "The Gravity Meter as a Geodetic Instrument," Geophysics, Vol. 15, No. 1, pp 1-29, 1950.

80. Woollard, G. P., "Crustal Structure from Gravity Seismic Measurements," Journal of Geophysical Research, Vol. 64, 1010, pp 1521-1544, 1959.

81. Woollard, G. P., "The Relation of Gravity Anomalies to Surface Elevation, Crustal Structure, and Geology," Research Report 62-9, AF23(601)-3455, University of Wisconsin, 1962.

82. Woollard, G. P., "Regional Isostatic Relations in the United States," in The Earth Beneath the Continents, AGU Geophysical Monograph No. 10, pp 557-594, 1966.

83. Woollard, G. P., "An Evaluation of Gravity Prediction in Mexico," HIG Technical Memo 68-1, AF Contract F23(601)-67-C-0168, 1968a.

84. Woollard, G. P., "Collection, Processing, and Geophysical Analysis of Gravity and Magnetic Data," Final Report to AF Contract F23(601)-67-C-0168, 1968b.

85. Woollard, G. P., "The Interrelationship of the Crust, the Upper Mantle, and Isostatic Gravity Anomalies in the United States," in The Crust and Upper Mantle of the Pacific Area, AGU Geophysical Monograph No. 12, pp 312-341, 1968c.

86. Woollard, G. P., "Regional Variations in Gravity," in The Earth's Crust and Upper Mantle, AGU Geophysical Monograph No. 13, pp 320-340, 1969a.

87. Woollard, G. P., "A Regional Analysis of Crustal Structure in North America and a Study of Problems Associated with the Prediction of Gravity in Europe," HIG-69-12, AF Contract F23(601)-68-C-0186, 1969b.

88. Woollard, G. P., Personal Communications to the author, 1969c.

89. Woollard, G. P., "The Interrelationship of Crustal and Upper Mantle Parameter Values in the Pacific," Hawaii Institute of Geophysics, University of Hawaii, 1973.

90. Woollard, G. P., and K. I. Daugherty, "Collection, Processing and Geophysical Analysis of Gravity and Magnetic Data: Gravity Gradients Associated with Sea Floor Topography," HIG-70-19, AF Contract F23(601)-69-C-0212, Hawaii Institute of Geophysics, University of Hawaii, 1970.

91. Woollard, G. P., and K. I. Daugherty, "Investigations on the Prediction of Gravity in Oceanic Areas," Hawaii Institute of Geophysics, University of Hawaii, 1973.

92. Woollard, G. P., and P. F. Fan, "The Evaluation of Gravity Data and the Prediction of Gravity in East Asia," Final Report to AF Contract AF23(601)-4375, 1967.

93. Woollard, G. P., and M. A. Khan, "Prediction of Gravity in Ocean Areas," HIG-72-11, AF Contract F23(601)-71-0187, Hawaii Institute of Geophysics, University of Hawaii, 1972.

284

94. Woollard, G. P., L. Mackesky, and J. M. Caldera, "A Regional
Gravity Survey of Northern Mexico and the Relations of Bouguer
Anomalies to Regional Geology and Elevation in Mexico," Hawaii
Institute of Geophysics Publication, HIG-69-13, 1969,

95. Woollard, G. P., and John C. Rose, International Gravity
Measurements, Society of Exploration Geophysicists, 1963.

96. Woollard, G. P., and W. E. Strange, "The Prediction of Gravity,"
in Gravity Anomalies: Unsurveyed Areas, AGU Monograph Series No. 9,
pp 96-113, 1966.